Universitat Autònoma de Barcelona

From underground to sunlight: characterization of PIF target genes define novel PIF-regulated processes

Arnau Rovira Freixa

UNIVERSITAT AUTONOMA DE BARCLONA

FACULTAT DE BIOCIENCIES

From underground to sunlight: characterization of PIF target genes define novel PIF-regulated processes

Arnau Rovira

2018

UNIVERSITAT AUTONOMA DE BARCLONA

FACULTAT DE BIOCIENCIES

Doctoral program of Plant Biology and Biotechonolgy

PhD Thesis

From underground to sunlight: characterization of PIF target genes define novel PIF-regulated processes

Dissertation presented by Arnau Rovira Freixa for the degree of Doctor of Plant Biology and Biotechnology at Autonomus University of Barcelona. This work was performed in the Center of Research in Agricultura Genomics

Thesis directors		Thesis tutor	PhD candidate
Dra. Elena Monte Collado	Dr. Pablo Leivar Rico	Dra. Mercè Llugany Ollé	Arnau Rovira Freixa

Barcelona
September 2018

Als meus pares

Agraïments

Començo escrivint aquestes paraules amb la sensació que una etapa s'acaba. Una etapa on vaig començar ja fa uns anys al CID a Barcelona i que acabo ara al CRAG. He de reconèixer que al principi, quan era un estudiant de Biologia en pràctiques, no tenia molt clar si centrar la meva recerca en plantes. No vaig tardar gens en adonar-me'n que aquell món m'agradava, i que volia continuar la meva carrera científica en el camp de la biologia molecular de plantes, no només per l'interès que em va despertar tot aquell camp que desconeixia en aquell moment, sinó també per la gent que en formava part.

Primer de tot, vull donar les gràcies a l'Elena per donar-me l'oportunitat de fer la tesi doctoral al seu laboratori. Han estat els anys de la meva vida on he après més, a nivell personal i professional. M'ha guiat sempre durant tot aquest període, ajudant-me en els moments més difícils i valorant la feina ben feta. Gràcies a l'Elena, he après a investigar, a qüestionar-me el perquè de les coses i ser rigorós amb la feina.

També vull agrair a en Pablo per tot el que m'ha ensenyat durant aquests anys. Tot i que va deixar el CRAG durant la meva tesi, va voler seguir formant part d'aquest projecte i sempre ha estat allà quan l'he necessitat, discutint resultats i proposant nous experiments.

Tots dos han estat un pilar fonamental durant tots aquests anys en la meva evolució com a científic. Tant és així que, fins i tot durant l'escriptura, els dos han estat fins a l'últim moment aportant idees que han fet que aquesta tesi sigui el que és ara.

Per suposat vull agrair als membres del Monte Lab: la Lot, la Liu i en Nil. Thank you guys for sharing with me grate moments inside and outside the CRAG. With you, my thesis have been less taught and more fun. Thank you for helping me in the most difficult moments. Ells han fet que el laboratori mantingués la mateixa essència que quan vaig començar. Sempre amb un somriure i ajudant en tot moment, tant a nivell científic com personal. Hem passat molt bones estones dins i fora del laboratori i, gràcies a això hem fet un gran equip. No puc oblidar-me de les integrants que ja no hi són al laboratori: la Judit, la Guiomar, la Celine i la Maria. Totes elles em van donar un cop de mà des del primer dia en que vaig entrar al laboratori. A la seva manera, totes em van ajudar i aconsellar durant la tota tesi. De totes elles he aprés molt.

Per descomptat, no em puc oblidar de la gent del CRAG em qui vaig compartir els meus primers anys. Vaig entrar sent un estudiant en pràctiques i de seguida em vaig sentir un més d'aquell grup. Gràcies a ells vaig descobrir que els científics tenen molta festa a les venes i tinc molt bons records de tots ells i elles tant dins com fora del CRAG.

Els predocs i postdocs que actualment estan al CRAG i que m'entenen la mateixa

essència de bon ambient. Aquests últims anys d'estrès i nervis s'han fet més amens gràcies a tots ells i elles. Les estones de "Happy Hour", celebracions de tesis, congressos i sopars, en són un bon exemple. Vull fer una menció especial als dies de cases rurals amb gent que actualment estar al CRAG i gent que ja ha marxat. Aquí és on es demostra el grup humà que s'ha creat durant aquests anys i espero seguir gaudint d'aquests caps de setmana molt més temps.

Però no tot és ciència. Abans que comencés aquesta aventura, ells i elles ja hi eren: La colla, els amics i amigues de Vic, la família que es tria. Gràcies a tots i totes per recolzar-me en tot moment, per ajudar-me a relativitzar les coses. Dies en què arribava estressat, preocupat, tard i cansat, han estat allà per fer-me desconnectar i oblidar-me dels problemes. Anàvem a sopar i arreglàvem el món amb unes cerveses. Tot i no saber res del que estava fent, el vostre interès per la meva feina i el que estava fent, molts cops desencadenava en una conversa científica on acabàvem discutint sobre l'existència de l'ésser humà. M'encanta! Membri, Marta, Jan, Guille, Núria D., Juli, Mariona, Edu, Núria P., Heri, Pauvi, Arroyo, Polgui i Marina: Gràcies per haver-hi estat tots aquests anys i, n'estic segur, que hi sereu sempre.

Òbviament vull agrair a la meva família. Primer de tot, vull donar les gràcies als meus pares. Per tot el que m'han ensenyat i per tot el que m'han donat. Sóc com sóc gràcies a ells. Ells em van donar l'oportunitat i la llibertat per estudiar el que més m'ha agradat sense qüestionar-m'ho, i van confiar cegament amb mi en totes les decisions que prenia. Sense ells mai hauria pogut començar aquesta etapa. És per aquesta raó que aquesta tesi els hi dedico especialment a ells.

A en Guilli i la Laura. Per animar-me a seguir, per estar pendents de la meva feina i animar-me en tot moment. Guilli, gràcies per deixar-me el pis els dies que sopava amb els del CRAG per Barcelona heheh.

Als meus avis del carrer nou i els de La Codina, que tot i no saber de què anava tota aquesta aventura, sempre em preguntaven si ja havia acabat d'estudiar, si treballava i si m'agradava la meva feina, que això últim era el més important. Als meus tiets i cosins, que tot i no saber res de biologia molecular de plantes, m'heu animat a seguir i en tot moment. A tu Jordi, que segur que m'haguessis donat suport en tot moment. No dubto ni un segon en què m'has ajudat quan més ho necessitava.

Vull mencionar també a la família Puigvert-Sànchez, que ja saben de què va tot això i m'han donat suport durant tota aquesta etapa.

Finalment a tu Marina, per ajudar-me tant en tot moment. Per confiar en mi i donar-me suport quan més ho necessitava. Per animar-me a seguir i fer treure el millor de mi. Per tot el que he après de tu durant aquesta etapa. Per tot això i molt més, gràcies.

Abbreviations

A.thaliana	Arabidopsis thaliana
ABA	Absicic acid
ABA-GE	ABA-glucose ester
aba2	ABA deficient 2
ABCG16	*ATP-BINDING CASSETTE G16*
ABI1/2	*ABA INSENSITIVE 1/2*
abi1	*ABI1* mutant
ACC	1-aminocyclo-propane-1-carboxylic acid
ACP4	*ACYL CARRIER PROTEIN 4*
ACS5/6/8	1-AMINOCYCLOPROPANE-1-CARBOXULATE SYNTHASE 5/6/8
ACTIN2	*DEFORMED ROOT HAIRS 1*
AHA2	PLASMA MEMBRANE PROTON ATPASE 2
APA	Active phytocrhome A domain
APB	Active phytochrome B domain
AUX1	*AUXIN RESISTANT 1*
BEH4	*BES1/BZR1 HOMOLOG 4*
bHLH	Basic helix-loop-helix
BIN2	*BRASSINOSTEROID-INSENSITIVE 2*
BR	Brassinosteroids
ChIP	Chromatin Immunoprecipitation
ChIP-qPCR	ChiP quantitative PCR
CHLI1	*LOW TEMPERATURE WITH OPEN-STOMATA 1*
CKX5	*CYTOKININ OXIDASE 5*
CO	CONSTANTS
Col-0	Columbia-0 ecotype in *A.thaliana*
COP1	CONSTITUTIVE PHOTOMORPHOGENIC 1
cop1	*COP1* mutant
cry	Crypthorchromes
cry1/2	Crypthochrome 1/2
CYP450	CYTOCHROME 450
CSLC04	*CELLULOSE-SYNTHASE-LIKE C4*
DELLAS	Negative regulator of gibberellin family protein
della	DELLA mutant
ELF3/4	EARLY FLOWERING 3/4
ET	Ethylene
EXLA2	*EXPANSIN-LIKE A2*
EXPA11	*EXPANSIN 11*
FAD	Flavine Adenine dinucleotide
FHL	*FAR-RED-ELONGATED HYPOCOTYL1-LIKE*
FKF1	FLAVING-BINDING KELCH REPEAT F-BOX 1

FR	Far red light
FT	*FLOWERING LOCUS T*
G-BOX	CACGTG sequence motif
GAs	Gibberallins
GFP	Green Fluorescence Protein
GLK2	*GOLDEN2-LIKE 2*
GMC	Guard mother cells
HAT2	*HOMEOBOX PROTEIN 2*
HEMA1	*GLUTAMYL-TRNA REDUCTASE*
HFR1	*LONG HYPOCOTYL IN FAR-RED 1*
HY5	*ELONGATED HYPOCOTYL 5*
IAA2/19/29	*INDOLE-3-ACETIC ACID INDUCIBLE 2/19/29*
KAT1	*POTASSIUM CHANNEL 1*
kat1	*KAT1* mutant
LAX	*LIKE AUXIN RESISTANT*
LD	Long day
LOV	Light Oxygen Voltage
LKP2	*LOV KELCH PROTEIN 2*
LUX	*PHYTOCLOCK 1*
M	Meristemoid
MGL	*METHIONINE GAMMA-LYASE*
MIDA1/9/10/11	*MISEXPRESSED IN THE DARK* 1/9/10/11
mida9	MIDA9 mutant
MMC	Meristemoid mother cells
MYB15/44	*MYB DOMAIN PROTEIN 15/44*
NFYA5	*NUCLEAR FACTOR Y 5*
OFP16	*OVATE FAMILY PROTEIN 16*
MS	Skoog medium
PA	Phaseic acid
PAO1	*POLYAMINE OXIDASE*
PBE-box	PIF-binding E-Boxes
PINs	*PIN-FORMED - AUXIN EFFLUX*
pd1	Mutated in AT3G17090
pd6	Mutated in AT4G38520
Pfr	Active far-red-absorbing phytochrome form
phot	Phototropin
phot1/2	Phototropin 1/2
phy	Phytochromes
PI	Propidium iodide
PIA1	PP2C induced by AvrRpm1
PIF	PHYTOCHROME INTERACTING FACTOR

PIF1/3/4/5	PHYTOCHROME INTERACTING FACTOR 1/3/4/5
pif1/3/4/5	*PIF1/3/4/5* mutants
PIFq	PIF QUARTET: *PIF1*, *PIF3*, *PIF4* and *PIF5*
pifq	PIFq quadruple mutant
PIL1	*PIF3-LIKE 1*
phy	Phytochrome
phyA/B/C/D/E	Phytochrome A/B/C/D/E
PP2C-D/A	Type 2C/A-protein phosphatases
PRR5/7/9	*PSEUDO-RESPONSE REGULATOR 5/7/9*
Pr	Inactive red-absorbing phytochrome form
PSB28	*PHOTOSYSTEM II REACTION CENTER 28*
R	Red light
Rc	Continuous red light
RCI2A	*RARE-COLD-INDUCIBLE 2A*
SAURs	*PSEUDOGENE OF AUXIN-RESPONSIVE FAMILY PROTEIN*
SD	Short day
SIGMA5	*SIGMA FACTOR 5*
SLGC	STOMATAL-LINEAGE GROUND CELLS
SPA1	*SUPRESSOR OF phyA-105 1*
SPCH	*SPEECHLESS*
TOC1	*TIMING OF CAB EXPRESSION 1*
TSS	Transcription start site
ST2B	*SULFOTRANSFERASE 2B*
WAG2	*PROTEIN KINASE 2*
WL	White light conditions
WT	Wild-type
XTH2/8/15	*XYLOGLUCAN ENDOTRANSGLUCOSYLASE/ HYDROLASE 2/8/15*
YFP	Yellow Fluorescence Protein
YUCCAs	*YUC-MEDIATED AUXIN BIOGENESIS FAMILY PROTEIN*
ZT	Zeitgeber time
ZTL	Zeitlupes

Contents

chapter 1

General introduction

Organisms have the ability to perceive and process information from the environment to adequate physiological responses in an optimal way. Because plants are sessile organisms, this adaptation to the environmental conditions are crucial for their survival. External factors such as temperature, light, humidity and salinity are sensed by plants and influence their development. Among all of these parameters, light is one of the most important because it has a dual role in plants: as a source of energy and as a source of information. It is well known that plants are able to transform light into chemical energy through the photosynthesis. Not less important is the fact that plants are able to perceive light signals and get information about season, time of the day, or local conditions (Kami *et al.*, 2010).

To inform about the dynamic changes of the spectral composition (light quality), light intensity and the light duration, plants are armed with a collection of light sensitive proteins called photoreceptors. Photoreceptors play an essential role throughout plant life cycle: seed germination, seedling deetiolation, plant growth and development, and flowering . Three classes of photoreceptors have been identified in *Arabidopsis thaliana* (or *A. thaliana* from now on*)* based on their absorption spectra: phytochromes (phy), which absorb red (R) and far-red (FR) light (Li *et al.*, 2011; Franklin and Quail, 2009), cryptochromes (cry), phototropins (phot) and zeitlupes (ZTL), specific for UV-A/blue

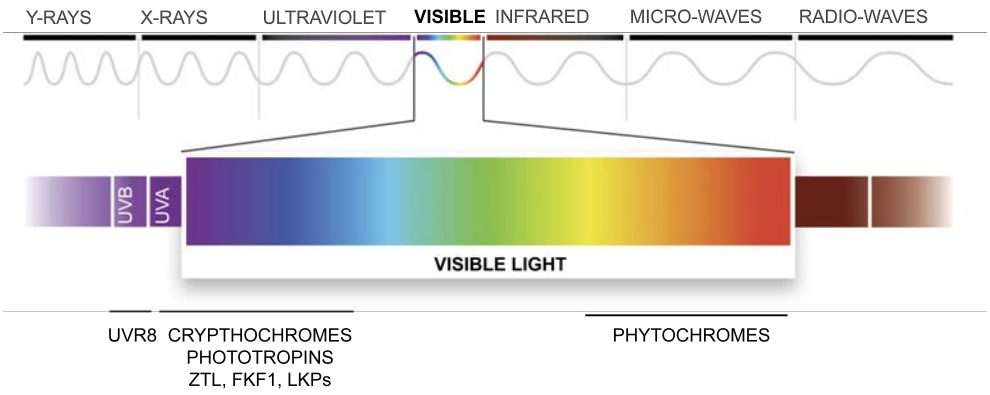

Figure 1.1 Light spectrum and plant photoreceptors.
Diagram representing the light spectrum. In grey, non-visible wavelengths of light. The spectrum of visible light is highlighted. The absorption spectra for each class of photoreceptors are indicated at the bottom of the diagram. Adapted from http://www.eyesafe.com/bluelight/

light perception (Liu *et al.*, 2011b; Ito *et al.*, 2012; Fankhauser and Christie, 2015) and UVR8, a UV-B light photoreceptor (Jenkins, 2014; Galvão and Fankhauser, 2015) (Fig 1.1).

1. Light perception and photoreceptors

Perception of UV-B light

The only photoreceptor found in *A. thaliana* to mediate the UV-B light responses is UVR8 (Rizzini *et al.*, 2011; Jenkins, 2014). Upon perception of UV-B light, UVR8 homodimers dissociate to active monomers (Yang *et al.*, 2015) that are able to interact with CONSTITUTIVE PHOTOMORPHOGENIC 1 (COP1) (Rizzini *et al.*, 2011) to mediate several developmental responses such as inhibition of hypocotyl elongation (Fierro *et al.*, 2015) and entrainment of circadian clock (Fehér *et al.*, 2011).

Perception of UV-A/blue light

Zeitlupe family of photoreceptors perceive UV-A/blue light. This family is comprised by ZEITLUPE (ZTL), FLAVING-BINDING KELCH REPEAT F-BOX (FKF1) and LOV KELCH PROTEIN 2 (LKP2) proteins. All members contain a characteristic Light Oxygen Voltage (LOV) domains (Ito *et al.*, 2012). Among other functions, it has been described that Zeitlupes control floral transition and entrainment of circadian clock (Christie *et al.*, 2015).

Phototropins also perceive UV-A/blue light and are part of the AGC Kinase family. This family contains two LOV domains (Christie *et al.*, 2015). *A. thaliana* possess two phototropins, phot1 and phot2 which regulate phototropism, stomatal opening and leaf flattening (Christie, 2007).

Another UV/A-blue light photoreceptors are the cryptochromes that contain a FAD chromophore (Flavin Adenine dinucleotide) (Chaves *et al.*, 2011). *A. thaliana* possess two cryptochromes (cry1 and cry2) with partially overlapping functions. In general, cry1 has been implicated in deetiolation while the main role of cry2 is the photoperiodic regulation of flowering (Chaves *et al.*, 2011; Liu *et al.*, 2011b). Cryptochromes are activated by blue light which leads to interact with signalling intermediates such as SUPPRESSOR OF PHYA-105 1 (SPA1) to supress COP1 activity (Liu *et al.*, 2011a; Holtkotte *et al.*, 2017). Recently, it has been described that cryptochromes can interact with PHYTOCHROME INTERACTING FACTOR 4 (PIF4) and PIF5, providing a crosstalk point between cry and phy signalling pathways (see below) (Pedmale *et al.*, 2016).

Perception of R and FR light

A. thaliana possess five phytochromes (phyA to phyE) and are classified in two groups according to their stability in light (Sharrock and Quail, 1989). PhyA belongs to light labile type I, and is most abundant in dark-grown seedlings. Its levels drop rapidly upon exposure to white light during seedling deetiolation. On the other hand, phyB to phyE are

considered light stable phytochromes and belongs to type II. In light-grown seedlings, phyB was demonstrated to be the most abundant of all of them (Quail, 2002a; Li *et al.*, 2011).

Phytochromes act as homodimers and, each monomer, is a chromoprotein consisting of an apoprotein of 120 kD covalently attached to the linear tetrapyrrole chromophore phytochromobilin (Quail *et al.*, 1995; Furuya, 1993). This chromophore is able to capture light of different wavelength, causing a conformational change on the protein structure that alters phytochrome activity.

Phytochromes are involved in the detection of specific range of wavelengths, in particular, they have an absorbance maxima in the red (660 nm) and far-red light (730 nm)(Neff *et al.*, 2000). They are synthesized as inactive form (Pr) that is converted to the active form (Pfr) upon absorption of red light. This reaction is reversible and, in this situation, the Pfr form is able to absorb far-red light, switching the Pfr back to Pr. In natural light conditions, this reversible photoconversion results in a dynamic photoequilibrium between active and inactive form of phytochromes (Strasser *et al.*, 2010; Franklin and Quail, 2009) (Fig 1.2).

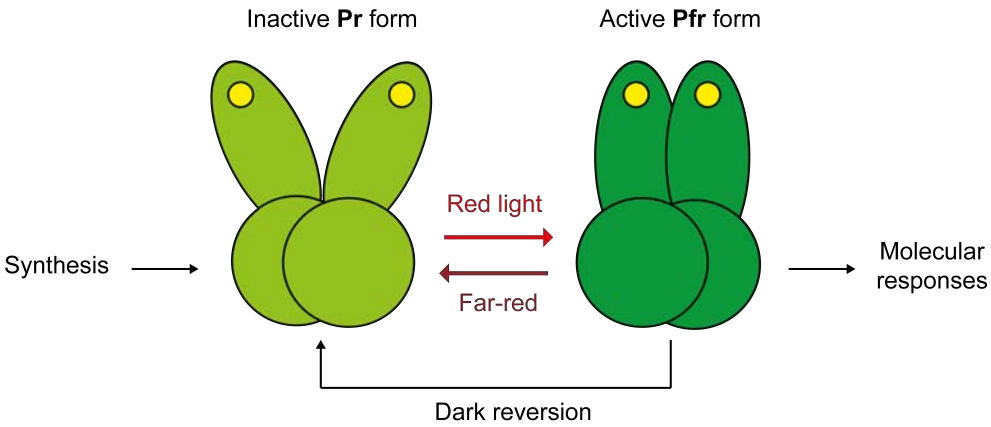

Figure 1.2 Phytochrome photoconversion.
The phytochrome is synthesized as the inactive Pr form (light green) and acts as a dimer. This Pr form is able to absorb red light and photoconvert into the Pfr biological active form (dark green). This is a reversible process mediated by FR light absorption, and in a slower fashion, by dark conditions. Yellow circles represent the associated tetrapyrrole chromophore phytochromobilin to each polypeptide.

Light activation of the phy also results in important changes in the cellular dynamics. The phy Pr inactive form is synthesized and accumulates in the cytoplasm in darkness. However, upon light exposure, the activated Pfr form translocates from the cytoplasm into the nucleus (Van Buskirk *et al.*, 2012; Klose *et al.*, 2015). Once in the nucleus, the active Pfr interacts and disrupt the activity of intermediary signalling components like the

E3 ubiquitin-protein ligase COP1 or the PIF transcription factors (Fig 1.3).
These molecular events result in the transduction of the light signal to the promoters of target genes through different mechanisms, and trigger changes in nuclear gene expression (Leivar *et al.*, 2009).

2. Skotomorphogenesis development

Just after seed germination in the subterranean darkness, seedlings undergo the skotomorphogenesis developmental program or etiolated growth, characterized by heterotrophic growth consuming seed reserves. The skotomorphogenic phenotype is defined by fast hypocotyl elongation to reach the sunlight at the soil surface, closed cotyledons and the formation and maintenance of the apical hook to protect the apical meristem when the seedlings are growing through the soil (Quail, 2002b) (Fig 1.4A).

When seedlings emerge to the soil surface, they are exposed to the environmental light. This light is perceived by plant and initiate a switch from skotomorphogenic to photomorphogenic development, a process that is called seedling deetiolation. This process is characterized by rapid formation of the photosynthetic apparatus to start to produce energy from light and to avoid photodamage. In addition, seedlings change

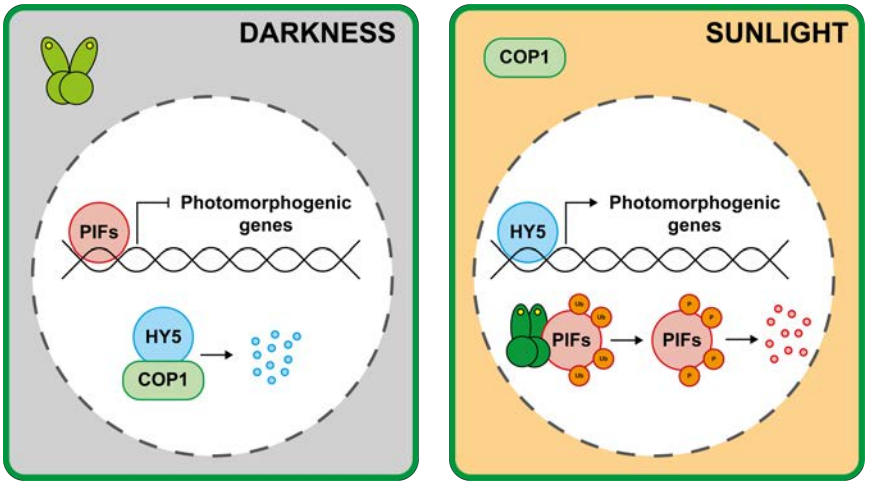

Figure 1.3 phy signalling pathways involving PIFs and COP1/HY5 proteins.
In darkness, phytochrome Pr inactive form localizes in the cytosol. Under these conditions, negative regulators of photomorphogenesis such as the PIF transcription factors are accumulated in the nucleus repressing the transcription of light-induced genes. Moreover, the E3-ubiquitin ligase COP1 is active and promote degradation of positive regulators of photomorphogenesis such as HY5. In contrast, under light conditions, phytochrome Pfr active form translocate into the nucleus where is able to interact and disrupt the activity of PIFs. Additionally, HY5 degradation by COP1 is abolished due to COP1 translocation to the cytoplasm. In this situation, HY5 activates the expression of light-induced genes.

their morphology to enhance light capture for photosynthesis. These changes comprise, among others, the inhibition of hypocotyl growth, the promotion of cotyledon aperture and expansion, and hook unfolding (Gommers and Monte, 2017) (Fig 1.4B and Fig 1.4C).

Skotomorphogenesis in the dark is achieved principally by the repression of proteins that promote deetiolation such as ELONGATED HYPOCOTYL 5 (HY5) and the induction of proteins that repress photomorphogenic development such as PIFs (Josse and Halliday, 2008).
During skotomorphogenesis, the phytochrome Pr inactive form is localized in the cytoplasm. In this situation, the E3 ubiquitin ligase COP1 is active and accumulates inside the nucleus, where is able to repress light signalling by targeting photoreceptors and downstream transcription factors for ubiquitination and subsequent proteasome-mediated degradation (Yi and Deng, 2005). One of the transcription factor targeted by COP1 for degradation is HY5, an important transcription factor that induce the expression of light-regulated genes (Ang *et al.*, 1998). In accordance, it has been established that dark-grown COP1 mutant (*cop1*) seedlings accumulate HY5 protein in the dark and display a phenotype resembling seedlings grown in the light (Deng *et al.*, 1991) (Fig 1.3).

Role of phy and PIFs during seedling deetiolation

PIFs and skotomorphogenesis

The absence of the phytochrome Pfr active form during skotomorphogenesis also allows the nuclear accumulation of phytochrome interacting factors (PIFs) (Fig 1.3). PIFs are nuclear proteins that belong to the basic helix-loop-helix (bHLH) family of transcription factors that function as a negative regulators of light responses by repressing photomorphogenesis. All the PIF members are characterized by their ability to interact with the active Pfr form of phyB through a domain located in the N-terminal part of the protein called APB (active phytochrome B binding). In addition, PIF1 and PIF3 also possess an APA domain (active phytochrome A), which confer them the ability to bind to the Pfr form of phyA (reviewed in Leivar and Quail, 2011). Seven PIFs have been described in *A. thaliana*: PIF1, PIF3, PIF4, PIF5, PIF6, PIF7 and PIF8, which have been reported to act regulating gene expression by direct binding to the DNA elements G-Box (CACGTG) and PBE-Box (PIF-binding E-Boxes), the latter including the E-Box variants CACATG and CATGTG. These DNA elements are located in specific promoter-regions of the target genes (Martínez-García *et al.*, 2000; Zhang *et al.*, 2013; Pfeiffer *et al.*, 2014).
Different studies have reported that the PIF quartet (PIFq) members PIF1, PIF3, PIF4 and PIF5 constitutively promote skotomorphogenesis by repressing photomorphogenesis state in darkness (Leivar *et al.*, 2008b). Whereas studies in *A. thaliana* single *pif1*, *pif3*,

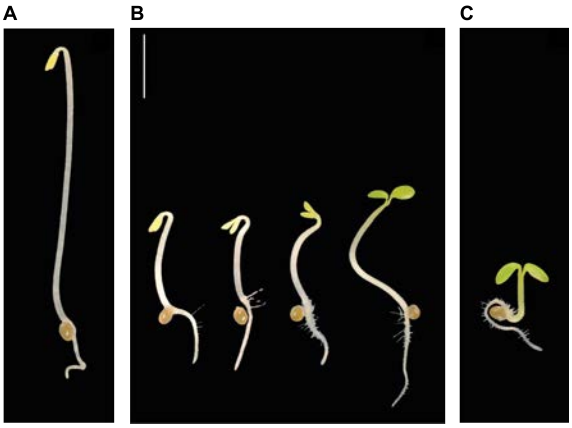

Figure 1.4 Morphological phenotypes of Arabidopsis seedlings during the seedling deetiolation developmental transition.
A. A 3-day-old dark-grown Arabidopsis WT seedling is shown. **B.** 2-day-old dark grown Arabidopsis WT seedlings exposed to (left to right), 0h, 2h, 6h or 24h of light. **C.** 3-day-old light-grown Arabidopsis WT seedlings is shown. Adapted from (Gommers and Monte, 2017).

pif4 and *pif5* mutants show a minor or absent photomorphogenic phenotype in darkness, additive to synergetic effects are observed in higher order mutant combinations. In accordance, *A. thaliana* seedlings deficient in PIFq members (*pif1*, *pif3*, *pif4* and *pif5*, also known as *pifq* mutant) grown under dark conditions, display a partial constitutive photomorphogenic phenotype similar to dark-grown *cop1* mutant (Leivar *et al.*, 2008b). Consistent with this observation, the transcriptomic profile of *pifq* mutants in the dark, largely resemble that of wild-type (WT) seedlings grown in the light (Leivar *et al.*, 2009; Shin *et al.*, 2009), demonstrating that PIFs are important to maintain the etiolated state (Fig 1.5).

PIFs and phy to regulate deetiolation

Several studies demonstrated that under dark conditions, phytochrome Pr inactive form localizes in the cytoplasm, which allows PIFq accumulation into the nucleus. However, upon light exposure, phytochrome Pfr active form translocates to the nucleus where it interacts with PIFq members through the APB domain. The phy-PIFs interaction triggers a rapid phosphorylation and subsequent ubiquitination, and proteasome-mediated degradation in photobodies (Quail, 2002a; Monte *et al.*, 2004; Al-Sady *et al.*, 2006; Van Buskirk *et al.*, 2012; Ni *et al.*, 2017) (Fig 1.3). Recently, it has been described that cry also physically interacts with PIF4 and PIF5 (Pedmale *et al.*, 2016), possibly to repress their transcriptional activity (Ma *et al.*, 2016).

All the PIFq members described so far are stable in the dark. After light exposure, the degradation of PIFq members is a fast event, with half-lives of 5 to 20 min (Park *et al.*, 2004; Bae and Choi, 2008).

Rapid phy-induced proteolytic degradation of PIFq members results in the disappearance of the PIF repressors, and thus the initiation of the deetiolation response. This mechanism partially explains the deetiolation response, since the *pifq* mutant

only show a partial constitutive photomorphogenic phenotype. In addition, once the deetiolation developmental transition is established, other mechanisms take place for the optimization of the response. For example, no function has been established during skotomorphogenesis for another PIF family member, PIF7, an instead, it participates as a negative regulator of deetiolation under prolonged light conditions. Interestingly, the physical interaction of PIF7 with phyB upon light exposure, does not lead to its proteolysis (Leivar *et al.*, 2008a), so alternative regulatory mechanisms must be involved. Among these, it has been well reported for PIF7 and other PIFs that the phyB-PIF interaction results in a concomitant degradation of the photoreceptor (Jang *et al.*, 2010; Park *et al.*, 2012; Ni *et al.*, 2013). This co-degradation of the photoreceptor is proposed to act to desensitize the seedling to the light and to optimize the photomorphogenesis. Other reported mechanisms include the phyB dependency on PIF1 and PIF3 for its translocation into the nucleus during the deetiolation in *in vitro* conditions. Furthermore, other PIFq members have been proposed as phyB transport facilitators based on the decreased nuclear phyB levels exhibited in the *pifq* mutant in *in vivo* assays (Pfeiffer *et al.*, 2012; Park *et al.*, 2012).

Figure 1.5 PIFs promote etiolated growth in Arabidopsis seedlings. 3-day-old WT and pifq seedlings grown in the dark, and WT seedlings grown in short day (SD) are shown. pifq mutants show a partial constitutive photomorphogenic phenotype in the dark. Adapted from (Gommers and Monte, 2017).

PIF-regulated transcriptional network

Given that PIFs are able to directly bind DNA to regulate gene expression, many transcriptomic studies of single or/and multiple *pif* mutants, ChiP-chip and/or ChiP-Seq data for individual PIFs in etiolated seedlings have been done to provide some insight into the transcriptional network downstream of PIFs (Monte *et al.*, 2004; Leivar *et al.*, 2009; Sentandreu *et al.*, 2011; Moon *et al.*, 2008; Lorrain *et al.*, 2009; Pfeiffer *et al.*, 2014). Among the multiple reported transcriptomic and ChiP-Seq studies, the microarray analysis described in Sentandreu et al. is of particular relevance for this thesis, as it defined PIF3-regulated genes misexpressed in the dark (*MIDAs*) (Sentandreu *et al.*, 2011), one of them being central to this thesis.

PIFs as system integrators

Multiple studies have showed that PIFs not only mediate light responses but also act as integrators of external and internal signals to coordinate plant growth and development. Recent studies have been performed to elucidate how seedling deetiolation is controlled by the

crosstalk between light and hormone transduction pathways, and how PIFs act as a hub where multiple light signals convey. On the one hand, genome-wide expression analysis have established that PIFs enhance the expression of auxin synthesis and signalling by regulating auxin-related genes such as *AUX1*, *LAX*, *PINS and YUCCAs* (Li *et al.*, 2012; Hornitschek *et al.*, 2012; Pfeiffer *et al.*, 2014). Furthermore, it has also been demonstrated that PIFs regulate ethylene levels by directly inducing *ACS5* and *ACS8* (Khanna *et al.*, 2007; Gallego-Bartolomé *et al.*, 2011).

In the other hand, hormone signals have also been described to modulate PIFs activity. For instance, it has been demonstrated that DELLAs, which are negative regulators of gibberellin (GA) signalling, interact with PIF3 and PIF4 to avoid the binding to the DNA and promote their degradation via proteasome (De Lucas *et al.*, 2008; Feng *et al.*, 2008; Li *et al.*, 2016). Additionally, it was defined that PIF4 has the capacity to interact with BZR1, a BR-activated transcription factor, to co-regulate light- and hormone-responsive genes (Oh *et al.*, 2012). In accordance, it has been reported that active BR signalling is required for growth promotion in response to DELLA destabilization. The same study reported that PIF4 directly interacts to a BR signalling kinase BIN2 *in vitro* and *in vivo*, which phosphorylates the PIF4 protein *in vitro*. The authors also demonstrated that this interaction plays and important role in modulating stability of PIF4 (Bernardo-García *et al.*, 2014).

Altogether, current data suggest that PIFs act as integrators of internal signals, such as hormones, and external signals, such as light, to modulate plant growth and development. However, some studies demonstrated that other external signals such as temperature or the circadian clock also convey on the PIFs, by modulating their activity.

Role of phy and PIFs in other photomorphogenic responses: Diurnal conditions

The phy-PIF interaction not only regulates the deetiolation transition, but also regulates other photomorphogenic developmental programs such as shade avoidance, responses to temperature and diurnal plant growth (Leivar and Monte, 2014; Lymperopoulos *et al.*, 2018). When post-germinative growth occurs under diurnal conditions, young seedlings are exposed to light/dark cycles of variable duration, and to a light intensity that depends on the time of the year. During the light hours, the plant photoreceptors are photoactivated and signal to the nucleus to induce photomorphogenesis. During this period, a large fraction of the carbon assimilated during photosynthesis, is stored transiently in the chloroplast as starch for its use during the following night. In this thesis, we focused on diurnal plant growth.

Under diurnal conditions, circadian clock and light regulate rhythmic development programs, such as hypocotyl growth (Soy *et al.*, 2012, 2016), photosynthesis and stomata opening (Tallman, 2004). As explained above, plant growth regulation under diurnal conditions is, in part, mediated by phy-PIFs interaction (Soy *et al.*, 2012). During the day, Pfr active form of phytochromes triggers the decrease in abundance of PIFs, whereas during the night, the gradual decline in the levels of Pfr form due to dark reversion leads on gradual reaccumulation of PIFq members, which peak at the end of the night. Therefore, under diurnal conditions, this rhythmic regulation of PIFq produces rhythmic processes, such as hypocotyl growth and photosynthesis (Monte *et al.*, 2004; Shen *et al.*, 2005; Nozue *et al.*, 2007; Niwa *et al.*, 2009; Soy *et al.*, 2012). PIFq accumulation depends on the length of the dark period. In consequence, the more dark hours the higher amount of PIFq accumulates at the end of the night. Accordingly, it has been previously described that PIF3 protein abundance stays low during the day and progressively accumulates during the dark hours to peak at the end of the night, coinciding with their physiological action in promoting hypocotyl elongation (Niwa *et al.*, 2009; Soy *et al.*, 2012). In consequence, seedlings grown in short day (SD) show longer hypocotyl than in long day (LD) conditions. Furthermore, *pifq* seedlings grown under SD are similar to WT seedlings grown in LD (Fig 1.6), demonstrating that hypocotyl growth under diurnal conditions is PIF-dependent.

Another regulatory layer of this rhythmic growth is imposed by the circadian clock, a biological oscillator that maintains rhythms of about 24 hours. Circadian clock is an endogenous signal that modulates diurnal growth, which is necessary to predict daily and seasonally environmental changes to coordinate physiological responses at the correct time in which they must occur. The connection between PIFs and circadian clock has been recently demonstrated. In this sense, it was published that circadian clock output pathways, such as the evening complex (LUX, ELF3 and ELF4), directly represses expression of PIF4 and PIF5 to gate the hypocotyl growth in the early evening (Nusinow *et al.*, 2012; Nakamichi *et al.*, 2012). In accordance, it was described that ELF3, one of the members of the evening complex, directly supresses PIF4 activity during early night. Furthermore, phyB-ELF3 interaction is essential to control ELF3 protein accumulation in the light phase of the day (Nieto *et al.*, 2015). Other studies

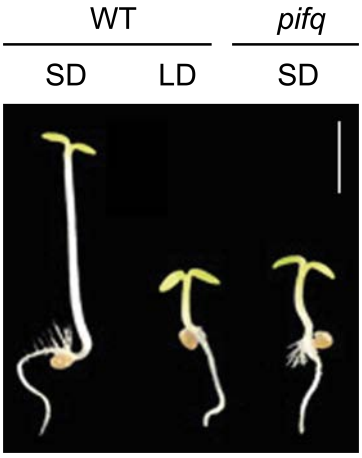

Figure 1.6 PIFs are required to promote growth under diurnal conditions. 3-day-old Arabidopsis WT seedlings grown under short day (SD) and long day (LD) conditions, and pifq seedlings grown in SD, are shown. Adapted from (Gommers and Monte, 2017).

defined that the core clock component Timing of CAB expression 1 (TOC1) and PIFs, directly interacts and represses PIFs activity in the middle of the night under SD conditions. PIFs-TOC1 interaction co-binds to the promoters of growth- and thermoresponsive-related genes to regulate their expression, which provides clock-imposed gating of PIFs-mediated responses (Soy *et al.*, 2016; Zhu *et al.*, 2016). Recently, it was described in our laboratory that circadian morning-to-midnight waves of PRR transcriptional repressors (PRR9, PRR7 and PRR5) jointly gate PIFs activity through sequential regulation of common PIF-PRR target genes, such as *CDF5* (Martín *et al.*, 2018).

Growth is induced by PIFq at the end of the night through the transcriptional regulation of growth related genes (Nozue *et al.*, 2011a; Soy *et al.*, 2012, 2014). Microarray expression analysis of multiple *pif* mutants under diurnal growth conditions have been performed to identify the regulatory network downstream of the PIFs. A microarray analysis was recently performed in our laboratory at the end of the night in 4-day-old SD-grown seedlings to define PIF-regulated and SD-regulated genes (Martin *et al.*, 2016). Interestingly, many of the PIF/SD-induced genes at the end of the night play a role in hypocotyl elongation and plant growth. They comprise several protein families, including transcriptional regulators (e.g., *PIL1*, *FHL*, *HFR1* and *HAT2*), auxin-related genes (e.g., *SAURs*, *IAA2*, *IAA19* and *IAA29*), genes involved in the response to gibberellins (GAs) and brassinosteroid (BR) stimuli, and cell wall-related genes (e.g., *XTH8*, *XTH15*, *ZTH33*, *CSLC04*, *EXPA11* and *EXLA2*). This analysis, together with previous studies (Nozue *et al.*, 2011b; Hornitschek *et al.*, 2012; Pfeiffer *et al.*, 2014), suggests that PIFq induce elongation during the dark period under diurnal conditions by upregulating the expression of hormonal pathways, transcription factors related in hypocotyl growth and genes involved in cell wall modification (Martin *et al.*, 2016).

In contrast, most of the PIF/SD-repressed gene sets are enriched in genes involved in photosynthesis, chlorophyll biosynthesis and chloroplast development (e.g., the photosystem I *PGR5-LIKE A*, the photosystem II PsbP, *PSB28*, *ACP4*, *CHLI1*, *HEMA1*, *GLK2* and *SIGMA5*). This data suggests that PIFq prevents the expression of chloroplast-related genes during the night (Martin *et al.*, 2016).

Altogether, understanding on how phy-PIFs mediate responses to light to regulate plant growth and photomorphogenesis is increasing over years. However, further work needs to be done to characterize the PIF-regulated transcriptional network and how it implements responses downstream of the PIFs, as well as to unveil novel phy-PIF functions in plant physiological responses other than growth. In this thesis, we shed some light on some of these questions.

Objectives

At the beginning of this thesis, PIF transcription factors had been described to play a key role in the integration of internal and external signals to modulate growth in the model plant *Arabidopsis thaliana*. Many studies had also contributed to the definition of the PIF-regulated transcriptional network. However, the downstream functions of this network and the implication of PIFs in physiological responses other than growth was poorly studied.

The main goal of this thesis was to expand the current knowledge of the regulatory network acting downstream of PIFs from skotomorphogenesis to photomorphogenesis, and to define novel regulatory roles of PIFs during plant development. The following specific objectives have been addressed:

- Characterization of the role of *MIDA9*, a PP2C clade D member that is regulated by PIF3, in the regulation of hook development during skotomorphogenesis.

- Characterization of the role of PIFs in the regulation of stomata rhythmic movements under diurnal conditions.

- Identification and characterization of novel PIF-regulated genes that are involved in the regulation of stomata movements under diurnal conditions.

chapter 2

Characterization of the role of MIDA9 during hook development

INTRODUCTION

After germination in the dark, young seedlings adopt a developmental strategy called skotomorphogenesis or etiolated growth, which is energetically sustained by reserves stored in the seed. This dark-grown strategy is characterized by fast hypocotyl elongation to rapidly reach the soil surface, together with an apical hook and appressed cotyledons, which protect the apical mersitem from damage during growth through the soil (Wei *et al.*, 1994; Gommers and Monte, 2017).

An important etiolated process to protect the apical meristem is the hook folding. The apical hook structure is a transient structure that develops after germination as a result of the curvature of the hypocotyl apex just below the cotyledons. Hook development proceeds through three different phases: formation, maintenance and opening (Zadnikova, Petra *et al.*, 2010; Vandenbussche *et al.*, 2010). The formation phase starts just after germination, when the seedling emerges from the seed coat. This phase lasts about 24-36h in which the hook reaches 180º when completely formed. The maintenance phase follows, in which the hook remains folded for another 24h-48h. Finally, the opening phase starts and hook progresively unfolds to become completely open (angle 0º) (scheme in Fig 2.2A). The formation phase is achieved by asymmetrical cell expansion and cell division at the apical part of the hypocotyl. Cell expansion is inhibited in the inner (concave) edge of the hook, while cell division and expansion is promoted in the outer (convex) border (Raz and Koornneef, 2001; Silk and Erickson, 1978; Vandenbussche *et al.*, 2010), which forms an apical hook bending of the hypocotyl apex. This asymmetrical cell expansion is caused by an auxin maximum in the concave part of the apical hook (Fig 2.1). Mutations in auxin transport genes or auxin-synthesis genes cause defects in hook development (Vandenbussche *et al.*, 2010; Zadnikova, Petra *et al.*, 2010; Willige *et al.*, 2012). In addition to auxin, other hormones like ethylene (ET) and gibberellins (GAs) are involved in hook formation. Exogenous treatment with the ethylene biosynthesis precursor ACC (1-aminocyclo-propane-1-carboxylic acid) induces a triple response of the etiolated seedlings characterized by an exaggerated hook, short and thickened hypocotyl (Fig 2.1). On the other hand, ethylene biosynthetic mutants as well as ethylene-insensitive mutants are hookless (Guzman and Ecker, 1990; Tsuchisaka *et al.*, 2009). GAs also participate in hook formation, given that inactivation of either GAs synthesis or signalling results in a hookless phenotype (Vriezen *et al.*, 2004; Alabadí *et al.*, 2004). Conversely, treatment with GA or mutations in *DELLA* genes (transcriptional regulators that negatively regulate the GA signalling pathway) exhibit an exaggerated hook (An *et al.*, 2012). It has been proposed that both GAs and ET modulate asymmetrical auxin distribution depending on the apical hook development (Vandenbussche *et al.*, 2010; Zadnikova, Petra *et al.*, 2010) (Fig 2.1).

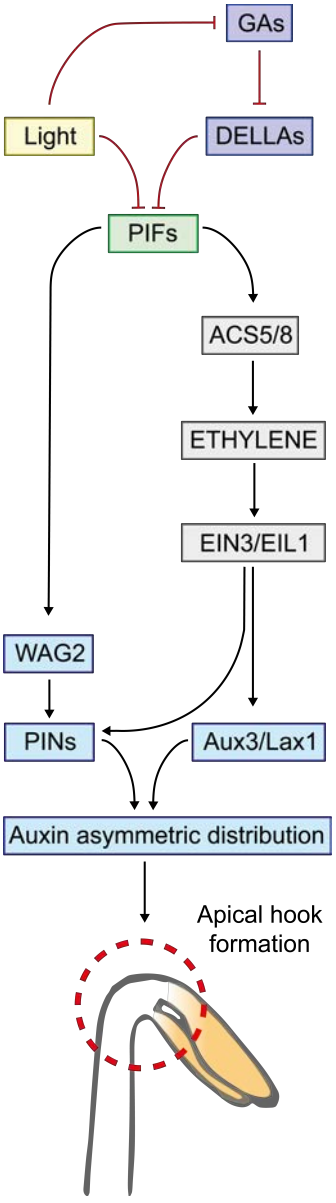

Figure 2.1 Simplified overview of the crosstalk between light and hormone signaling network involved in auxin asymmetric distribution during apical hook formation.
Green arrows indicate positive regulation. Red blunt arrows indicate negative regulation. Adapted from (Mazzella, 2014).

PIFs negatively regulate photomorphogenesis in the dark. This is well studied in *A. thaliana pif* quadruple mutant (*pifq*) deficient in multiple PIF proteins (PIF1, PIF3, PIF4 and PIF5). *pifq* mutant grown in the dark, results in photomorphogenic phenotype: short hypocotyl, unfolded hook and expanded cotyledons, which resembles a wild type plant grown in the light (Leivar *et al.*, 2008; Josse and Halliday, 2008). Light rapidly induces complete hook opening, within a few hours, through the action of phy and cry (Wu *et al.*, 2010; Liscum and Hangarter, 1993). This hook unfolding occurs due to faster cell elongation at the inner compared to the outer edge (Vandenbussche and Van Der Straeten, 2004; Vriezen *et al.*, 2004). During hook opening, the auxin gradient is greatly reduced (Wu *et al.*, 2010; Willige *et al.*, 2012). Recent reports have established several direct targets of PIF activity through which PIFs could be contributing to hook development in the dark. PIF5 affects generation of the auxin gradient by directly regulating *WAG2*, which encodes a protein kinase that regulates auxin transport, and this regulation is modulated by GAs and DELLAs (Willige *et al.*, 2012) (Fig 2.1). PIF5 also directly induce expression of ethylene biosynthesis genes 1-aminocyclopropane-1-carboxulate synthase (ACS) such as ACS5 and ACS8 in a GAs and DELLA-dependent manner (Gallego-Bartolomé *et al.*, 2011; Khanna *et al.*, 2007) (Fig 2.1).

In our laboratory, Maria Sentandreu *et al.* reported in 2011 a combination of a microarray-based approach with a functional profiling strategy to identify novel regulators of seedling deetiolation downstream of PIF3 (Sentandreu *et al.*, 2011). Four PIF3-regulated genes misexpressed in the dark (*MIDAs*) were defined as novel regulators of seedling deetiolation involved in hypocotyl elongation (*MIDA11*), hook maintenance (*MIDA9* and *MIDA10*) and cotyledon appression

(*MIDA1*). One of them, *MISEXPRESSED IN THE DARK* 9 (*MIDA9*) was a repressor of photomorphogenesis in the dark with a specific role in hook unfolding (Sentandreu *et al.*, 2011). Etiolated seedlings deficient in *MIDA9* (*mida9)* was not able to fully form the apical hook compare to Col-0 control (Sentandreu *et al.*, 2011). *MIDA9* encodes a type-2C phosphatase belonging to clade D of the type-2C phospahatase superfamily in *A. thaliana*. Clade D (PP2C.D) consists of 9 members and is characterized by having a distinc nuclear localization signal and prediction of possible plasma membrane localization (Schweighofer *et al.*, 2004). Recently, MIDA9 has been reported to modulate H^+-ATPase phosphorylation status by protein-protein interaction to regulate cell expansion in the hypocotyl in long day-grown seedlings (Spartz *et al.*, 2014). Interestingly, this activity of MIDA9 can be directly inhibited by SMALL AUXIN UP-RNA (SAUR) proteins (Spartz *et al.*, 2014).

In the current chapter we combine phenotypic and molecular analysis to characterize in more detail the role of *MIDA9*, and find that *MIDA9* specifically regulates hook formation. Furthermore, based on previous studies pointing at possible functional redundancy among family members (Spartz *et al.*, 2014 Add NEW REF o Ren et al), we explore the possible role of PP2C.D phosphatases in regulating hook formation together with *MIDA9*.

EXPERIMENTAL PROCEDURES

Plant material and seedling growth

A. thaliana seeds used in this chapter include the previously described *mida9-1* mutant (*mida9*) in the ecotype Col-0 background (Sentandreu *et al.*, 2012). The new *A. thaliana* seeds *pd1*/SALK_203806 and *pd6*/SALK_049798 described in this thesis were T-DNA lines in the ecotype Col-0 background, which were identified by searching the Salk Institute Genomic Analysis Laboratory database (Alonso *et al.*, 2003) (http://signal.salk.edu/cgi-bin/tdnaexpress). Homozygous T-DNA insertion lines and WT siblings were identified using PCR with T-DNA and gene-specific primers (Table S2.1).

MIDA9-YFP transgenic lines were generated by cloning the 2kb region upstream of the ATG (*MIDA9* promoter) in the pDONR-P4-P1R vector, the *MIDA9* coding sequence (CDS) in the pDONR-P2R-P3 vector, and the GFP CDS in the pDONR221 vector. LR recombination reaction using the Gateway cloning system (Invitrogen) was done to generate proMIDA9::MIDA9:YFP in the pH7m34gw vector. The resulting vector was used to transform *mida9* to generate MIDA9-YFP.

MIDA9-GFP-OX transgenic lines were generated by cloning the *MIDA9* CDS under the regulation of the 35S promoter in the pH7WG2 vector by the Gateway cloning system. The resulting 35S::MIDA9:GFP was transformed into *mida9* to generate MIDA9-GFP-OX lines.

Seeds were sterilized and plated on Murashige and Skoog medium (MS) without sucrose as previously described (Monte *et al.,* 2003). For $AgNO_3$ experiments, seeds were sterilized and plated on MS without sucrose with $AgNO_3$ (50µM). Seedlings were then stratified for 4 days at 4ºC in the dark. 3h of whit light were done to induce germination and after that seedlings were placed in darkness for the indicated period of time.

Hypocotyl, hook and cell measurements

For hypocotyls and hook measurements, seedlings grown for 2, 3 and 4 days were arranged horizontally on a plate and photographed using a digital camera (Nikon D80). Measurements were performed using NIH image software (Image J, National Institutes of Health), as described before (Leivar *et al.,* 2008). The angle of a completely closed apical hook was defined as 180°, whereas the angle of a fully opened hook was defined as 0°. Measurements of at least 30 seedlings for each mutant line were tested using in R for statically significant differences with the wild-type sibling controls. Cell size and hook length measurements was visualized at 2-day-old dark-grown seedlings stained with propidium iodine (10µg/mL) (Calbiochem) using confocal laser microscope Leica SP5 (Emission window: 570nm – 666nm).

Gene expression analysis

RNA was extracted using Maxell RSC plant RNA Kit (Promega). 1µg of total RNA extracted were treated with DNase I (Ambion) according to the manufacturer's instructions. First-strand cDNA synthesis was performed using the SuperScript III reverse transcriptase (Invitrogen) and oligodT as a primer. RNase Out (invitrogen) was used to treat the cDNA. 2 µl of 1:25 diluted cDNA with water was used for real-time PCR (LightCycler 480 Roche) using SYBR Premix Ex Taq (Takara) and primers at 300nM concentration. For figure 2.3B, 3 independent biological replicates, with three technical replicates for each biological samples, and the mean of the biological replicates +/- SE is shown. Dots indicate each replicate. For figure 2.5C, 2 independent biological replicates were performed, and one of them is shown as representative. *PP2A (AT1G13320)* was used for normalization. Primers uses for gene expression analysis are listed in Table S2.2.

Fluorescence microscopy

2-day-old dark-grown hypocotyl and apical hook for MIDA9-YFP and *MIDA9-GFP-OX* #1.4/#2.2 transgenic lines were visualized using a confocal laser scanning microscope Olympus FV1000 (Emission window: 500nm - 600nm). *mida9* was used as a negative control.

Protein extraction and immunoblots

Protein extracts were prepared from 2-day-old dark-grown seedlings. Tissue samples were collected and frozen in liquid nitrogen. Samples were manually ground under frozen conditions and resuspended in extraction buffer (100mM MOPS (pH 7.6), 2% SDS, 10% glycerol, 4mM EDTA, 50mM Sodium Metabisulfite ($Na_2S_2O_5$), $2gl^{-L}$ apoprotein, $3gl^{-L}$ leupeptine, $1gl^{-L}$ pepstatin and 2mM PMSF) (Soy *et al.*, 2014; Martín *et al.*, 2018). Total protein was quantified using a Protein DC kit (Bio-Rad), and B-mercaptoethanol was added just before loading. 100µg for each sample were treated for 5min at 95ºC and subjected to 12.5% SDS-PAGE gels. Proteins were then transferred to Immobilon-P membrane (Millipore), and immunodetection of MIDA9-GFP was performed using an anti-GFP antibody (1:10,000 dilution). Peroxidase-linked anti rabbit secondary antibody (1:10,000) and SuperSignal West Femto chemiluminescence kit (Pierce) were used for detection of luminescence using LAS-4000 image imaging system (Fujifilm). The membrane was stained with Ponceau as a loading control.

Statistical analysis

Levene's test was performed to verify equal variances ($P<0.05$). When the variances were equal, Student *t*-test ($P<0.05$) or ANOVA test ($P<0.05$) followed by a post-hoc Tukey-b test was performed. If needed, data were ln transformed. For not equal variances, Kruskal-Wallis test ($P<0.05$) followed by a post-hoc Dunn test was performed. All analyses were conducted in R.

RESULTS

MIDA9 is required for hook formation during skotomorphogenesis development

To characterize in detail the role of *MIDA9* during apical hook development under skotomorphogenesis, we followed the apical hook dynamics in wild-type (Col-0) and *mida9* mutant seedlings lacking *MIDA9* (Sentandreu *et al.*, 2011). The three phases in hook development (formation, mantainance, aperture) were monitored by measuring the angle of hook curvature at different time points after germination under darkness conditions.

After germination, we observed that Col-0 and *mida9* mutants emerged from the seed coat at the same time (Fig 2.2). However, compared to Col-0, which reached about 160º hook 40h post-germination, we observed that *mida9* hooks were only about 125º. Therefore, *mida9* mutants were not able to fully form the apical hook during the formation phase. After formation, the differences in the hook between Col-0 and *mida9* were maintained during the maintenance phase, which lasted up to 60h post-germination. Finally, hook opening started at similar time in both genotypes (>60h post-germination), eventually resulting in similar hook unfolding (about 25º) at 108 hours after germination (Fig 2.2).

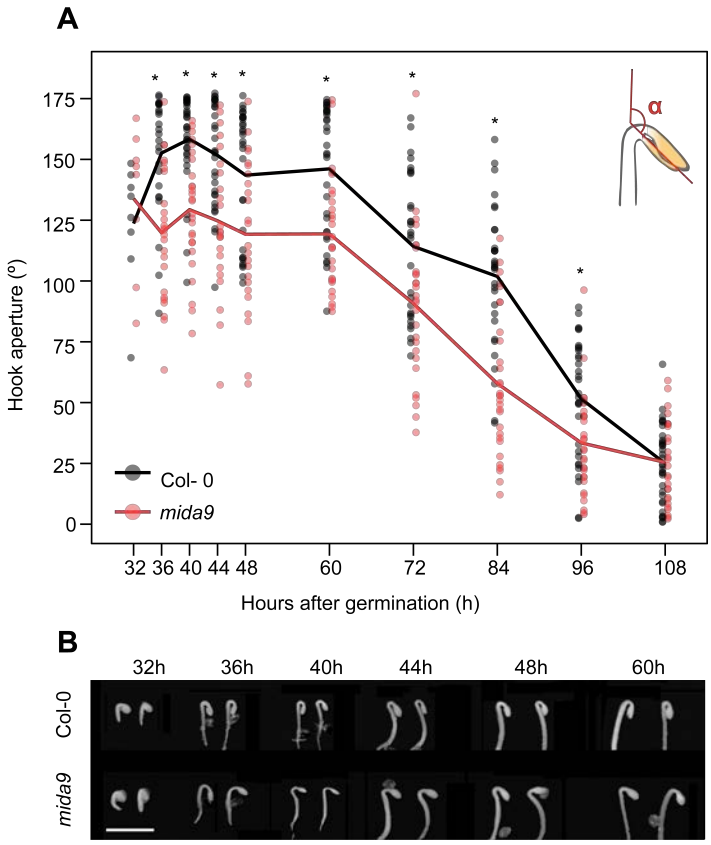

Figure 2.2. *MIDA9* is necessary to induce hook formation after germination.
A. Time course analysis of apical hook aperture after germination in the dark of Col-0 and *mida9*. Lines represent mean values, dots indicate each measurement. Statistical significant relative to Col-0 are indicated by an asterisk (Student *t*-test, $P<0.05$) n=40. **B.** Visible phenotypes of seedlings grown in the dark are shown. Bar = 2 mm.

Together, these data extended our previous observation that *MIDA9* participates in hook development (Sentandreu *et al.*, 2011) and determine that *MIDA9* activity is required for hook formation during the first hours of post-germinative growth. Our data also suggest that MIDA9 does not participate during the maintenance or opening phase of hook development under skotomorphogenesis development.

MIDA9 is required to establish the asymmetric growth necessary for hook formation

To understand how *MIDA9* might regulate hook formation, we combined confocal microscopy images and phenotypic measurements to study the early stage of *mida9* hook development in more detail. To examine the hook development under dark-grown

conditions, we stained Col-0 and *mida9* with propidium iodide (PI), which is used to visualize plasmatic membrane to delimit cells. Compared to Col-0, which closed the hook as described above, *mida9* mutants failed to form the apical hook (Fig 2.3A) (Fig2.2A), indicating that *MIDA9* is necessary for hook formation. Because hook formation is achieved mainly as a result of asymmetric elongation of the cells on the outer (convex) edge of the hook compared to the inner edge (concave) (Raz and Koornneef, 2001; Silk and Erickson, 1978), we hypothesized that *mida9* seedlings might be affected in establishing this asymmetric growth. The length of the outer and the inner border of the hook were measured in 2-day-old dark-grown seedlings (Fig 2.3B). Whereas the inner concave side was similar in Col-0 and *mida9*, the outer convex side was significantly longer in Col-0 compared to *mida9* (Fig 2.3C right panel). Cell length of the outer and the inner side

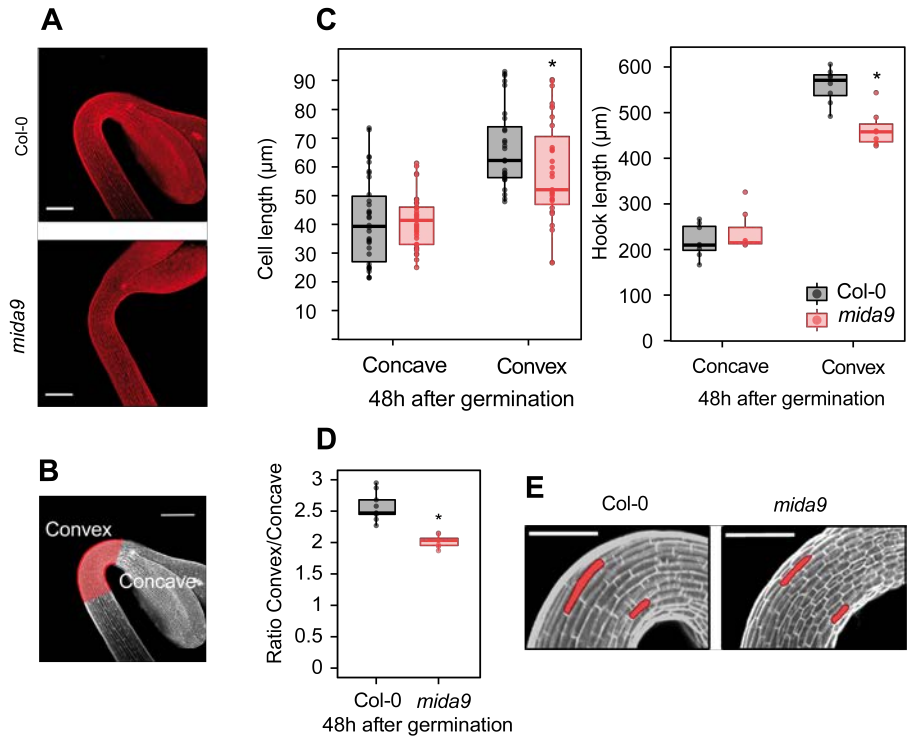

Figure 2.3. *MIDA9* induces cell expansion in the outer edge of the apical hook.
A. Visual phenotypes of the apical hook in 2-day-old dark-grown Col-0 and *mida9*. Bar = 200 µm. **B.** In red, apical hook is highlighted. Bar = 200 µm. **C.** Cell length (left panel) and hook length (right panel) measurements in the concave and convex side of the apical hook of 2-day-old dark-grown Col-0 and *mida9*. Dots indicate each measurement. Statistical significance relative to Col-0 are indicated by an asterisk. Left panel, (Kruskal-Wallis, P>0,05), left panel (Student *t*-test, *P*>0,05). n=15. **D.** Apical hook length ratio between convex and concave in Col-0 and *mida9*. Data come from panel B. Statistical significance relative to Col-0 is indicated by an asterisk (Student *t*-test, *P*<0,05). **E.** Visual phenotypes of 2-day-old dark-grown Col-0 and *mida9*. Cells from concave and convex part of the hook are highlighted. Bar = 60 µm.

of the hook were also measured and compared, and no differences in cell length were found in the inner edge of the apical hook in Col-0 and *mida9*. However, cells in the outer convex side of the hook were longer in Col-0 compared to *mida9* (Fig 2.3C left panel). No apparent difference in cell number was observed between both genotypes. As a result, the convex/concave ratio was higher in Col-0 compared to *mida9* (Fig 2.3D), indicating that asymmetric growth in the hook structure in *mida9* was less pronounced than that of Col-0. Together, these results demonstrate that *MIDA9* induces the elongation of the cells in the outer edge of the hook, necessary to establish the asymmetric growth that results in the hook organ formation after germination in the dark.

MIDA9 localizes to the nucleus and cytoplasm in the apical hook

To characterize MIDA9 function at the molecular level, two different transgenic lines were previously generated in the laboratory by Maria Sentandreu that express a fluorescent-tagged fusion (GFP/YFP) under the strong constitutive 35S promoter (MIDA9-GFP-OX) or the endogenous *MIDA9* promoter (MIDA9-YFP) in a *mida9* mutant background (see Experimental Procedures for details). These transgenic lines were characterized here and used to study the molecular role of *MIDA9* in regulating hook formation.

First, we checked the *MIDA9* gene expression in our transgenic lines by qRT-PCR. Compared to Col-0, *MIDA9* expression levels were about 4-fold higher in MIDA9-YFP transgenic lines. In contrast, two selected independent MIDA9-GFP-OX lines showed highly increased *MIDA9* levels compared to Col-0 plants. In particular, *MIDA9* expression in MIDA9-GFP-OX #2.2 was 4-fold higher than MIDA9-GFP-OX #1.4, and they were 20- and 80-fold, respectively, higher than Col-0. We did not detect *MIDA9* expression in *mida9*, consistent with previous results (Sentandreu *et al.*, 2011) (Fig 2.4A). Western blot analyses confirmed higher accumulation of the fusion protein in the overexpressing MIDA9-GFP-OX lines with respect to the MIDA9-YFP (Fig 2.4B). MIDA9-YFP transgenic lines complemented the hook formation phenotype of *mida9* (Fig 2.4C), indicating that the expressed fusion protein is active and functional.

MIDA9 belongs to the clade D of the type 2C-protein phosphatases (PP2C), the only clade in the family in which all members present a nuclear localization signal in their sequence (Schweighofer *et al.*, 2004). Functional characterization of the members of PP2C clade D in overexpressing lines, showed several cellular localizations in root tips over the family such as plasma membrane, cytosol, endomembranes system and nucleus (Tovar-Mendez *et al.*, 2013). Visualization of 2-day-old dark-grown MIDA9-YFP by confocal microscopy showed subcellular localization of MIDA9 to the nucleus and cytoplasm in the apical hook and hypocotyl (Fig 2.4D), consistent with the predicted nuclear localization signals (Schweighofer *et al.*, 2004). A comparable pattern was

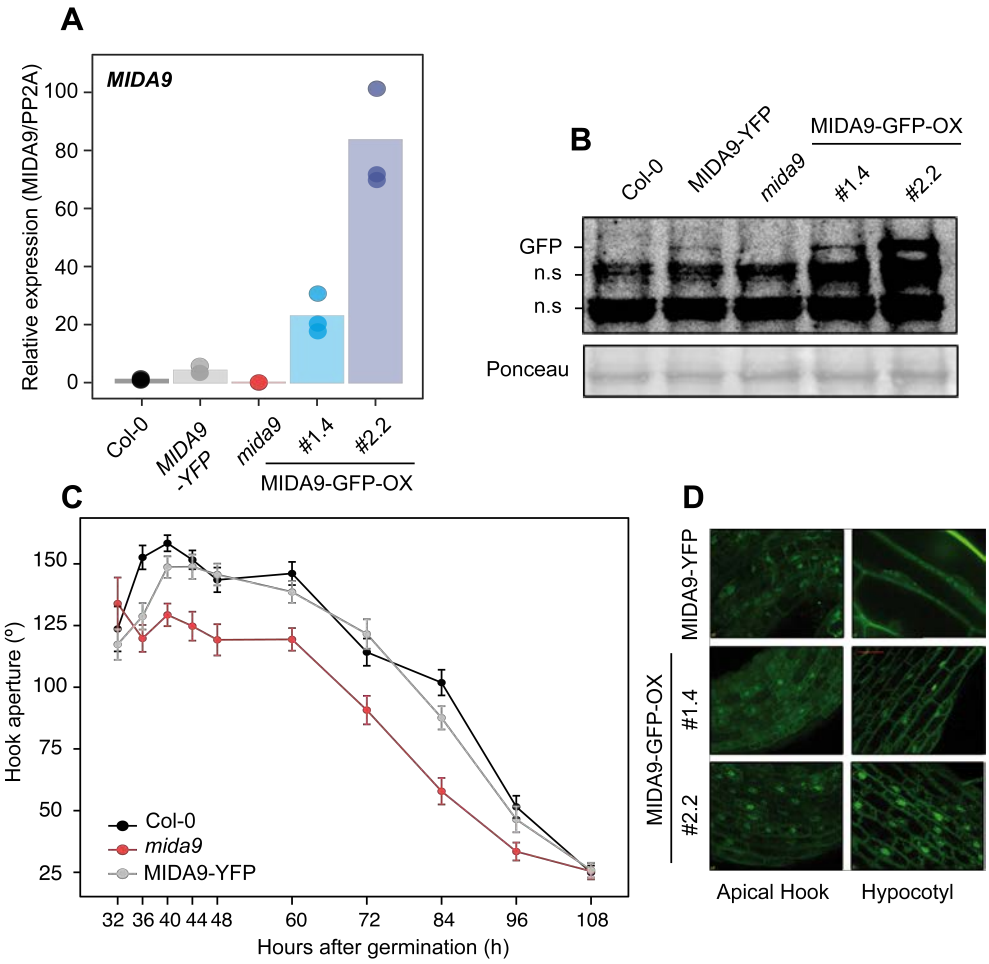

Figure 2.4. MIDA9 is localized into the nucleus and cytoplasm in darkness.
A. qRT-PCR analysis of 2-day-old dark-grown Col-0, MIDA9-YFP, *mida9*, MIDA9-GFP-OX #1.4 and MIDA9-GFP-OX #2.2. *MIDA9* expression levels were normalized to *PP2A* and expressed relative to the Col-0 value set at unity. Bars represent mean values, dots indicate each measurements. n= 3 biological replicates. **B.** Immunoblot of protein extracts of 2-day-old dark-grown Col-0, MIDA9-YFP, *mida9*, MIDA9-GFP-OX #1.4 and #2.2 seedlings. Protein extract from Col-0 and *mida9* was used as a negative control. GFP-specific polyclonal antibody was used as a probe. Ponceau staining was used as a loading control. Non-specific cross-reacting bands were marked as n.s. **C.** Time course analysis of apical hook aperture after germination in the dark of Col-0, *mida9* and MIDA9-YFP. Lines indicate mean values. Dots indicate each measurement. n=40. **D.** MIDA9-YFP, MIDA9-GFP-OX #1.4 and #2.2 subcellular localization in dark-grown seedlings was determined by confocal microscopy.

observed in cells of the MIDA9-GFP-OX lines. However, signal was higher in MIDA9-GFP-OX overexpressing transgenic lines, in agreement with higher transcript and protein accumulation compared to MIDA9-YFP. In MIDA9-GFP-OX overexpressing lines, signal was ubiquitous and cytoplasm localization was also detected (Fig 2.4D). Interestingly, a recent study defined localization patterns of MIDA9 similar to our results (Ren *et al.*, 2018).

Assessing a role for other PP2C.D members in the regulation of hook formation

We hypothesized that the other eight members of the PP2C clade D could also be involved in the regulation of developmental processes during skotomorphogenesis. Therefore we characterized PP2C clade D members to address whether they have similar roles to *MIDA9* in regulating hook formation phase during skotomorphogenesis. T-DNA insertional mutant lines were available for all the PP2C clade D members. We identified homozygous mutants together with the corresponding wild-type siblings for all members of the PP2C clade D. The eight mutated loci were screened for statistically significant differences compared to Col-0 at a late phase of hook development in 4-day-old dark-grown seedlings. This preliminar assay allowed us the identification of two members of the PP2C clade D that could be potentially involved in the regulation of hook development: *pd1* (mutated in *AT3G17090*) and *pd6* (mutated in *AT4G38520*) (data not shown). We thus decided to perform a more detailed genetic study to characterize the role of *PD1* and *PD6* during hook development. To this end, all combinations of *mida9*, *pd1* and *pd6* double and triple mutants were constructed, and the three phases in hook development (formation, mantainance, aperture) were monitored by measuring the angle of hook curvature over 4 days after germination in the dark.

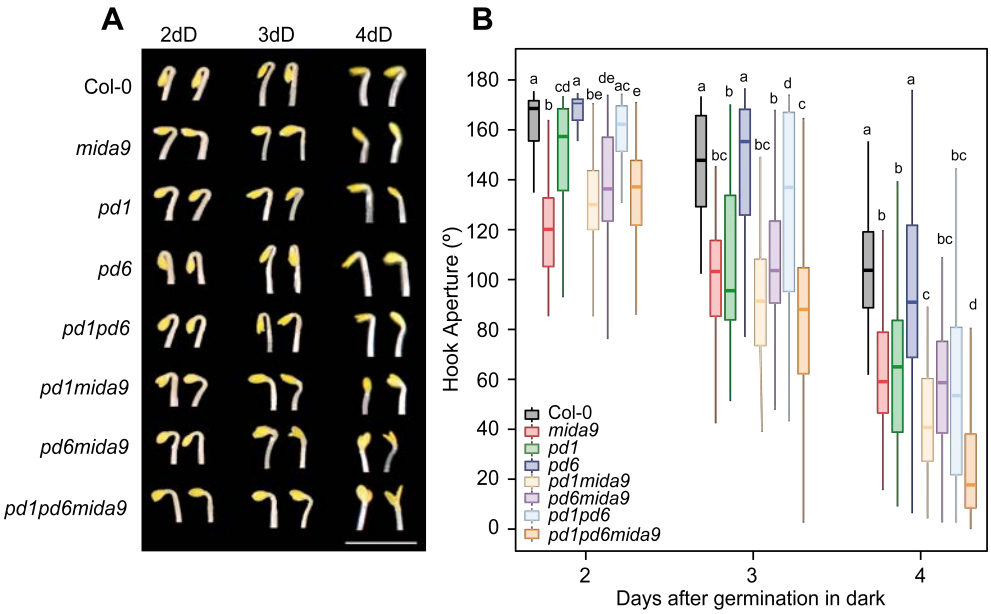

Figure 2.5. PP2C Clade D members present temporally-space function regulating hook development.
A. Visible hook phenotypes of seedlings grown at 2, 3 and 4 days in the dark are shown. Bar = 3 mm. **B.** Apical hook aperture was measured in 2-, 3-, 4-day-old dark-grown seedlings in Col-0, *mida9*, *pd1*, *pd6*, *pd1pd6*, *pd1mida9*, *pd6mida9* and *pd1pd6mida9*. Different letters denote statistical differences between means by Kruskal-Wallis test ($P<0.05$) followed by a post-hoc Dunn test. n=40.

Single mutant analysis at the hook formation phase at 2 days showed a prominent open hook of *mida9* (Fig 2.5), consistent with our previous observations (Fig 2.2A). A significant but relatively minor phenotype was observed in *pd1*, whereas *pd6* showed no apparent hook phenotype compared to Col-0. This tendency was also observed at the maintance (3d) and at the aperture (4d) phases, only that *pd1* mutant displayed now displayed a prominent open hook phenotype similar to *mida9*, and in contrast to our initial screening conditions, *pd6* did not show an observable phenotype. Together, these results suggest that (i) *MIDA9* and *PD1* act together to promote hook formation, with a dominant role of *MIDA9* and a relatively marginal role of *PD1*; (ii) *PD1* gains importance to promote hook mantainance together with *MIDA9*; and (iii) *PD6* have a minor or absent contribution in the presence of the other clade D PP2C members.

In order to test for possible redundancy between family members, we next characterized higher order mutants between *MIDA9*, *PD1* and *PD6*. No significant additive or synergistic genetic interactions were identifyed at the hook formation phase at 2d, as the observed differences are relatively minor in magnitude (Fig 2.5). A similar tendency was observed at the mantainance phase at 3d, only that the increased role of *PD1* in mantaining the hook was also evidenced in the absence of the other two members MIDA9 and PD6 (compare *mida9pd6* with *mida9pd1pd6*). Interestingly, additive/synergistic genetic interactions were clearly observed at the opening phase at 4d. First, relative to the *mida9* and *pd1* single mutants, *mida9pd1* showed a significant more open hook phenotype. Second, in striking contrast to 2d and 3d, a clear contribution of *PD6* was observed in the triple mutant *mida9pd1pd6* in the absence of *MIDA9* and *PD1* (compare *mida9pd1* with *mida9pd1pd6*).

Together, this genetic analysis unvails a complex scenario where *MIDA9*, *PD1* and *PD6* clade D family members collectively participate in the hook develeopment, but that they do so in a temporal and hirerchical manner. *MIDA9* has a prevalent role in promoting hook formation, whereas *PD1* plays a relatively marginal role at this phase. In contrast, at the maintanance phase, *PD1* gains quantitative importance and equals *MIDA9*. Finally, *PD6*, with no apparent role during hook formation or mantainance, act at the aperture phase to prevent hook opening in combination with *MIDA9* and *PD1*. These results are oveverally consistent with recent reports performed in slighlty different conditions (older seedlings in the presence of sucrose known to alter photomophogenic responses), which suggest that except for *mida9,* minor or absent hook phenotypes are observed in clade D PP2C single mutants, but that prominent phenotypes are observed in higher order mutants indicating additive/synergistic genetic interactions among family members (Spartz *et al.*, 2014; Ren *et al.*, 2018).

Exploring an interplay between MIDA9 and ethylene biosynthesis in the dark

We observed a marginal effect of MIDA9-GFP-OX seedlings in complementing hook formation phenotype of *mida9* mutants (Fig 2.6A), suggesting that hook formation is highly sensitive to the amount of MIDA9, and highly increased levels of MIDA9 in MIDA9-GFP-OX lines might be detrimental to hook formation. In contrast, MIDA9-GFP-OX seedlings displayed shorter and thickened hypocotyls under dark-grown conditions compared to Col-0 and *mida9* seedlings (Fig 2.6A). Because this feature has been previously described in mutants with increased ethylene levels (Guzman and Ecker, 1990), we decided to explore whether the observed phenotype of etiolated MIDA9-GFP-OX lines may be related to ethylene levels. Treatment with $AgNO_3$ that blocks accessibility to ethylene receptors (Beyer, 1976), resulted in greater hypocotyl elongation responses in MIDA9-GFP-OX lines compared to Col-0 in 3-day-old dark-grown seedlings (Fig 2.6B lower panel). As a result, the hypocotyl growth differences calculated by subtracting the hypocotyl length of plants grown in MS (mock) and the hypocotyl length of plants grown in $AgNO_3$ was calculated. The hypocotyl growth difference was higher in MIDA9-GFP-OX compared to Col-0 (Fig 2.6B lower panel). Together, these results suggest that the short hypocotyl phenotype of MIDA9-GFP-OX lines is possibly caused by increased ethylene levels, and indicates that the activity of MIDA9 might impact ethylene biosynthesis.

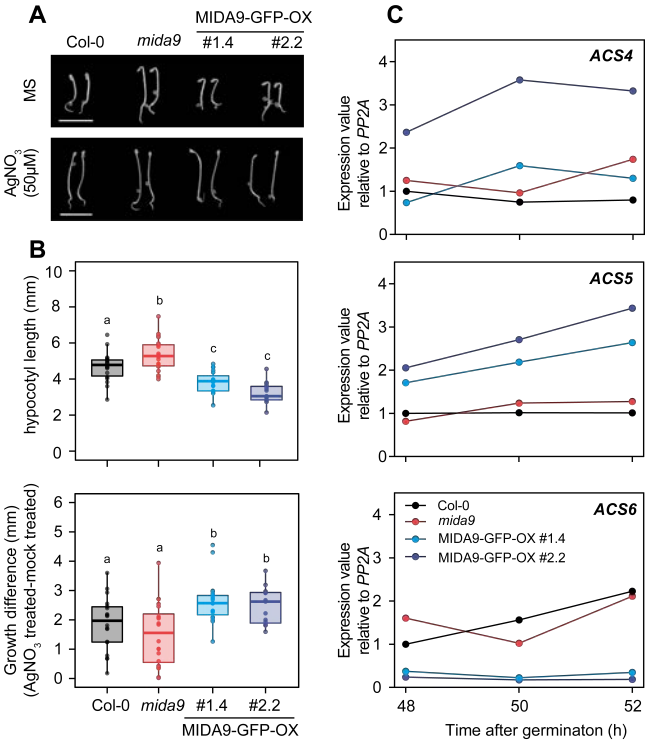

Figure 2.6. *MIDA9* participates in ethylene responses modulating *ACS* expression in dark-grown seedlings.
A. Visible phenotypes of 2-day-old dark-grown seedlings in MS or MS + $AgNO_3$ (50μM) of Col-0, *mida9*, MIDA9-GFP-OX #1.4 and #2.2. Bar = 5 mm **B**. Upper panel, hypocotyl length of 2-day-old dark-grown Col-0, *mida9*, MIDA9-GFP-OX #1.4 and #2.2. Lower panel, hypocotyl growth differences of $AgNO_3$ (50μM) treated compared to mock treated plants. In both panels, different letters denote statistical differences between means by ANOVA ($P<0.05$) followed by post-hoc Tukey-b test. **C.** qRT-PCR time course analysis of Col-0, *mida9*, MIDA9-GFP-OX #1.4 and #2.2. *ACS* expression levels were normalized to *PP2A* and expressed relative to the Col-0 at 48h after germination value set at unity. n=2 biological replicates and only one is represented.

At the molecular level, stimulation of ethylene production is achieved through upregulation of the transcript levels of enzymes involved in ethylene biosynthesis. Conversion of ACC by ACC synthase (ACS) is the first committed step in ethylene biosynthesis and is considered to be the rate-limiting step. *ACS* is encoded by a multigene family containing at least 8 functional members in *A. thaliana* (Yamagami *et al.*, 2003). *ACS6* is regulated by negative feedback when ethylene levels are increased in tomato fruit ripening (Chang *et al.*, 2007). We analysed the levels of *ACS4*, *5* and *6* at 48, 50 and 52 hours after germination in the dark, when the short hypocotyl phenotype is robust (Fig 2.6A). Compared to Col-0, we detected elevated levels of ACS5 in the MIDA9-GFP-OX lines (Fig 2.6C). In contrast, only MIDA9-GFP-OX #2.2 line show elevated ACS4 expression levels compared to Col-0. The fold-change increase was greater in the MIDA9-GFP-OX #2.2 compared to #1.4, in agreement to #2.2 having greater *MIDA9* levels compared to #1.4 (Fig 2.4B and 2.4C). In contrast, the ACS6 expression levels, which is under negative feedback regulation, were greatly reduced in MIDA9-GFP-OX lines compared to Col-0 and *mida9*. Together, these results suggest elevated levels of ethylene in MIDA9-GFP-OX, suggesting that MIDA9 levels might impact the regulation of ethylene biosynthesis.

DISCUSION

Although much progress has been achieved in the past years, the role of PIF-regulated genes during seedling deetiolation still remains incomplete. Here, we perform a detailed genetic and phenotypic characterization of the role of *MIDA9* (a previously described PIF3-regulated gene) in the regulation of the different phases of hook development (Sentandreu *et al.*, 2011). *MIDA9* encodes one of the nine members of type 2C-protein phosphatases belonging to clade D (PP2C.D) (Schweighofer *et al.*, 2004), and in this work, we define *MIDA9* as a prominent positive regulator of hook formation during skotomorphogenesis. In accordance with other studies, we defined that MIDA9 localizes in the nucleus and cytoplasm in the apical hook and hypocotyl cells. Finally, we described a potential connection between *MIDA9* and ethylene biosynthesis, which is described to be implicated in apical hook development.

MIDA9 is required for cell expansion in the outer part of the apical hook

Apical hook development is a complex process that takes place in three different phases: formation, maintenance and opening (Zadnikova, Petra *et al.*, 2010; Vandenbussche *et al.*, 2010). Therefore, it is important not just to focus at the final stage but to analyze all temporal stages of the whole dynamic process. Here, we defined that *MIDA9* is specially involved in the early stage of hook development: hook formation (Fig. 2.1). For this reason,

we decided to understand how *MIDA9* participates in this process at the cellular level. It is well-known that the hook is formed because of the bending of the hypocotyl, determined by an asymmetric growth that is the result of an inhibition of the cell expansion at the inner side of the hook coinciding with a local maxima of the auxin gradient. Importantly, our phenotypic analysis establishes that *MIDA9* induces cell elongation in the outer edge of the hook, with no effect observed in the inner side.

Previous studies demonstrated that plants expressing an artificial microRNA which partially knocks down the expression of five PP2C clade D family members (amiD2/5/7/8/9), exhibit increments in hypocotyl elongation in 8-day-old diurnal-grown seedlings (Spartz *et al.*, 2014). This study also showed a reduction in hypocotyl length on plants overexpressing *MIDA9* (referred to as *PP2C-D1*) due to a diminished cell expansion in hypocotyl epidermal cells, when compared to WT control seedlings grown under diurnal conditions. Recently, the same authors reported that the *pd1*/*at4g38520*/*at3g51370* (referred to as *pp2c-d2/d5/d6* in these publications) triple mutant exhibits a long hypocotyl phenotype and an increase in cell expansion compared to WT seedlings (Ren *et al.*, 2018). Considering these observations, the authors conclude that *MIDA9* as well as other clade C PP2C are negative regulators of hypocotyl cell expansion. In accordance, it had been described that MIDA9 interacts with a proton pump (AHA2) to regulate cell expansion in hypocotyls of diurnal-grown seedlings (Spartz *et al.*, 2014; Ren *et al.*, 2018), and that SAURs interact with MIDA9 proteins to inhibit its activity and repressing cell expansion. However, these results do not correlate with our observations that *mida9* showed less cell expansion in the outer edge of the apical hook compare to control plants. This inconsistency could be explained by the fact that we described the role of *MIDA9* in the apical hook in etiolated seedlings, whereas the previously mentioned studies characterized *MIDA9's* function within the hypocotyl in diurnal growth conditions. Therefore, it remains plausible that *MIDA9* plays different roles depending on the organ and diurnal conditions.

Since apical hook is a complex organ in which the balance between asymmetric cell elongation and cell division at the opposite sides of the apical portion of the hypocotyl, it is essential to promote normal hook formation. In this sense, apical hook might be highly sensitive to differential protein concentrations in the outer and inner edges, caused by a gene expression imbalance at either edge of the hook. The fact that *MIDA9* (*PP2C-D1*) is more strongly expressed in the inner side of the apical hook (Ren *et al.*, 2018), further reinforces this hypothesis. Therefore, it would not be surprising that *mida9* mutant seedlings could have an altered downstream function -such as target protein phosphorylation or hormonal balance- between the outer and inner edges of the apical hook, ultimately resulting in an unfolded hook due to less cell expansion in the outer side.

The role of PP2C.D family in the different stages of hook development

MIDA9 belongs to clade D of the type 2C-portein phosphatases (PP2C.D), whose function has been proposed to be redundant (Spartz *et al.*, 2014; Ren *et al.*, 2018). In fact, most of the living organisms showed gene redundancy between members of the same family. For example, redundancy has been previously demonstrated within the PP2C genes. This is the case of the *ABI1* and *ABI2* members of PP2C clade A, which showed redundant functions in ABA signaling (Leung *et al.*, 1997). Additionally, clade C contains the POL and PLL phosphatases which have been shown to act redundantly in promoting stem-cell identity (Song and Clark, 2005). Even proteins with different functions, such as transcription factors like PIFs, have also been described to have some redundancy. In this case, PIF1 plays a prominent role in promoting etiolated growth while PIF3, PIF4 and PIF5 act together with PIF1 in a partially redundant manner (Leivar and Monte, 2014).

Here, a temporal analysis of single, double and triple mutants of PP2C.D family, suggest that they participate in a hierarchical and complex manner during hook development. We defined that *MIDA9* has a predominant role in promoting hook formation and maintenance. However, *PD1* showed a negligible role during hook formation but equals to *MIDA9* during the maintenance phase. In contrast, *PD6* act at the aperture phase to prevent hook opening in combination with *MIDA9* and *PD1*.

Recently, it has been described that *MIDA9* (*PP2C.D1*) exhibits stronger expression and protein localization on the inner side of the apical hook, and it is present in both nuclei and the cytoplasm at the subcellular level (Ren *et al.*, 2018). Moreover, PD1 (PP2C.D2) and PD6 (PP2C.D5) are broadly expressed in etiolated seedlings and both proteins localize exclusively to the cell periphery of root cells, consistent with a plasma membrane localization (Schweighofer *et al.*, 2004; Ren *et al.*, 2018). The fact that these proteins display differential gene expression patterns in etiolated seedlings and that they show different protein localization at the subcellular level, further reinforce our results. Although the authors study apical hook development in etiolated *pd1*/*at4g38520*/*at3g51370* (*pp2c-d2/d5/d6*) triple mutant in the presence of sucrose, which is known to alter photomorphogenic responses, the mutant appeared to be affected in apical hook at a late stage of hook development (Ren *et al.*, 2018). Altogether, these evidences suggest that *MIDA9, PD1* and *PD6* could play distinct roles at each stage of the hook developmental process.

In this thesis, we define for the first time a temporal function as well as the genetic interaction between *PD1*, *PD6* and *MIDA9* during the different phases of hook development in etiolated seedlings.

A connection between MIDA9 and ethylene biosynthesis in etiolated seedlings

The first PP2C in plants was identified as a mutation that gave rise to an ABA-insensitive phenotype of the mutant *abi1* (ABA insensitive 1) (Meyer *et al.*, 1994). Moreover, the homologous of ABI1, ABI2 (ABA insensitive 2), was also found to mediate the full range of ABA responses (Rodriguez *et al.*, 1998). Both proteins are involved in the regulation of transpiration, vegetative growth and seed germination, and cluster together with seven other PP2Cs in clade A. These results were the first evidence that PP2C proteins are connected with phytohormones to mediate stress signaling responses. Furthermore, one member of clade F (*PIA1* - PP2C induced by AvrRpm1) also appeared to be involved in hormone-mediated responses, by regulating the accumulation of stress hormones such as ethylene and salicylic acid (Widjaja *et al.*, 2010).

Different studies demonstrated that ethylene is involved in the regulation of hook development. In fact, dark-grown seedlings treated with the ethylene biosynthesis precursor ACC, exhibit an exaggerated apical hook, which is one of the components of the classical triple response. It has been described that ethylene has a role during the formation and maintenance phase of hook development through the induction of auxin biosynthesis and regulating its transport and signaling in the apical hook (Raz and Koornneef, 2001; Mazzella, 2014).

Here, we defined that *MIDA9* regulates the expression of genes involved in ethylene biosynthesis (*ACS*) in etiolated seedlings, adding new evidence on the link between PP2C phosphatases and phytohormones. As it cannot be discarded that the affected *ACS* levels in MIDA9-GFP-OX could be caused by an alteration in the hormone regulatory feedback, further experiments should be performed to elucidate the connection between PP2C.D family and ethylene. For that reason, it would be necessary to analyze *ACS* expression and ethylene levels in all the PP2C.D single mutants lines.

SUPPLEMENTAL DATA

Table S2.1. Primers used to genotype new T-DNA mutant lines.

Mutant line	AGI	PCR Reaction	Forward	Reverse
pd1	At3g17090	WT	GGTGATGAAGATGGTGATTGG	TCATCAGAAACCCATTACTTGC
		T-DNA	TGGTTCACGTAGTGGGCCATC	TCATCAGAAACCCATTACTTGC
pd6	At4g38520	WT	GAGAAGTCACCAAAGACGTGC	ATTCTTTGCCACTGTTTGGTG
		T-DNA	TGGTTCACGTAGTGGGCCATC	ATTCTTTGCCACTGTTTGGTG

Table S2.2. Primers used for gene expression analyses.

Gene	AGI	References	Forward	Reverse
ACS4	At2g22810	Thain *et al.*, 2004	GTTTACGAAGTGAAGCTCAAC	GTCTCATCAATCATGTTCGCG
ACS5	At5g65800		GCGGCAAGTCTCAAGAGGA	TTCTGGGCTTGTTGGTAAGC
ACS6	At4g11280		GTTCCAACCCCTTATTATCC	CCGTAATCTTGAACCCATTA
PP2A	At1g13320		TATCGGATGACGATTCTTCGT	GCTTGGTCGACTATCGGAATG

chapter 3

Definition of an interplay between light and PIFs that determines stomata movements

INTRODUCTION

Upon reaching the soil surface, etiolated seedlings growing in the subterranean darkness are exposed to sunlight, which triggers the deetiolation response and a developmental transition from skotomorphogenesis to photomorphogenesis. Under diurnal photoperiodic conditions, where dark and light periods alternate, seedlings display rhythmic responses regulated by circadian clock and light, such as hypocotyl growth (Soy *et al.*, 2012, 2016), photosynthesis and stomata opening (Tallman, 2004).

These rhythmic responses are in part determined by phytochrome regulation of PIF levels. During the light period, activated phytochromes induce the degradation of PIFs, whereas during the night phase, the decreasing levels of Pfr due to dark reversion, allows PIF1, PIF3, PIF4 and PIF5 accumulation which peak at the end of the night. The regulation of hypocotyl growth and the PIFs accumulation depends on the number of dark hours within a diurnal cycle. In SD conditions, with extended night periods, seedlings grow more than in LD conditions (Niwa *et al.*, 2009).

Under diurnal cycles, seedlings exhibit rhythmic growth, with maximal elongation rate occurring at the end of the night, coinciding with maximum PIF accumulation (Niwa *et al.*, 2009; Soy *et al.*, 2012; Nozue *et al.*, 2007). The circadian clock also contributes to restrict PIFs activity towards the end of the night period (Niwa *et al.*, 2009). In our laboratory we demonstrated that Timing of CAB expression 1 (TOC1), an essential core component of the central oscillator, directly interacts and represses the activity of PIF3 during the first part of the night under SD. We proposed that this mechanism provides clock-imposed gating of PIF3-mediated growth patterns (Soy *et al.*, 2016).

In consequence, under diurnal conditions, the more the dark hours the higher amount of PIFs accumulate at the end of the night. In the case of PIF3, it has been described that PIF3 protein abundance stays low during the day and progressively accumulates during the dark hours to peak at the end of the night, coinciding with their physiological action in promoting hypocotyl elongation (Soy *et al.*, 2012). Accordingly, PIF3 levels drop below the detection limit after exposure of seedlings to continuous light (Nozue *et al.*, 2011; Soy *et al.*, 2012). In agreement, Col-0 plants grown under SD conditions for 2 days, and then transferred to constant white light (WL) at the end of the third day (ZT8) for 16 hours, showed undetectable levels of PIF3 at ZT24 compared to Col-0 seedlings grown under SD. In consequence, seedlings grown under SD conditions, with extended night periods, exhibit longer hypocotyl than those grown in continuous light (WL). Similar to PIF3, other PIFs such as PIF1, PIF4 and PIF5 also participate in the regulation of this growth responses. Superimposed on this regulation, a circadian output pathway involving the evening complex (LUX, ELF3 and ELF4) directly represses the gene expression of *PIF4*

and *PIF5* to gate their expression the end of the night (Nusinow *et al.*, 2012; Nakamichi *et al.*, 2012). Genetic analyses demonstrate that PIFq promote hypocotyl elongation at the end of the night, given that *pifq* mutant grown in SD are more similar to wild type (WT) seedlings grown in WL (Soy *et al.*, 2014).

We hypothesize that other rhythmic processes under diurnal conditions could be regulated by phytochromes and PIFs. It has been described that stomata are closed in darkness but open in response to light. Experiments performed in 5-week-old *V. faba* leaves showed rapid stomata opening at the onset of light and stomata closing during the night (Talbott and Zeiger, 1996). It is well described that phytohormones and blue light are required for a normal function of these stomata movements. In contrast, little is known about the role of red/far-red light, phytochromes and PIFs in regulating this process. Previous data have suggested a function of phytochromes and PIFs in regulating stomata opening under non diurnal conditions (Wang *et al.*, 2010). Altogether, we decided to investigate whether stomata movement is rhythmic and regulated by the number of dark and light hours, and whether PIFs have a role in the regulation of stomata movement under SD conditions.

Stoma consists of two specialized epidermal guard cells and serves as a major gateway both for CO_2/O_2 influx from the air and transpiration water loss of plants, which is necessary for optimal photosynthesis (Pillitteri and Dong, 2013).

Stomata are formed by specialized epidermal linage, which go through an organized series of cell divisions. In cotyledons, a subset of protodermal cells becomes meristemoid mother cells (MMC). Through an asymmetric cell division, an MMC produce small cell called meristemoid (M) and a larger cell called a stomatal-lineage ground cell (SLGC). Finally, the M differentiates into a guard mother cell (GMC). The GMC then gives rise to two guard cells that form the stomata (Pillitteri and Dong, 2013). M cells are generated during the first 2 days of seedling development. During skotomorphogenesis, stomata development is arrested by COP1-SPA complex (Lee *et al.*, 2017). CRYs, phyA and phyB complete guard cell differentiation, with phyB having a dominant role in white light during photomorphogenesis. During this stage, COP1 is degraded and PIF4 has a major role in regulating stomatal development in responses to changes in light quantity. Recently, it has been demonstrated that in high temperature, PIF4 directly inhibit SPEECHLESS (*SPCH*), bHLH transcription factor that serves as the master regulator of stomatal lineage initiation (Lee *et al.*, 2017; Casson *et al.*, 2009; On Sun Lau *et al.*, 2018).

Mature stomata can integrate internal and environmental signals such as humidity, CO2, calcium, phytohormones, pathogens and light to modulate the guard cell turgor, necessary to regulate stomata opening or closure. The action of ion channels,

transporters and pumps are essential for normal stomata function. During the opening of the stomata, the H⁺-ATPase pump mediates efflux of H⁺ from the guard cells, which hyperpolarizes the plasma membrane and leads to cation uptake via activation of cation channels (Araújo *et al.*, 2014).This results in water transported inside the guard cells via aquaporins which generate the turgor necessary to keep stomata open. During the stomata closure, H⁺-ATPase is inhibited and anion channels are activated, which result in membrane depolarization, creating an efflux of cations outside of the guard cell. This leads to a reduced turgor and stomata closure (Fig 3.1).

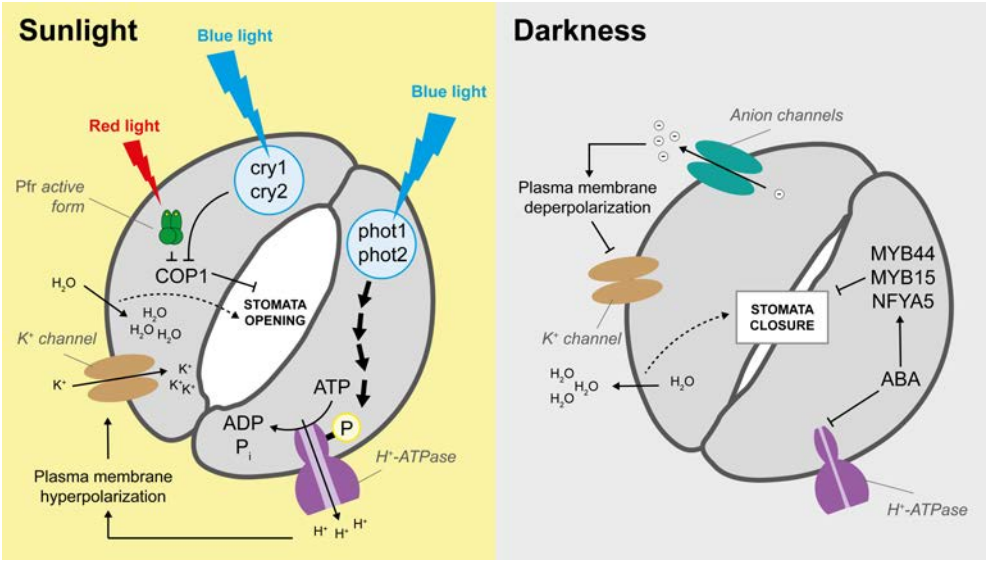

Figure 3.1 Simplified overview of stomata movements during light and dark phase under diurnal conditions. Arrows indicate positive regulation, blunt arrows indicate negative regulation, dotted arrows indicate the effect of accumulation or expulsion of water within or outside of guard cells in either case. Anions are represented as circles with a negative sign.

One of the most important internal signals regulating stomata movements are phytohormones. Among these, abscisic acid (ABA), is the best-known stress hormone with a role in stomata movement. It has been hypothesized that during the dark phase of the day, intensive ABA accumulation induce stomata closure (Daszkowska-Golec and Szarejko, 2013). This accumulation of ABA is the result of an induction of ABA biosynthetic genes (Charron *et al.*, 2009), the import of endogenous ABA from the apoplast to the guard cell, and a reduction of ABA catabolic genes. In this situation, high endogenous ABA levels inhibit the H⁺-ATPase to induce stomata closure. Furthermore, elevated endogenous ABA regulate the expression of transcription factors involved in stomata

closure such as *R2R3MYB (MYB44 and MYB15)* (Jung *et al.*, 2008; Ding *et al.*, 2009) and *NF-YA (NFYA5)* family (Li *et al.*, 2008) (Fig 3.1).

Upon light exposure, a depletion of ABA biosynthesis genes is observed (Charron *et al.*, 2009), triggered by the isomerization of ABA precursors and the activation of ABA catabolism enzymes such as cytochrome 450 (CYP450) (Charron *et al.*, 2009). This ABA depletion causes stomata opening during the light phase of the day.

Light is one of the most variable and essential environmental parameter regulating stomata movement. Stomata are closed in darkness but open in response to blue light and, less efficiently, in red light. It has been published that cryptochromes (CRY) and phototropins (PHOT), a family of UV-A/blue-light-absorbing photoreceptors, participate in mediating blue light-induced stomata opening. CRYs and PHOTs activate the plasma membrane H^+-ATPase (Kinoshita and Shimazaki, 1999), which hyperpolarizes the plasma membrane and opens the stomata (Sharkey and Raschke, 1981). CRYs and PHOT also regulate stomata movements through COP1 (Mao *et al.*, 2005), a repressor of photomorphogenesis. CRYs interact with COP1 by protein-protein interaction (Sang *et al.*, 2005). The stomata pore in *Arabidopsis cop1* mutant, deficient in COP1 protein, is constitutively open in the dark (Mao *et al.*, 2005; Wang *et al.*, 2010). It was proposed that COP1 could act downstream of phyB in regulating this process (Wang *et al.*, 2010) (Fig 3.1).

It has been described that red light, through the photosynthesis in mesophyll and guard cell, induce stomata opening (Assmann and Shimazaki, 1999). More recently, it was proposed that phyB might regulate stomata opening in part by regulating *MYB60* expression (Wang *et al.*, 2010), a transcription factor involved in stomatal opening (Cominelli *et al.*, 2005). In spite of these facts, little is known about the mechanism underlying the regulation of stomata movements by phytochromes and red light. Further experiments are needed to define new components downstream of phytochromes that could regulate stomata movements.

The main goal of this chapter is to study the role of PIFs in regulating stomata movements under diurnal conditions in Arabidopsis. This goal is addressed in two specific aims: (i) To characterize whether stomata movement is rhythmic and the implications of light/dark cycles during early Arabidopsis seedling deetiolation in SD conditions. (ii) To study the involvement of PIFs in regulating these stomata movements in cotyledons.

EXPERIMENTAL PROCEDURES

Seedling growth and measurements

A. thaliana seeds used in this chapter include the previously described *aba2/gin1-3*

(*aba2*) (Cheng *et al.*, 2002), *pif1-1pif3-3* (*pif1pif3*)(Leivar *et al.*, 2008b), *pif3-3* (*pif3*) (Monte *et al.*, 2004), *pif4-2* (*pif4*) (Leivar *et al.*, 2008a), *pif5-3* (*pif5*) (Khanna *et al.*, 2007) and *pif1-1pif3-3pif4-2pif5-3* (*pifq*) (Leivar *et al.*, 2009) mutants, pPIF3::YFP:PIF3 (YFP-PIF3) (Al-Sady *et al.*, 2006).

Seeds were sterilized and plated on Murashige and Skoog medium (MS) without sucrose as previously described (Monte *et al.,* 2003). Seedlings were stratified for 4 days at 4 ºC in darkness, and then placed in SD conditions [8 h white light (85 µmol m-2 s1-) + 16 h dark] for 3 days at 21 ºC. For photobiology experiments, during the third day at ZT8, seedlings were either kept in SD conditions, transferred to continuous white light conditions (WL) or exposed to continuous dark conditions (Dark).

Hypocotyl and stomata measurements

Hypocotyls were measured as described in chapter 2. For stomata aperture measurements, 4-day-old dark-grown cotyledons were wet mounted with water on a microscope slide with a cover glass, and pictures were taken with and optical microscope (AixoPhot DP70) at 60X magnification. Stomata pore area was measured using NIH image software (Image J, National Institutes of Health).

ABA by LC-ESI-MS

ABA levels were determined in Gianfranco laboratory at 3-day-old SD-grown seedling. Next, plants were freeze-dried at different time points. 100 mg of powder were extracted (3 biological replicates) for 1h at 50°C using 0.5 mL of unbuffered 50 mM Tris and samples were then spiked with 50 ng of (±)-2-cis,4-trans-ABA-d6 (Icon Isotopes), used as internal standard. After centrifugation (5,000g, 10 min), the supernatant was transferred into new tubes, acidified with 3N HCl and partitioned three times with ethyl acetate. Combined epiphases were then dried and re-dissolved in 100 µl Acetonitrile: H_20 (15:85) with 12mM acetic acid (pH 3.3); 10 µl were injected. Separation was carried out using an Ultimate 3000 HPLC coupled to a Q-EXACTIVE mass spectrometer (ThermoFisher) equipped with a C18 Luna reverse-phase column (Phenomenex, Macclesfield, UK) and a gradient system as previously described for the semi-polar metabolome analysis. The Exactive Plus Orbitrap mass spectrometer was equipped with a heated electrospray probe (H-ESI). ESI and MS parameters were as follows: spray voltage –5.0 kV, sheath gas and auxiliary nitrogen pressures 30 and 10 arbitrary units, respectively; capillary and heater temperatures were set at, respectively 250 and 150 ºC, while tube lens voltage was 50 V. Data were acquired in profile mode. ABA levels were expressed as fold internal standard levels, and normalized on the sample dry weight.

Fluorescence microscopy

Stomata of 3-day-old SD-grown at ZT23 and same stomata maintained in white light 1h (4-day-old ZT1) after dawn of PIF3-YFP transgenic line were visualized using a confocal laser scanning microscope Olympus FV1000 (Emission window: 500nm - 660nm). *pif3* was used as a negative control. Nuclei were stained using DAPI.

Statistical analysis

Levene's test was performed to verify equal variances ($P<0.05$). When the variances were equal Student *t*-test ($P<0.05$) or ANOVA test ($P<0.05$) followed by a post-hoc Tukey-b test was performed. If needed, data were ln transformed. For not equal variances, Kruskal-Wallis test ($P<0.05$) followed by a post-hoc Dunn test was performed. All analyses were conducted in R.

RESULTS

Stomata movement oscillates during early Arabidopsis deetiolation under SD conditions

The stomata pore area in Col-0 cotyledons was measured over 24 hours during the fourth day of seedling growth under SD conditions (Fig 3.2A). At the beginning of the light period, stomata were closed in Col-0 seedlings. Between 0 - 3 hours after the beginning of the day, stomata started to open, reaching the maximum aperture at 3 hours after dawn

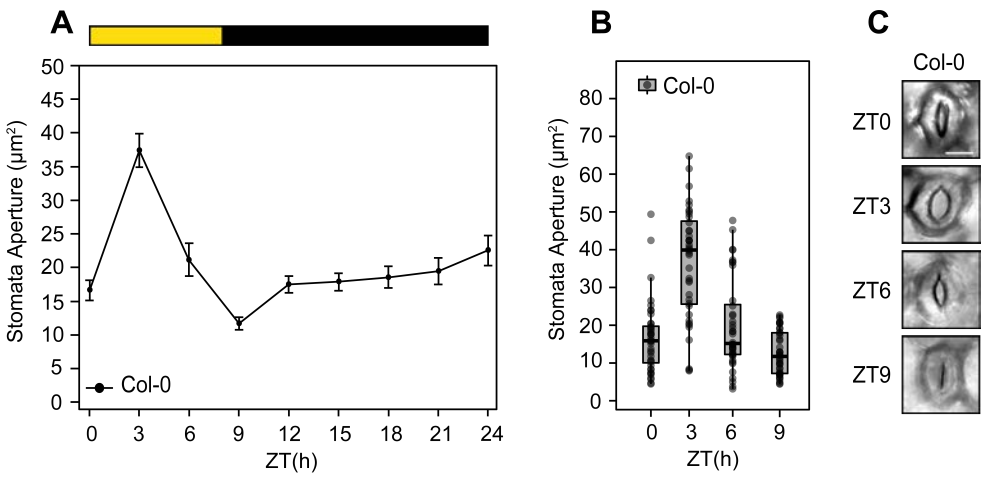

Figure 3.2. Stomata movements oscillate during early Arabidopsis deetiolation under SD conditions.
A. Time course analysis of stomata aperture in Col-0 cotyledons over 24 hours during the fourth day of seedlings grown under SD conditions. Lines represent mean values +/- SE. n=40. **B.** Same data from panel A are represented over 9 hours after dawn. Dots represent each measurement. C. Visible phenotypes of panel B are shown. Bar = 10 µm.

(Fig 3.2A, Fig 3.2B and Fig 3.2C). At the end of the light period in SD (6-h time point), stomata started to close, resulting in the maximum closing 1 hour after the transition from light to dark at Zeitgeber time (ZT) ZT9 (Fig 3.2A, Fig 3.2B and Fig 3.2C). Finally, stomata remained closed during the dark phase (Fig 3.2A). Together, these results suggest that the dark-to-light transition induces stomata aperture, whereas prolonged light during the day promote stomata closure that remains closed during the night period. These data extend previous observations that describe stomata movements oscillations under photoperiodic growth conditions in older seedlings (Wang *et al.*, 2010).

The night period under SD is required to induce stomata opening at dawn

To better understand how diurnal light/dark cycles regulate stomata movements, Col-0 seedlings were first grown under SD conditions for 2 days, and then transferred to constant white light (Col-0 WL) at the end of the third day (8 hour time point, ZT8) for 16 hours. Controls were kept under SD conditions (Col-0 SD) (Fig 3.3A). Next, stomata pore area was monitored during the fourth day every 3 hours over a period of 9 hours. At the beginning of the day (ZT0), no difference in stomata aperture was observed between

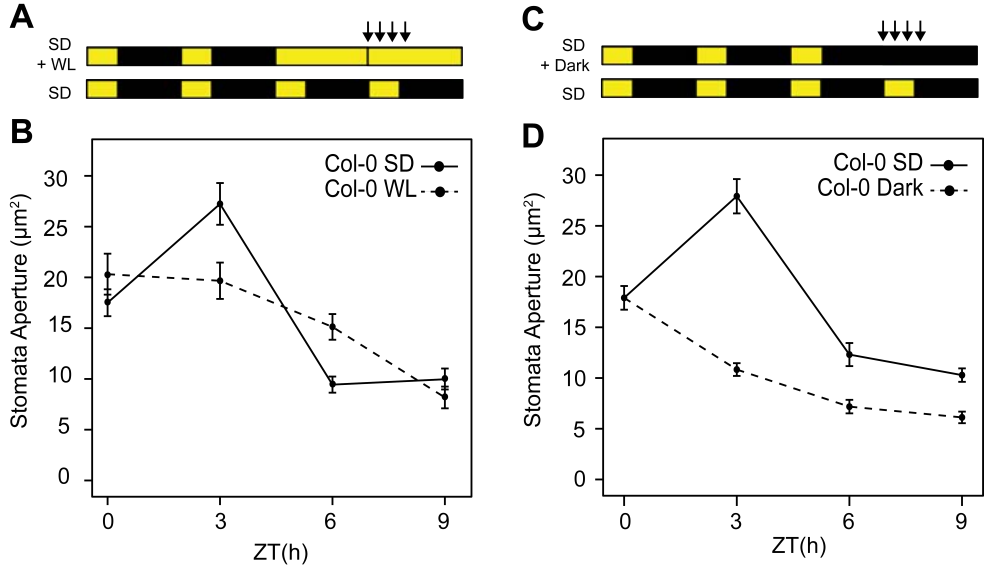

Figure 3.3. Dark and light signals are required to induce stomata opening at the beginning of the day.
A. Schematic diagram of growth regime used in B. Seedlings were grown under SD conditions for 2 days, then at ZT8 of the third day they were either kept under SD as a control (SD) or they were transferred to continuous light (WL). Stomata measurements were performed during the fourth day at ZT0, 3, 6 and 9 (indicated by arrows). **B.** Stomata aperture measurements of Col-0 grown in SD or WL as described in A. Lines represent mean values +/- SE. n=40. **C**. Schematic diagram of growth regime used for D. Seedlings were grown under SD conditions for 3 days, and then during the fourth day they were either kept under SD as a control (SD) or were transferred to continuous dark (Dark). Arrows indicate the timepoints when stomata aperture was measured. **D.** Stomata aperture measurements at ZT0, 3, 6 and 9 h of Col-0 SD grown in SD or in Dark as described in C. Lines represent mean values +/- SE. n=40.

Col-0 SD and Col-0 WL (Fig 3.3B). However, in striking contrast to Col-0 SD, Col-0 WL seedlings were not able to open the stomata after dawn (ZT3). Stomata closure in Col-0 SD during ZT3-ZT9 also took place in Col-0 WL, resulting in similarly closed stomata at ZT9 (Fig 3.3B). Together, these results demonstrate that the night period is required for stomata opening at dawn, but not for complete closure at the end of the day.

PIFs are necessary to induce stomata aperture at dawn

The results above prompted us to hypothesize that the PIFs, which accumulate during the dark in SD conditions (Soy *et al.*, 2012), might be involved in stomata regulation. To test this, we measured stomata pore in *pifq* mutants over 24 hours in 4-day-old seedlings (Fig 3.4A). At the beginning of the light period (ZT0), no differences in stomata aperture was shown in Col 0 compared to *pifq*. 3 hours after dawn, compared to Col 0, *pifq* was not able to fully open the stomata. Before the light-to-dark transition (ZT6), Col 0 started to close the stomata, reaching the same aperture than *pifq*, showing no differences in stomata aperture between them at ZT6 (Fig 3.4A, Fig 3.4B and Fig 3.4C). Compare to Col

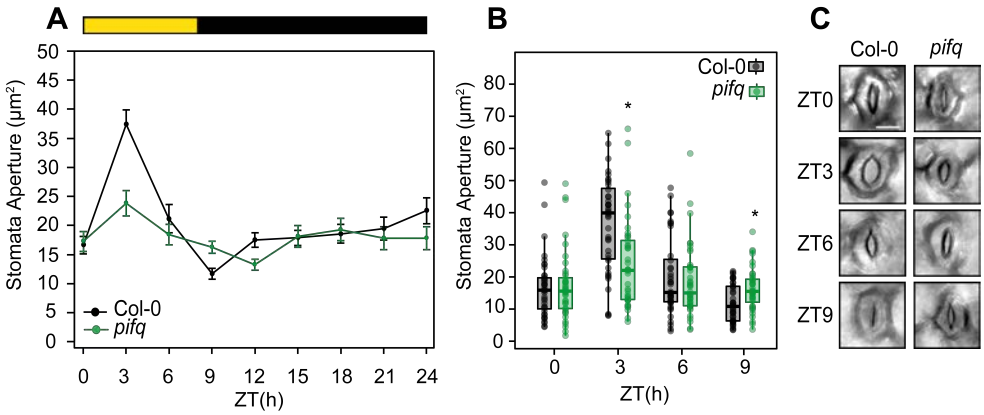

Figure 3.4. *PIFs* are required to induce stomata aperture at dawn.
A. Time course analysis of stomata aperture in Col-0 and *pifq* cotyledons over 24 hours during the fourth day of seedlings grown under SD conditions. Lines represent mean values +/- SE. n=40. **B.** Detail of ZT0 to ZT9 data from panel A. Dots represent each measurement. Statistical differences relative to Col-0 for each time point are indicated by an asterisk (Student *t*-test. $P<0.05$). **C.** Visible phenotypes of panel B data are shown. Bar = 10 µm.

0, *pifq* displayed same stomata aperture during the dark phase of the day (ZT12 - ZT21). Under SD+WL conditions, where PIF3 and likely other PIFs do not accumulate (Soy *et al.*, 2014), *pifq* SD/WL was also not able to open the stomata in the morning (Fig 3.5B). These results let us to conclude that PIFs accumulated during the dark/night period are required to induce stomata opening in the subsequent light/day phase under SD.

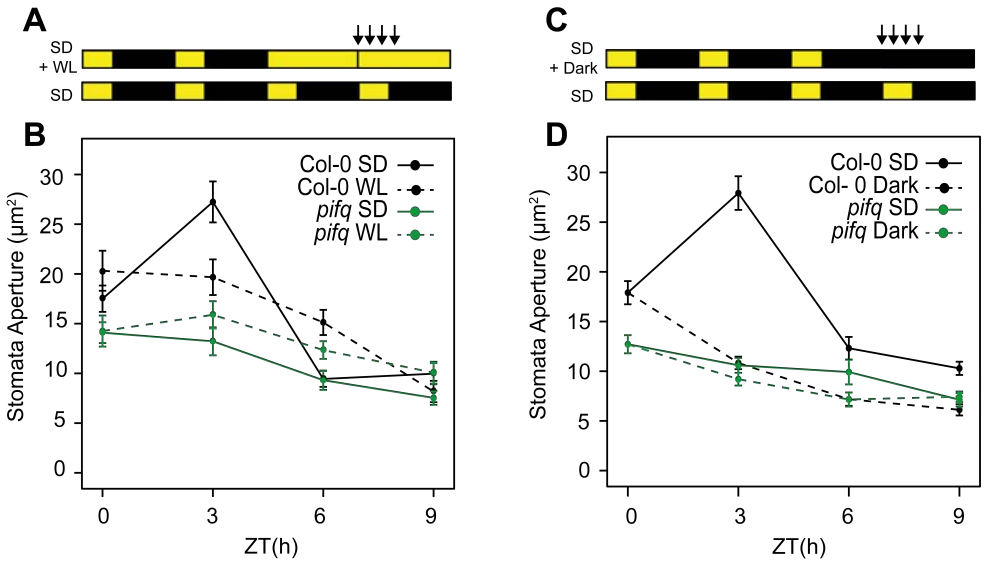

Figure 3.5. *PIFs* mediate the light and dark responses that determine stomata opening at the beginning of the day.
A. Schematic diagram of growth regime used in B. Seedlings were grown under SD conditions for 2 days, then at ZT8 of the third day they were either kept under SD as a control (SD) or they were transferred to continuous light (WL). Stomata measurements were performed during the fourth day at ZT0, 3, 6 and 9 (indicated by arrows). **B.** Stomata aperture measurements of Col-0 and *pifq* grown in SD or WL as described in A. Lines represent mean values +/- SE. n=40. **C.** Schematic diagram of growth regime used for D. Seedlings were grown under SD conditions for 3 days, and then during the fourth day they were either kept under SD as a control (SD) or were transferred to continuous dark (Dark). Arrows indicate the timepoints when stomata aperture was measured. **D.** Stomata aperture measurements at ZT0, 3, 6 and 9 h of Col-0 and *pifq* SD grown in SD or in Dark as described in C. Lines represent mean values +/- SE. n=40.

PIF3 localizes in the guard cells nucleus at the end of the dark phase under SD and is degraded by light at dawn

Our previous analysis suggested that PIFs accumulate at the end of the night and this is required for the subsequent stomata aperture at dawn. In order to test this hypothesis, we studied PIF3 accumulation in the nucleus of guard cells at the end of the night and upon 1h illumination. Visualization of 3-day-old SD-grown pPIF3::YFP:PIF3 (YFP-PIF3) at ZT23 by confocal microscopy, confirmed accumulation of PIF3 in the nucleus of guard cells at the end of the night (Fig 3.6A). Notably, YFP fluorescence in the nucleus of guard cells was absent after 1 hour of white light treatment (4dSD ZT1), demonstrating that PIF3, and presumably other PIFq members, are degraded by light in guard cells (Fig 3.6B). These data demonstrate that PIF3 protein is expressed in the nucleus of guard cells at the end of the dark period under SD and is light-degraded at dawn.

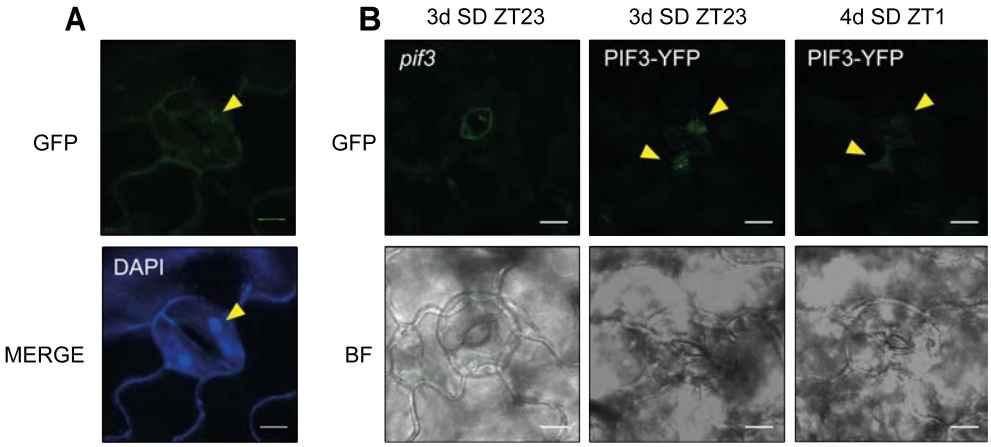

Figure 3.6. PIF3 localizes in the nucleus of guard cells at the end of the night and is rapidly degraded by light. **A.** PIF3-YFP localization in guard cells at 3-day-old SD-grown (ZT23). DAPI for nucleic acid staining was used. **B.** PIF3-YFP localization in guard cells at 3-day-old SD-grown (ZT23) and 4-day-old SD-grown (ZT1) after 1 hour of white light. Images correspond to the same stoma. *pif3* was used as a control. Bar = 10 µm. Bright field (BF) is shown.

PIF3, PIF4 and PIF5 contribute to induce stomata aperture in the morning under SD

Considering the previous results suggesting that PIFq members are required at the end of the night to induce stomata opening at dawn, we next decided to define the individual contribution of PIF1, PIF3, PIF4 and PIF5 in regulating stomata movements under SD. To this aim, stomata aperture was measured in Col-0, *pif13, pif3*, *pif4*, *pif5* and *pifq* over 9 hours after dawn at 4-day-old seedlings (Fig 3.7A). At the beginning of the day (ZT0), no statistically significant differences in stomata aperture were shown between all the genotypes. Upon light exposure, no differences in stomata aperture at ZT3 relative to ZT0 were observed in *pif13*, *pif3*, *pif4*, *pif5* and *pifq*. In contrast, Col-0 showed statistically significant difference in stomata aperture relative to ZT0 (Fig 3.7B). In addition, between ZT3 and ZT6, stomata closure was observed in all genotypes (Col-0, *pif13*, *pif3*, *pif4*, *pif5* and *pifq*), which resulted in same stomata aperture between them at ZT6. Altogether, our results suggest that PIF3, PIF4 and PIF5 contribute to regulate stomata opening in the morning under SD. Further analysis is required to determine whether PIF1 also participates in this process.

Role of endogenous ABA in stomata movements under SD

It has been published that under stress conditions, ABA biosynthesis is induced and results in accumulation of ABA levels which promote stomata closure. In accordance, exogenous application of ABA also increases stomata closure (Araújo *et al.*, 2014). Given that *pifq* mutant is not able to fully open the stomata at the beginning of the light period

under SD, we wondered whether existed a connection between PIFs and ABA pathway to modulate stomata movements.

To understand how endogenous ABA affects stomata movements under SD, we measured stomata pore in a previously described ABA deficient synthesis mutant (*aba2*) (Cheng *et al.*, 2002), which does not synthesize ABA (Fig 3.8A). At dawn, compared to Col-0 and *pifq*, *aba2* showed fully open stomata. Upon light exposure at ZT3, stomata remained completely open in *aba2* and no differences were shown compared to Col-0. These data suggest that endogenous ABA is required to keep the stomata closed at night, and a reduction in bioactive ABA levels is required to open the stomata in response to light. In addition, between ZT3 and ZT6, stomata closure was observed in the three genotypes (Col-0, *pifq* and *aba2*) which resulted in similar stomata aperture between them at ZT6, and suggesting that this effect does not requires ABA biosynthesis.

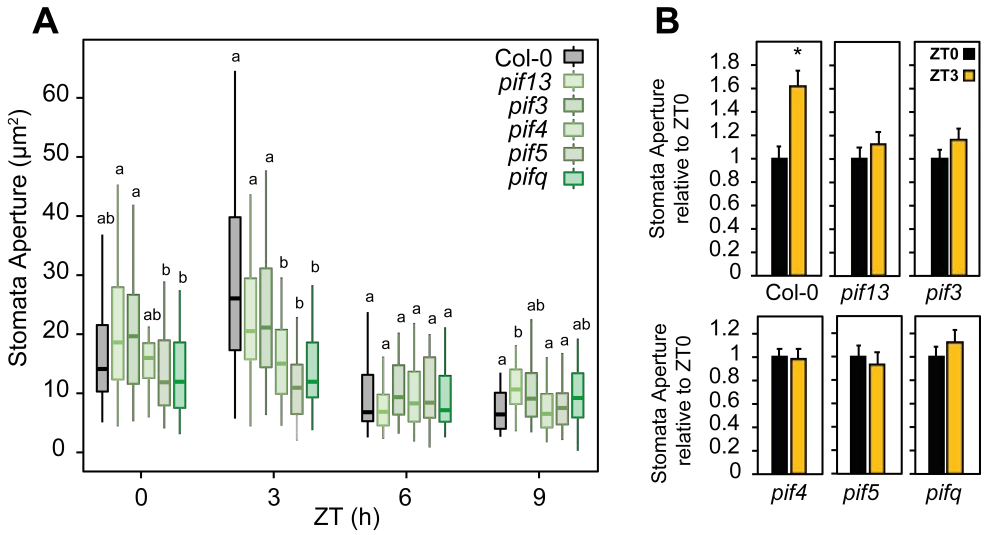

Figure 3.7 *PIF3*, *PIF4* and *PIF5* regulate stomata aperture at the beginning of the day in SD-grown seedlings. **A.** Stomata aperture of Col 0, *pif13*, *pif3*, *pif4*, *pif5* and *pifq* at ZT0, 3, 6 and 9 h in 4-day-old SD-grown seedlings. Different letters denote statistical differences between means by Kruskal-Wallis test ($P<0.05$) followed by a post-hoc Dunn test. n=40. **B.** Same data from A. represented by stomata aperture at ZT3 relative to ZT0 for each genotype. The data present the mean +/- SE. Statistical differences relative to ZT0 for each genotype are indicated by an asterisk (Student *t*-test, $P<0.05$).

However, whereas stomata continued to close in Col-0 and *pifq* at the beginning of the night at ZT9 and remained closed during the rest of the night, *aba2* did not completely close the stomata at ZT9 and progressively opened until completion at the end of the night (Fig 3.8A, Fig 3.8B and Fig 3.8C). Together, these results suggest that endogenous ABA is necessary to maintain stomata closed during the night/dark hours of the day, and

that ABA degradation or inactivation may permit stomata opening in response to light. Furthermore, we concluded that stomata closure at the end of the light period (ZT3 to ZT9) is partially independent of the endogenous ABA.

A light-induced reduction in bioactive endogenous ABA has been suggested as a mechanism to induce stomata opening. Moreover, it was described that dark periods

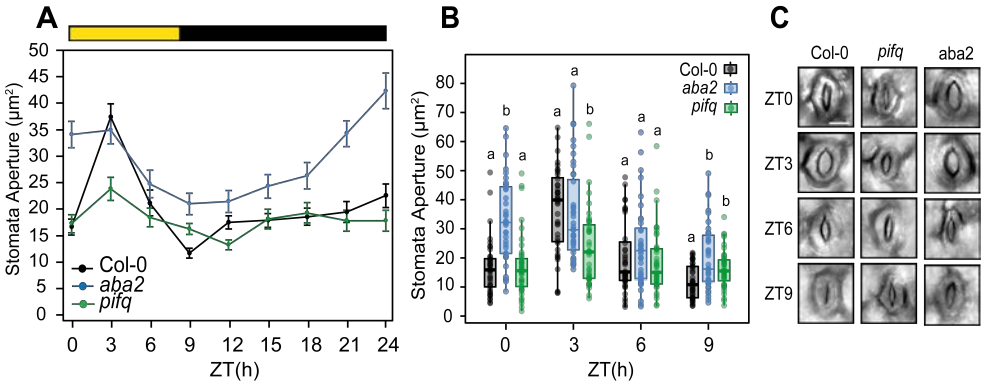

Figure 3.8. Endogenous ABA is necessary to maintain the stomata closed during the night period under SD. **A.** Time course analysis of stomata aperture in Col 0, *aba2* and *pifq* seedlings during the fourth day of growth under SD conditions. Lines represent mean values +/- SE. n=40. **B.** Detail of ZT0 to ZT9 data from panel A is represented. Dots represent each measurement. Different letters denote statistical differences between means for each time point by ANOVA test ($P<0.05$) followed by post-hoc Tukey-b test. If needed, data was ln transformed. **C.** Visible phenotypes of panel B data are shown. Bar = 10 µm.

are necessary to accumulate endogenous ABA (Weatherwax *et al.*, 1996; Arve *et al.*, 2013). Two different mechanisms resulting in ABA inactivation have been described: (i) hydroxylation of ABA at the 8′ position by P-450 type monoxygenases to give an unstable intermediate (8′-OH-ABA) that is isomerized to phaseic acid (PA), and (ii) esterification of ABA to ABA-glucose ester (ABA-GE) (Finkelstein, 2013). Some evidence indicates that light might induce ABA catabolism (Sawada *et al.*, 2008; Nambara *et al.*, 2010). We therefore hypothesized that ABA accumulates during the night to maintain the stomata closed, and upon illumination levels of active ABA decrease to allow for stomata opening. To test this idea, we submitted the Col-0, *pifq* and *aba2* seedlings to a SD + DARK regime: seedlings were first grown for 3 days in SD conditions and then transferred to dark before dawn. Controls were kept under SD conditions (SD) (Fig 3.6C and 3.9C). In this scheme, we expected WT seedlings to remain closed, as active ABA levels would still be high in the absence of inactivation by light. Indeed, we observed that this was the case not only in Col-0 but also in *pifq* (Fig 3.6D), whereas *aba2* mutants remained opened during the morning (Fig 3.9D). These results indicate that light-induced inactivation of endogenous ABA is necessary to allow for stomata opening in the morning.

Together, our results are consistent with a scenario where ABA prevents stomata

opening during the night, whereas stomata opening in the morning requires two distinct processes to occur: (1) accumulation of PIFs during the night, and (2) light-induced inactivation of ABA.

Our data also provide evidence suggesting that stomata closure at the end of the light period is partially independent of ABA levels (Fig 3.8), as this closure is observed in *aba2* biosynthetic mutant. A similar response is observed when the seedlings are released in constant darkness (Fig 3.9A and Fig 3.9B). In order to get more insight into the nature

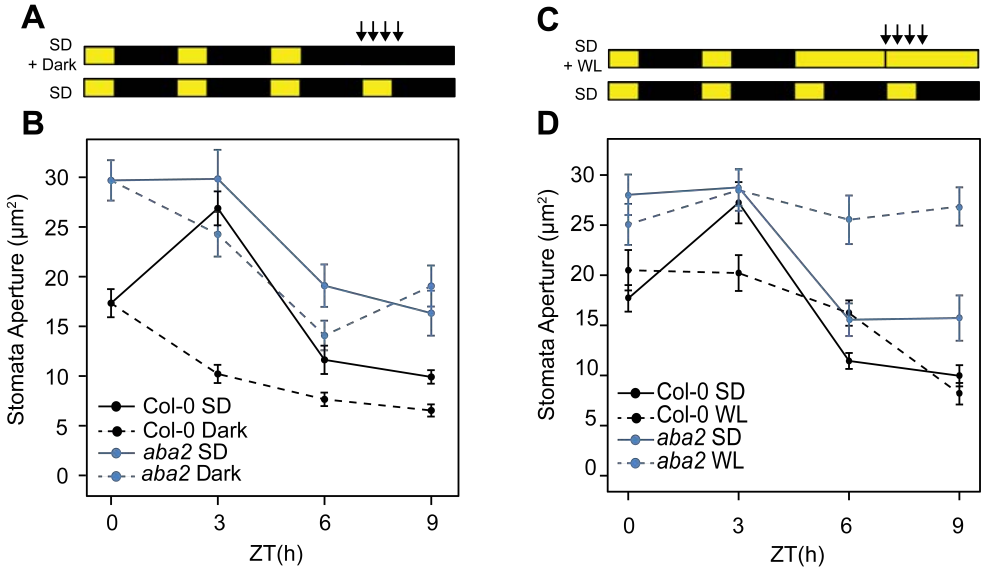

Figure 3.9. Stomata closure at the end of the light phase under SD is partially independent of ABA.
A. Schematic diagram of growth regime used for B. Seedlings were grown under SD conditions for 3 days, and then during the fourth day they were either kept under SD as a control (SD) or were transferred to continuous dark (Dark). Arrows indicate the timepoints when stomata aperture was measured. **B.** Stomata aperture measurements at ZT0, 3, 6 and 9 h of Col-0 and *aba2* SD grown in SD or in Dark as described in A. Lines represent mean values +/- SE. n=40. **C.** Schematic diagram of growth regime used in D. Seedlings were grown under SD conditions for 2 days, then at ZT8 of the third day they were either kept under SD as a control (SD) or they were transferred to continuous light (WL). Stomata measurements were performed during the fourth day at ZT0, 3, 6 and 9 (indicated by arrows). **D.** Stomata aperture measurements of Col-0 and *aba2* grown in SD or WL as described in C. Lines represent mean values +/- SE. n=40.

of this ABA-independent signal, Col-0 and *aba2* seedlings were first grown under SD conditions (SD) for 2 days, and then transferred to constant white light (WL) at the end of the third day (8 hour time point, ZT8) for 16 hours (Fig. 3.9C). Controls were kept under SD conditions (Fig 3.9C). Strikingly, whereas *aba2* mutants in SD partially closed the stomata between ZT3-ZT9 (Fig 3.8 and Fig 3.9D), they showed no response in WL. These data suggest that the ABA-independent signal partially promoting stomata closure at the end of the day is generated during the dark/night period of the previous day.

DISCUSION

Light regulation of stomata aperture contributes to the control of stomata rhythmic movement under diurnal conditions. The regulatory pathway has also been studied extensively at the molecular level, identifying the blue light photoreceptors cry1/2 and phot1/2 as important components of this regulation (Mao *et al.*, 2005). In contrast, phyB-mediated red light regulation of stomatal opening remains largely unclear. In this work, we studied the role of phytochrome interacting factors (PIFs) in the regulation of stomata aperture under diurnal conditions because: I) the molecular mechanism downstream of phyB to control stomata aperture was ill-defined, and II) PIF3, PIF4 and PIF5 have been identified as promoters of rhythmic growth under diurnal conditions (Soy *et al.*, 2012), suggesting that they could also be involved in the regulation of other rhythmic processes. Here, we set up an experimental system to study stomata movements under diurnal conditions in young seedlings and we observed that stomata is closed during the night and it is transiently open at dawn. Moreover, light is required to induce stomata aperture, as seedlings kept in darkness are not able to open the stomata. Strikingly, the light-induced stomata opening requires a period of darkness during the previous night, a process that requires the PIFq members. Finally, the stomata aperture by light is temporary and as of ZT3 stomata progressively started to close. We observed that this closure at the end of the light period is partially independent of ABA. Based on our data we propose that this closure at the end of the day is generated during the dark/night period of the previous day. The mechanism by which PIFs regulate this processes remains unclear and our studies side light to this question.

Stomata aperture at dawn: The interplay between light and endogenous ABA

Our results suggest that PIFs accumulation at the end of the night is necessary to induce stomata aperture in the subsequent light/day phase under SD. In accordance, *pifq* is not able to fully open the stomata during the light period. Moreover, stomata measurements performed in a previously described *aba2* mutant (Cheng *et al.*, 2002) led us to concluded that (i)endogenous ABA is necessary to maintain stomata closed during the dark phase of the day, and (ii) ABA degradation or inactivation may permit stomata opening in response to light. Taken our results together we hypothesizes that, PIFs accumulation during the night, and light-induced inactivation or/and degradation of ABA, are necessary to promote stomata opening for the subsequent day. In agreement, it has been described that the reduction of bioactive endogenous ABA is induced by light (Fig 3.10). Furthermore, dark periods are essential to accumulates endogenous ABA through the conversion of ABA-GE inactive form to ABA bioactive form (Weatherwax *et al.*, 1996; Arve *et al.*, 2013), reinforcing our hypothesis.

Additionally, we observed that stomata closure at the end of the light period is partially independent of ABA levels, suggesting that a ABA-independent signal might contribute to promote closure stomata at the end of the day. We conclude that light/dark periods are essential to accumulate this signal at the end of the night, necessary to induce stomata closure at the end of the subsequent day. However, further experiments are required to better understand stomata movement regulation mediated by interaction between light and ABA.

Since *pifq* mutant is not able to open the stomata at during the day, endogenous inactive or/and bioactive ABA levels are necessary to be analysed in Col-0 and *pifq* mutant seedlings. Here, preliminary results performed in Gianfranco laboratory suggest no difference in bioactive endogenous ABA levels in *pifq* compare to Col-0 at ZT3 in 4-day-old SD-grown seedlings. Moreover, *aba2* was used as a control. As expected, reduced levels of ABA was detected in *aba2* compare to Col-0 and *pifq* (Fig. S3.1). As our ABA levels measurements were taken from whole seedlings, we cannot discard the possibility that *pifq* has higher endogenous ABA levels compared to Col-0 specifically in guard cells. In addition, it has been described that ABA is synthesized in vascular tissue but, under stress conditions, ABA can be also synthesized in guard cells (Bauer *et al.*, 2013). Therefore, it would be interesting to measure endogenous ABA levels in Col-0 and *pifq* mutants specifically in protoplast guard cells in the future.

Stomata movements mechanism: the role of PIFs

As we discovered that PIFq members at the end of the night are necessary to promote stomata aperture at dawn, we decided to determine PIF3 localization in stomata nuclei at the end of the night. It had been previously proposed that PIFq members accumulates in the nucleus of hypocotyl cells during the dark phase in dark-grown seedling, becoming actives at the end of the night under diurnal SD conditions. After light-dawn, PIFq members are degraded trough the direct binding to either phyA or phyB (Bauer *et al.*, 2004; Al-Sady *et al.*, 2006; Castillon *et al.*, 2007; Soy *et al.*, 2012). Accordingly, we found that PIF3 accumulates in stomata nuclei of 3-day-old SD-grown seedlings at the end of the dark phase, and that it was degraded after 1 hour of light exposure. In accordance, we propose that the mechanism described in which accumulation of PIFs at the end of the night and their subsequent phy-degradation upon light exposure, also take place in stomata.

Moreover, we observe that PIF3, PIF4 and PIF5 are involved in stomata aperture, as *pif3*, *pif4* and *pif5* mutants showed no difference in stomata aperture at ZT3 compare to ZT0 under SD conditions. Further experiments are necessary to elucidate PIF1 implication in stomata aperture.

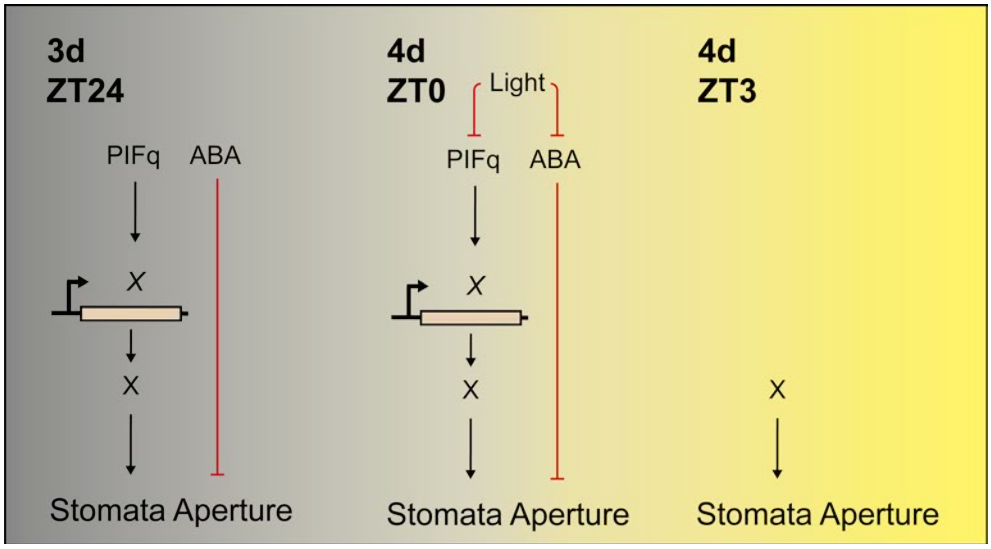

Figure 3.10. Proposed model of the interplay between *PIFq* and endogenous ABA to open stomata during the day.
Arrows indicate positive regulation and blunt-red arrows indicate negative regulation.

As it has been described that growth is induced by PIFq at the end of the night through the transcriptional regulation of growth related genes (Nozue *et al.*, 2011a; Soy *et al.*, 2012, 2014), we propose that a novel regulatory network regulated by PIFs is implicated in the regulation of stomata opening (Fig 3.10).

SUPPLEMENTAL DATA

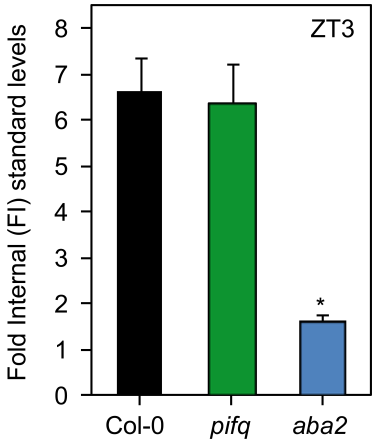

Figure S3.1 ABA levels are not effected in *pifq* during light phase under SD conditions at ZT3.
ABA levels analysis of Col 0, *pifq* and *aba2* at ZT3 in 4-day-old short-day-grown seedlings. The data present the mean +/- SE. Statistical differences relative to Col 0 at each ZT are indicated by an asterisk (Student *t*-test, $P<0.05$). n= 3 biological replicates.

chapter 4

Identification of novel components acting downstream of PIFs that regulate stomata movements

INTRODUCTION

Living in ever-changing environments, plants have evolved the capacity to sense and respond to various stimuli. Capability to respond to environmental stimuli is a basic essence for plants to take adaptive actions before serious harms occur.

Stomata, a cellular structure to control CO_2 uptake and water loss, are capable of responding positively or negatively to various stimuli, such as temperature, humidity, CO_2, hormones and light. For example, while ABA hormone induces stomata closure, light reverses the effect of ABA and induces stomata opening. Integration of the positive and negative signalling pathways in guard cells to regulate stomata movements is crucial to response rapidly and effectively to environmental changes (Kim *et al.*, 2010).

In chapter 3 we proposed a new role for PIFs in regulating stomata aperture after dawn. Specifically, it was concluded that PIFs accumulation at the end of the night is necessary to promote stomata aperture during the light phase of the following day. The identification of PIFs-regulated genes and genes involved in the regulation of stomata movement, would provide new insights into the transcriptional network regulated by PIFs during stomata movements.

Several transcriptomic analyses using single and/or multiple *pif* mutants have been published and provide a genome-wide overview of genes that are PIFs-regulated. ChiP-chip and/or ChiP-Seq data for individual PIFs, together with the transcriptomic analyses contribute to define genes that are potential direct targets of transcriptional regulation by the PIFs. The first expression profile study of PIFs network regulation was performed to define the role of PIF3 in phy signalling during the initial period of seedling deetiolation after exposure to continuous red light (Rc) (Monte *et al.*, 2004). After that, most the sequent studies were performed in darkness to define the contribution of individual PIFs in regulating gene expression (Monte *et al.*, 2004; Leivar *et al.*, 2009; Sentandreu *et al.*, 2011; Moon *et al.*, 2008; Lorrain *et al.*, 2009; Pfeiffer *et al.*, 2014) and the identification of the transcriptomic profile of *pifq* mutants in the dark, that resemble that of wild-type seedlings grown in the light (Leivar *et al.*, 2009). RNA-seq studies identified twice the number of genes previously identified by microarray analysis under equivalent growth conditions (Zhang *et al.*, 2013). ChiP-seq technology was performed to define high confidence binding sites and associated genes in the genome for PIF1 (Kim *et al.*, 2016), PIF3 (Zhang *et al.*, 2013), PIF4 (Oh *et al.*, 2012) and PIF5 (Hornitschek *et al.*, 2012).

However, a limited number of genome-wide analyses using single or/and multiple *pif* mutants have been performed under diurnal conditions. Microarray analysis of *pif4pif5* double mutant under a modified SD schedule after entrainment in SD was performed

to identify PIF-induced and PIF-repressed genes associated with growth (Nozue *et al.*, 2011). Furthermore, in our laboratory, a microarray analysis was performed to define PIF/SD-regulated genes at the end of the night period (ZT24) under SD conditions in 4-day-old seedlings (Martin *et al.*, 2016).

In the other hand, reduced genome-wide analyses have been done in guard cells to provide an overview of new candidate genes involved in stomata movements. Only a couple of expression profile studies have been performed applying exogenous ABA into the guard cell protoplasts to define ABA-regulated genes potentially involved in stomata movement (Leonhardt *et al.*, 2004; Wang *et al.*, 2011). Same studies were used to define guard cell-enriched genes. Finally, a microarray analyses have been performed in guard cells to assess the role of sucrose in the modulation of stomata movements (Bates *et al.*, 2012).

The objective of this chapter was to identify (using these previously-published expression data) PIF-regulated genes that might be involved in the regulation of stomata movements in SD. Furthermore, the top candidates were assayed by functional studies using mutants.

EXPERIMENTAL PROCEDURES

Seedling growth and measurements

A. thaliana seeds used in this chapter include the previously described *aba2/gin1-3* (*aba2*) (Cheng *et al.*, 2002), *mida9-1* (*mida9*) (Sentandreu *et al.*, 2011), *pif1-1pif3-3pif4-2pif5-3* (*pifq*) (Leivar *et al.*, 2009) mutants, pPIF3::YFP:PIF3 (YFP-PIF3) (Al-Sady *et al.*, 2006), *kat1-1* and *kat1-2* (Kazunari Nozue and Robinson, 2015). MIDA9-GFP/YFP transgenic lines were constructed as described in chapter2.

Seeds were sterilized and plated on Murashige and Skoog medium (MS) without sucrose as previously described (Monte *et al.,* 2003). Seedlings were stratified for 4 days at 4 ºC in darkness, and then placed in SD conditions [8 h white light (85 µmol m-2 s1-) + 16 h dark] for 3 days at 21 ºC. For photobiology experiments, during the third day at ZT8, seedlings were either kept in SD conditions, transferred to continuous white light conditions (WL) or exposed to continuous dark conditions (Dark).

Gene expression analysis

RNA was extracted using Mawxell RSC plant RNA Kit (Promega). 1µg of total RNA extracted were treated with DNase I (Ambion) according to the manufacturer's instructions. First-strand cDNA synthesis was performed using the NZYtech First-strand cDNA Synthesis Kit (NZYtech). 2 µl of 1:25 diluted cDNA with water was used for real-time PCR (LightCycler

480 Roche) using SYBR Premix Ex Taq (Takara) and primers at 300nM concentration. Gene expression was measured in three independent biological replicates, and at least two technical replicates were done for each of the biological replicates. *ACTIN2* (AT3G18780) was used for normalization (Table S4.1)

Chromatin Immunoprecipitation (ChIP) Assays

Chromatin immunoprecipitation (ChIP) and ChIP-qPCR assays were performed as in (Soy *et al.*, 2016; Toledo-Ortiz *et al.*, 2014). For PIF3-YFP, all process was performed in the dark under green safelight. Seedlings (3g) were vacuum-infiltrated with 1 % formaldehyde and cross-linking was quenched by vacuum infiltration with 0.125 M glycine for 5 min. Tissue was ground, and nuclei-containing cross-linked protein and DNA were purified by sequential extraction on Extraction Buffer 1 (0.4M Sucrose, 10 mM Tris-HCL pH8, 10 mM MgCl2, 5mM ß-mercaptoethanol, 0.1 mM PMSF, 50 mM MG132, proteinase inhibitor cocktail), Buffer 2 (0.25M Sucrose, 10mM Tris-HCL pH8, 10mM MgCl2, 1% Triton X-100, 5mM ß-mercaptoethanol, 0.1mM PMSF, 50 mM MG132, proteinase inhibitor cocktail), and Buffer 3 (1.7M Sucrose, 10mMTris-HCL pH8, 0.15% Triton X-100, 2mMMgCl2, 5mM ß-mercaptoethanol, 0.1mM PMSF, 50 mMMG132, proteinase inhibitor cocktail). Nuclei were resuspended in nuclei lysis buffer (50 mM Tris-HCL pH8, 10 mM EDTA, 1% SDS, 50 mM MG132, proteinase inhibitor cocktail), sonicated for 10X 30sec, and diluted 10X in Dilution Buffer (0.01% SDS, 1% Triton X-100, 1.2 mM EDTA, 16.7 mM Tris-HCL pH8, 167 mM NaCl). Overnight incubation was performed with the GFP antibody at 4 ºC overnight, and immunoprecipitation was performed using dynabeads. Washes were done sequentially in Low Salt Buffer (0.1% SDS, 1% Triton X-100, 2 mM EDTA, 20 mM Tris-HCL pH 8, 150 mM NaCl), High Salt Buffer (0.1% SDS, 1% Triton X-100, 2 mM EDTA, 20 mM Tris-HCL pH 8, 500 mM NaCl), LiCl Buffer (0.25M LiCl, 1% NP40, 1% deoxycholic acid sodium, 1mM EDTA, 10 mM Tris-HCL pH 8), and TE 1X. Immunocomplexes were eluted in Elution Buffer (1%SDS, 0.1MNaHCO3), de-crosslinked overnight at 65 ºC in 10 mM NaCl, and then treated with proteinase K. DNA was purified using QIAGEN columns, eluted in 100 µL of QIAGEN elution buffer, and 2 µl were used for qPCR (ChIP-qPCR) using *KAT1* promoter-specific primers (Table S4.2) spanning the region containing the predicted binding sites for the PIFs and an intergenic region as a negative control (Pfeiffer *et al.*, 2014). Three independent biological replicates were performed and PIF3 binding were represented as % of input and relative to Col-0 set at unity.

Stomata measurements

Stomata aperture was measured in 4-day-old dark-grown cotyledons. Cotyledons were wet mounted with water on a microscope slide with a cover glass, and pictures were taken with and optical microscope (AixoPhot DP70) at 60X magnification. Stomata pore

area was measured. Measurements were performed using NIH image software (Image J, National Institutes of Health).

Fluorescence microscopy

Stomata of 3-day-old SD-grown at ZT23 and same stomata maintained in white light 1h (4-day-old ZT1) after dawn of MIDA9-GFP-OX #2.2 transgenic line were visualized using a confocal laser scanning microscope Olympus FV1000 (Emission window: 500nm - 660nm). *mida9* was used as a negative control.

Statistical analysis

Levene's test was performed to verify equal variances ($P<0.05$). When the variances were equal, Student *t*-test ($P<0.05$) or ANOVA test ($P<0.05$) followed by a post-hoc Tukey-b test was performed. If needed, data were ln transformed. For not equal variances, Kruskal-Wallis test ($P<0.05$) followed by a post-hoc Dunn test was performed. All analyses were conducted in R.

Microarray data analysis

Gene expression data shown in Fig 4.1 were obtained from the published microarray experiments GSE19520 (Wang *et al.*, 2011) and GSE81813 (Martin *et al.*, 2016). A 0.05 *p*-value was used as a cut-off.

Diurnal profile expression

Transcript abundance were analysed using the publicly available genome-wide expression data DIURNAL5 (http://diurnal.mocklerlab.org) (Mockler *et al.*, 2007) using a cut-off of 0.2 for the following conditions: SD (Col-0_SD) names as Col-0 SD and free running (LL23_LDHH) named as Col-0 LL.

RESULTS

Identification of guard cell specific, PIF- and ABA-regulated genes under SD conditions

Previously, in our laboratory, a microarray analysis was performed to define PIF/SD-regulated genes at the end of the night period (ZT24) under SD conditions in 4-day-old seedlings (Martin *et al.*, 2016). Most of the genes found in this subset were previously described as growth regulated genes. To define new PIF roles in regulating diurnal processes, promoter analysis of PIF-regulated genes under SD was performed. It was found that most of PIF/SD-regulated genes contained the ABA-responsive elements ABRE in their promoter (Martin *et al.*, 2016). These results prompted us to speculate that

ABA and PIFs regulate common genes at the end of the night under SD conditions.

Given that in the previous chapter we confirmed that PIFs accumulation at the end of the dark phase is necessary to induce stomata opening at dawn and the new possible connection between ABA and PIF/SD-regulated genes, we decided to identify PIF-regulated and ABA-regulated genes specifically in guard cells.

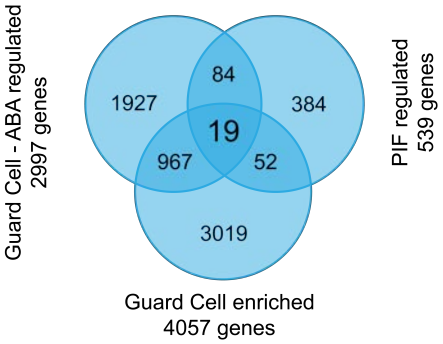

Figure 4.1. Comparison of PIF-regulated genes, ABA-regulated genes in guard cells and guard cells enriched genes.
Venn diagram showing the overlap between the 2,997 genes in gen set Guard Cell – ABA regulated genes, 4057 genes enriched in guard cells (Wang et al., 2011) and 539 PIF-regulated genes (Martin et al., 2016).

To this end, we performed a 3-way comparison analysis between previously described PIF-regulated genes in SD (Martin *et al.*, 2016), ABA-regulated genes in guard cells, and genes that are enriched in guard cells (Wang *et al.*, 2011) (Fig 4.1). Interestingly, 19 genes enriched in guard cells and ABA-regulated, were PIF-regulated in SD, suggesting that ABA and PIFs can act together in regulating common genes to modulate stomata responses, such as stomata aperture, in SD (Table S4.3).

Among the identified genes, we found enzymes that have been related with metabolic processes such as Methionine Gamma-Lyase (*MGL*), Sulfotransferase 2B *(ST2B*), Polyamine Oxidase (*PAO1*) and GDSL esterase/lipase (*AT1G29660*) (Jander and Joshi, 2009; Gidda *et al.*, 2003; Takahashi *et al.*, 2010). Moreover, three of them are hormone-related genes that mediate plant growth (*CKX5*, *OFP16* and *BEH4*) (Nomoto *et al.*, 2012; Wang *et al.*, 2016; Yin *et al.*, 2005). Furthermore, one gene is described to mediate dehydration responses (*RCI2A*) (Medina *et al.*, 2005). Importantly, we found ABA-related genes which are described that are involved in ABA-mediated responses (*KAT1* and *ABCG16*) (Ji *et al.*, 2014). Among these two genes, *KAT1* belongs to a potassium channel family (Hedrich, 2012) which have been involved in the regulation of stomata movements (Kollist *et al.*, 2014). Surprisingly we found *MIDA9*, a previously characterized gene in the chapter 2 of this thesis. Moreover, *MIDA9* has been described to mediate cell expansion through proton pump (*AHA2*) (Spartz *et al.*, 2012) which is involved in the regulation of stomata movements mediated by blue light (Wang *et al.*, 2014).

For these reasons, we decided to characterize the possible connection between PIFq and endogenous ABA in the mediation of stomata movements through *KAT1* and *MIDA9* under diurnal conditions.

KAT1 expression is dark dependent, peaks at the end of the night and is repressed by exogenous ABA in guard cells

Since plasma membrane K+ channels are involved in stomata movements (Pandey *et al.*, 2007) and our data suggest a possible coregulation by PIFs in SD, and exogenous ABA in guard cells, we analysed the *KAT1* expression profile *In silico* under diurnal conditions.

To this end, we first used publicly available genome-wide expression data from the web-based DIURNAL5 resource (Mockler *et al.*, 2007), to define the expression profile of *KAT1* under different light regimes, including 8-day-old Col-0 seedlings grown under SD (Col-0 SD) and under free running conditions (Col-0 LL). This analysis shows that at the end of the night period (ZT20 - ZT24), Col-0 SD presents a clear peak of *KAT1* expression compared to Col-0 LL, consistent with a diurnal regulation of *KAT1* that requires the night hours to induce its expression (Fig 4.2A).

To elucidate the spatial expression of *KAT1* and regulation by exogenous ABA in guard cells, we used the bioinformatic web-based resource ePlant (Waese *et al.*, 2017). Col-0 plants were grown for 60 weeks under SD conditions and *KAT1* expression was measured in leaves and guard cells of plants treated with 50um of exogenous ABA over 3 hours. Plants treated with ethanol (solvent control) over 3 hours was used as a negative control

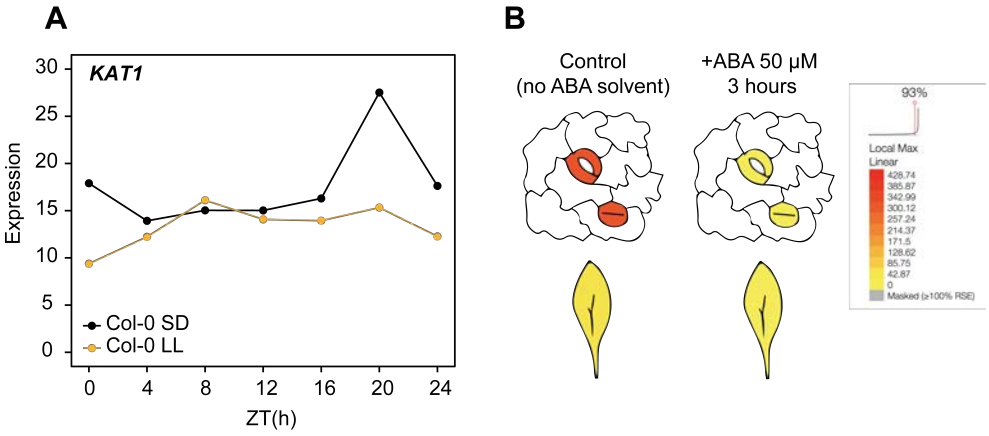

Figure 4.2. *KAT*1 expression is dark dependent, peaks at the end of the night and it is repressed by exogenous ABA in guard cells.
A. Time course analysis of *KAT1* expression in Col-0 under SD and continuous light condition (LL). Data obtained from DIURNAL5 (http://diurnal.mocIker.org) (Mockler et al., 2007). **B.** *KAT1* expression in Col-0 guard cells and leaves in 60-week-old SD-grown plants. Plants treated 3 hours with 50 µm of ABA or ethanol (solvent control) are shown. Data obtained from ePlant (https://bar.utoronto.ca/eplant/) (Pandey et al., 2010).

(Pandey *et al.*, 2010). After 3 hours of ABA treatment, *KAT1* expression levels were strongly reduced in guard cells of treated plants compared to control plants. However, undetectable levels of *KAT1* were observed in neighbouring leaf cells either in control or in treated plants (Fig 4.2B).

Together, this results suggest that *KAT1* accumulation in SD requires the dark/night hours. Furthermore, *KAT1* is enriched in guards cells compared to leave cells, and its expression is repressed by exogenous ABA.

End-of-night expression of *KAT1* under SD requires PIFs but not endogenous ABA

The presented genome-wide expression analysis suggests that *KAT1* expression is dependent of the light/dark cycles (Fig 4.2A). To test *KAT1* regulation by diurnal cycles under the same growth conditions where we validated the function of PIFs in regulating stomata movements (chapter 3), Col-0 seedlings were first grown under SD conditions for 2 days, and then either maintained in SD (SD) or transferred to constant WL (SD + WL) for one additional day (Fig 4.3A). *KAT1* expression levels were then examined at the end of the third day (3d ZT24) and 3 hours after dawn of the following day (4d ZT3).

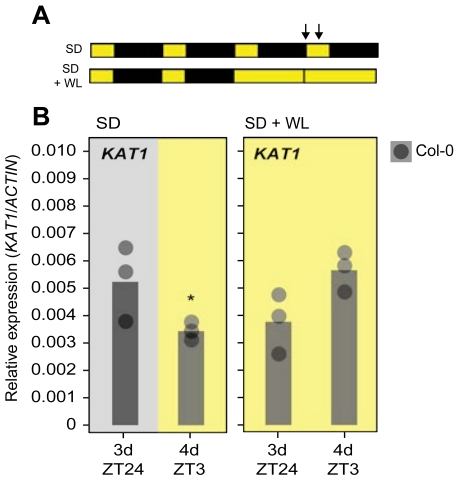

Figure 4.3. KAT1 accumulation is dependent of dark hours under SD.
A. Schematic diagram of growth regime used for B. Seedlings were grown under SD conditions for 2 days and 8h (ZT8), at which time they were either kept under SD as a control (SD) or were transferred to the light (WL). Arrows indicate at which timepoint the *KAT1* expression levels was measured. **B.** Left: *KAT1* levels in Col-0 seedlings at 3d ZT24 and 4d ZT3 under SD conditions. Right: *KAT1* levels in Col-0 seedlings at 3d ZT24 and 4d ZT3 under SD + WL conditions. *KAT1* expression levels were normalized to *ACTIN2*. Bars represent mean values, dots indicate individual measurements. N=3 biological replicates. Statistical differences between mean values relative to 3d ZT24 for each growth condition are indicated by an asterisk (Student *t*-test. $P<0.05$).

Under SD conditions, 4d ZT3 grown seedlings experienced reduced expression levels of *KAT1* compared to 3d ZT24 (Fig 4.3B left). Under SD + WL conditions, no statistically significant differences in *KAT1* expression were observed between 3d ZT24 and 4d ZT3 grown seedlings (Fig 4.3B right). These data suggest that *KAT1* accumulation is dependent of the dark period in SD at dawn, and it is repressed by morning light.

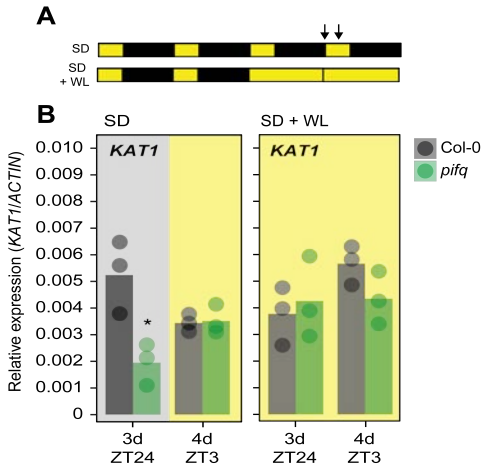

Figure 4.4. *KAT1* accumulation is regulated by PIFs at the end of the night under SD.
A. Schematic diagram of the growth regime used for B. **B.** Left: *KAT1* levels in Col-0 and *pifq* seedlings at 3d ZT24 and 4d ZT3 under SD conditions. Right: *KAT1* levels in Col-0 and *pifq* seedlings at 3d ZT24 and 4d ZT3 under SD + WL conditions. *KAT1* expression levels were normalized to ACTIN2. Bars represent mean values, dots indicate individual measurements. N=3 biological replicates. Statistical differences between mean values relative to Col-0 for each time point are indicated by an asterisk (Student *t*-test. $P<0.05$).

Moreover, in the previous chapter we demonstrated that PIFs accumulation at the end of the night (3d ZT24) are necessary to promote stomata aperture during the light phase of the following day (4d ZT3) under SD. In accordance with previous published data, night period under SD allows the accumulation of PIF3 (and probably other PIFs) which is necessary to induce PIF3-target genes at the end of the night (Soy *et al.*, 2014). To test whether the dark induction of *KAT1* at the end of the night under SD is controlled by PIFs, we analysed *KAT1* expression levels in *pifq* mutants seedlings grown in SD and SD + WL at 3d ZT24 and 4d ZT3 (Fig 4.4A). Under SD conditions, at the end of the third day (3d ZT24), the levels of *KAT1* were reduced in *pifq* mutants compared to Col-0. In contrast, no differences in *KAT1* expression levels were found 3 hours after dawn (4d ZT3) between Col-0 and *pifq* (Fig 4.4B left). In contrast, under SD + WL conditions, no differences in *KAT1* levels were observed either at 3d ZT23 or 4d ZT3 between Col-0 and *pifq* (Fig 4.4B right). Together, these results suggest that *KAT1* expression is regulated by PIFs at the end of the night period.

In the previous chapter we concluded that endogenous ABA is necessary to maintain stomata closed at the end of the night period. Furthermore, previous analysis suggest that *KAT1* expression is regulated by 3 hours of exogenous ABA treatment. To test whether endogenous ABA regulates *KAT1* levels under our experimental set up, we analysed *KAT1* expression levels of in *aba2* mutant seedlings grown in SD and SD + WL (Fig 4.5A). Under SD conditions, no statistically significant differences in *KAT1* expression were observed between Col-0 and *aba2* at the end of the night period during the third day (3d ZT24) and 3 hours after dawn during the fourth day (4d ZT3) (Fig 4.5B left). Similar results were obtained under SD + WL conditions (Fig 4.5B right). Together, these data suggest that endogenous ABA is not involved in the regulation of *KAT1* expression at the end of the night and 3 hours after dawn.

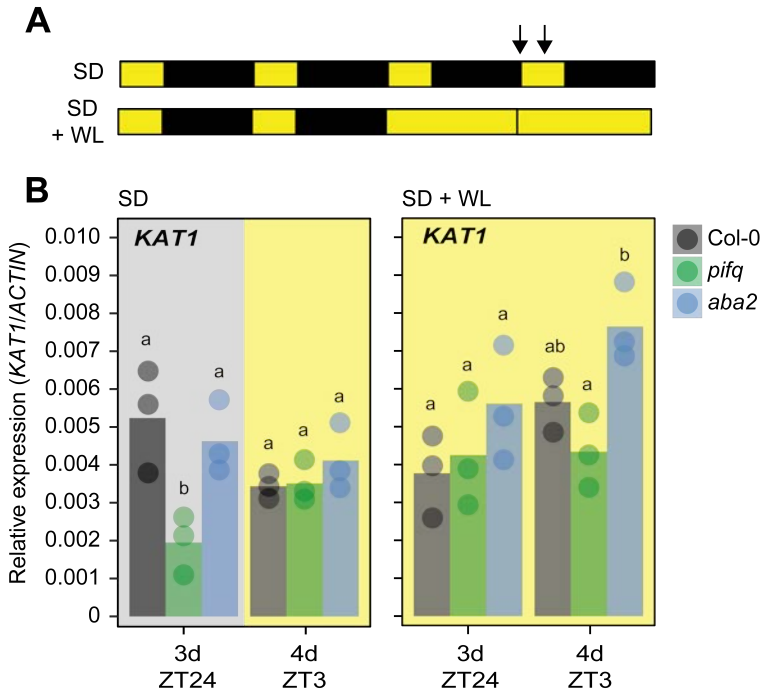

Figure 4.5. *KAT1* accumulation is not regulated by endogenous ABA at the end of the night under SD.
A. Schematic diagram of growth regime used for B. **B.** Left: *KAT1* levels in Col-0, *pifq* and *aba2* seedlings at 3d ZT24 and 4d ZT3 under SD conditions. Right: *KAT1* levels in Col-0, *pifq* and *aba2* seedlings at 3d ZT24 and 4d ZT3 under SD + WL conditions. *KAT1* expression levels were normalized to *ACTIN2*. Bars represent mean values, dots indicate individual measurements. N=3 biological replicates. Different letters denote statistical differences between means for each time point by ANOVA test ($P<0.05$) followed by post-hoc Tukey-b test.

Taken together, we defined that *KAT1* accumulation is dependent of the dark period and it is regulated by PIFs at the end of the night under SD. Moreover, endogenous ABA is not required to regulate *KAT1* expression at the end of the night.

KAT1 expression is directly regulated by PIFs at the end of the dark period under SD

Given that *KAT1* levels are regulated by one or more PIFq members at the end of the night, we next addressed whether this is regulation is direct. We found multiple G-BOX and PBE binding motifs (Fig 4.6A) in the *KAT1* promoter that could act as potential PIF binding sites. Available ChiP-seq data for PIF1, PIF3, PIF4 and PIF5 (Pfeiffer *et al.*, 2014) showed that PIF3 and PIF5 bind to the same promoter region of *KAT1* in 2-day-old dark-grown seedlings (Fig 4.6A). We verified the binding of PIF3 to this promoter region by ChiP-qPCR analysis performed at the end of the night period during the third day (3d ZT24). For that, PIF3 tagged line driven by the endogenous *PIF3* promoter was used (YFP-PIF3).

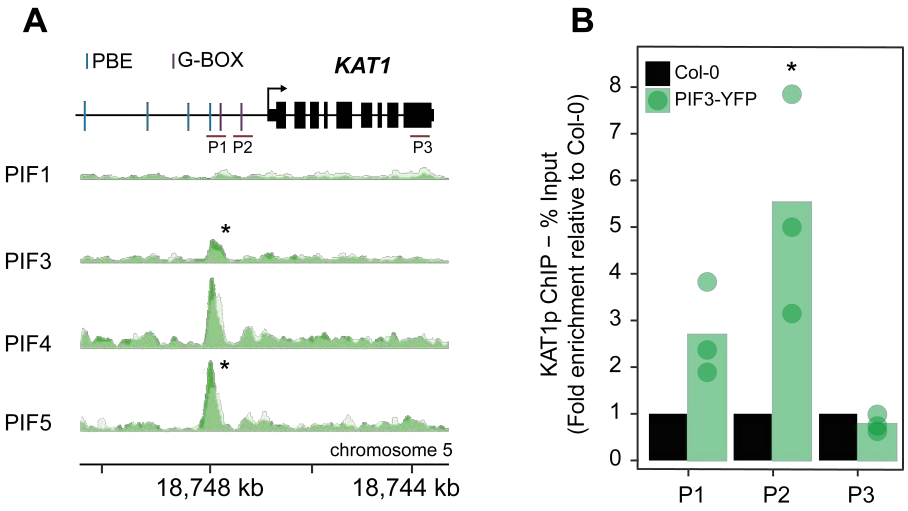

Figure 4.6. ***KAT1*** **expression is directly regulated by PIFs at the end of the night.**
A. Visualization of ChiP-Seq data in the genomic region encompassing the *KAT1* locus. Identified significant binding sites are indicated by an asterisk on top of the pile-up ChiP-Seq tracks. Shadow tracks indicate negative binding control. G- and PBE-box motif in the promoter are indicated. Data obtained from (Pfeiffer et al., 2014). **B.** PIF3 binding to the *KAT1* promoter at ZT24 of 3-days-old SD-grown seedlings is shown. PIF3 binding was represented as % of input and relative to Col-0 set at unity. Col-0 and an intergenic primer (P3) were used as negative controls. Bars represent mean values, dots indicate individual measurements. N=3 biological replicates. Statistical differences between mean values relative to Col-0 for each pair of primers are indicated by an asterisk (Student *t*-test. $P<0.05$).

Statistically significant YFP-PIF3 binding was observed at ZT24 of 3-day-old SD-grown seedlings compared to Col-0 (Fig 4.6B). A primer that binds in the last exon was used as a negative control (P3) (Fig 4.6A). Together, these data validate the binding of PIF3 to the *KAT1* promoter region on G/PBE boxes, localized approximately 1,000 bp upstream of the transcription start site (TSS).

KAT1 is required to induce morning stomata opening after the light-dawn under SD

Our previous data demonstrate that *PIFs* accumulation at the end of the night are required to induce stomata opening 3 hours after dawn. Moreover, *KAT1* expression is dark and PIFs induced at the end of the night under SD. To evaluate whether *KAT1* is required to induce stomata opening during the light phase under SD, we measured stomata aperture over 9 hours after dawn in 4-day-old SD-grown seedlings in the following genotypes: Col 0, *pifq* mutant and 2 two independent mutant lines lacking *KAT1* (*kat1-1* and *kat1-2*) (Kazunari Nozue and Robinson, 2015) (Fig 4.7). In these experiments we observed that at the beginning of the day (ZT0), *kat1-1*, *kat1-2* and *pifq* experienced slightly more stomata closure compared to Col-0. Noticeably, at 3 hours after dawn (ZT3), while Col-0 was

able to fully open the stomata, minor or absent responses to light were detected in *kat1-1*, *kat1-2* and *pifq* mutants, which resulted in closed stomata. At the end of the light phase (ZT6), stomata remained closed in *kat1-1*, *kat1-2* and *pifq*. Furthermore, as expected Col-0 closed the stomata at between ZT3 and ZT6, resulting in a closed stomata similar to *kat1-1*, *kat1-2* and *pifq* at ZT6. At the beginning of the night (ZT9), Col-0, *kat1-1*, *kat1-2* and *pifq* showed stomata fully closed, and no differences between them were observed (Fig 4.7).

Altogether, these data lead us to conclude that PIFq induces *KAT1* expression at the end of the night and, at least, *KAT1* is directly regulated by PIF3. This *KAT1* regulation mediated by PIFq could be essential to promote stomata aperture during the subsequent light period under SD.

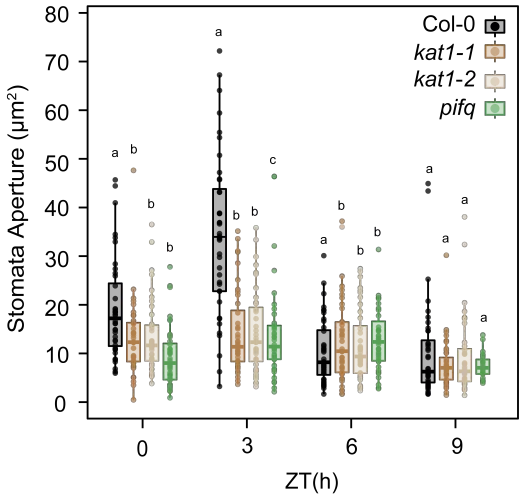

Figure 4.7. *KAT1* is required to induce stomata opening during the light period under SD. Stomata aperture of Col 0, *kat1-1*, *kat1-2* and *pifq* at ZT0, 3, 6 and 9 at 4-day-old SD-grown seedlings are represented. Different letters denote statistical differences between means by Kruskal-Wallis test ($P<0.05$) followed by a post-hoc Dunn test. n=40.

MIDA9 expression is dark dependent, peaks at the end of the night and its repressed by exogenous ABA in guard cells

In chapter 2, we proposed that *MIDA9* is required to form the apical hook through the regulation of cell expansion, during hook development under skotomorphogenesis. Moreover, it has been published that *MIDA9* is involved in cell expansion in the hypocotyl organ (Spartz *et al.*, 2014) under diurnal conditions. Our gene expression comparison analysis showed that *MIDA9* could be regulated by PIFs and exogenous ABA in guard cells (Fig 4.1). This finding pointed to the direction of new roles of *MIDA9* under diurnal conditions mediated by light and hormones.

To this end, we first performed In silico analysis of *MIDA9* expression in the Diurnal website (cita), similar to what we did above for *KAT1*. These analysis showed that under SD conditions (Col-0 SD), *MIDA9* expression decreased during the light period after dawn (ZT0 - ZT8). In contrast, expression levels increased over dark period (ZT8 - ZT24), reaching the peak of expression at the end of the night (ZT24), similar to *KAT1* expression in SD (Fig 4.2A). However, under free running conditions (Col-0 LL) *MIDA9* showed two peaks of expression: in the middle of the light period (ZT4) and in the middle of the night period (ZT16). Furthermore, compared to Col-0 at ZT24, *MIDA9* levels was highly reduced in Col-0 LL at ZT24 (Fig 4.8A). The *MIDA9* expression pattern in Col-0 LL was completely different than *KAT1*.

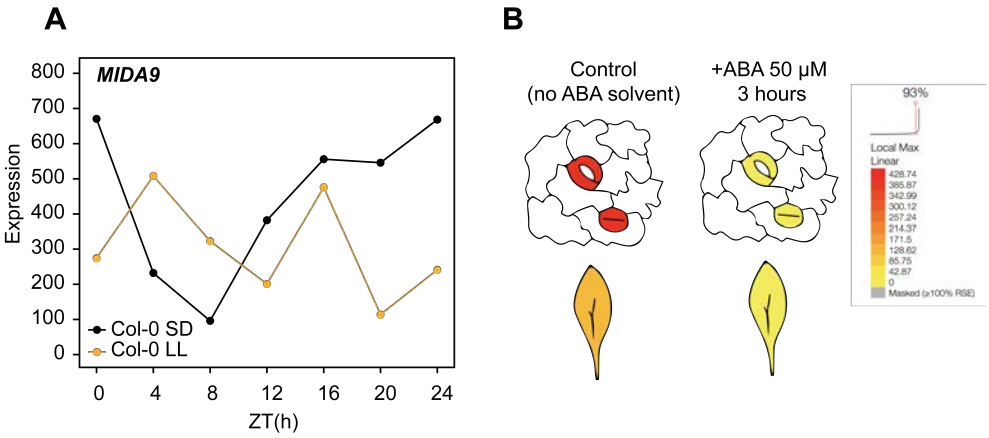

Figure 4.8. *MIDA9* expression is dark dependent, peaks at the end of the night and it is repressed by exogenous ABA in guard cells.
A. Time course analysis of MIDA9 expression in Col-0 under SD and continuous light condition (LL). Data obtained from DIURNAL5 (http://diurnal.mocIker.org) (Mockler et al., 2007). **B.** *MIDA9* expression in Col-0 guard cells and leaves in 60-week-old SD-grown plants. Plants treated 3 hours with 50 µm of ABA or ethanol (solvent control) are shown. Data obtained from ePlant (https://bar.utoronto.ca/eplant/) (Pandey et al., 2010).

Regarding to the spatial expression and regulation by ABA in guard cells of *MIDA9*, after a 3 hours of ABA treatment, *MIDA9* expression levels were strongly reduced in guard cells of treated plants compared to control plants. However, undetectable levels of *MIDA9* were observed either in surrounding leave cells of control and treated plants (Fig 4.8B).

Together, these results suggest that *MIDA9* accumulation in SD is strongly dependent on the dark hours. Furthermore, *MIDA9* is enriched in guards cells compared to leaves and its expression is repressed by exogenous ABA in guard cells.

MIDA9 expression is dependent of dark hours and its expression is regulated by PIFs but not by endogenous ABA at the end of the night under SD

Previous results suggested that *MIDA9* expression is dependent of the light/dark cycles under diurnal conditions (Fig 4.8A). To demonstrate whether *MIDA9* regulation by diurnal cycles take place at the same growth conditions where we validated the function of PIFs in regulating stomata movements (chapter 3), *MIDA9* levels were analysed in Col-0 seedlings grown in SD compared to seedlings grown SD + WL at the end of the third day (3d ZT24) and 3 hours after dawn of the following day (4d ZT3) (Fig 4.9A). Under SD conditions, compared to 4d ZT3, Col-0 seedlings at 3d ZT24 experienced statistically significant higher levels of *MIDA9* (Fig 4.9B left). In contrast, no statistically significant differences were shown between Col-0 seedlings grown under SD + WL at 3d ZT24 and 4d ZT3 (Fig 4.9B right). These results showed that *MIDA9* accumulation is dependent of the dark period in SD and it is repressed by light.

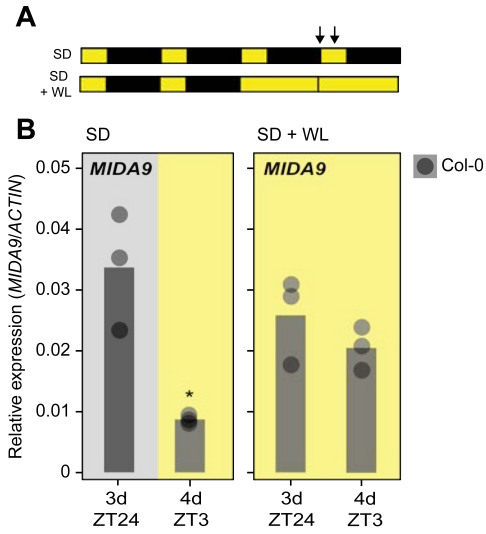

Figure 4.9. *MIDA9* accumulation is dependent of dark hours under SD.
A. Schematic diagram of growth regime used for B. Seedlings were grown under SD conditions for 2 days and 8h (ZT8), at which time they were either kept under SD as a control (SD) or were transferred to the light (WL). Arrows indicate at which timepoint the *MIDA9* expression levels was measured. **B.** Left: *MIDA9* levels in Col-0 seedlings at 3d ZT24 and 4d ZT3 under SD conditions. Right: *MIDA9* levels in Col-0 seedlings at 3d ZT24 and 4d ZT3 under SD + WL conditions. *MIDA9* expression levels were normalized to *ACTIN2*. Bars represent mean values, dots indicate individual measurements. N=3 biological replicates. Statistical differences between mean values relative to 3d ZT24 for each growth condition are indicated by an asterisk (Student *t*-test. $P<0.05$).

Next, we wondered whether the dark induction of *MIDA9* at the end of the night is controlled by PIFs. To this end, we analysed *MIDA9* expression levels in *pifq* grown in SD and SD + WL at 3d ZT24 and 4d ZT3 (Fig 4.10A). Under SD conditions, at the end of the third day (3d ZT24), *MIDA9* levels were significantly reduced in *pifq* mutants compared to Col-0. However, no differences in *MIDA9* expression were shown at 3 hours after dawn (3d ZT3) between Col-0 and *pifq* (Fig 4.10B left). Under SD + WL conditions, no statistically significant differences in *MIDA9* accumulation were observed at 3d ZT23

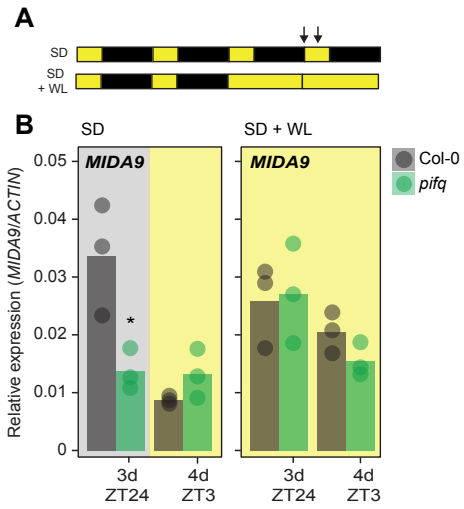

Figure 4.10. *MIDA9* accumulation is regulated by PIFs at the end of the night under SD.
A. Schematic diagram of growth regime used for B. **B.** Left: *MIDA9* levels in Col-0 and *pifq* seedlings at 3d ZT24 and 4d ZT3 under SD conditions. Right: *MIDA9* levels in Col-0 and *pifq* seedlings at 3d ZT24 and 4d ZT3 under SD + WL conditions. *MIDA9* expression levels were normalized to *ACTIN2*. Bars represent mean values, dots indicate individual measurements. N=3 biological replicates. Statistical differences between mean values relative to Col-0 for each time point are indicated by an asterisk (Student *t*-test. $P<0.05$).

and 4d ZT3 between Col-0 and *pifq* (Fig 4.10B right). Together, these data demonstrate that *MIDA9* expression is regulated by PIFq members at the end of the night period.

Finally, we decided to elucidate the implication of endogenous ABA in regulating *MIDA9* levels at the end of the night period. To this end, we analysed the *MIDA9* expression in *aba2* mutant seedlings grown in SD and SD + WL at 3d ZT24 and 4d ZT3 (Fig 4.11A). No statistically significant differences were observed in *MIDA9* accumulation between Col-0 and *aba2* mutant seedlings in SD and SD + WL conditions at 3d ZT24 and 4d ZT3 (Fig 4.11B). These results suggest that endogenous ABA is not involved in the regulation of *MIDA9* levels at the end of the night and 3 hours after dawn. Taken together, we concluded that *MIDA9* accumulation is dependent of the dark period and it is regulated by PIFs at the end of the night under SD. Furthermore, endogenous ABA is not required to regulate *MIDA9* levels at the end of the night.

MIDA9 localizes in the nucleus and in the cytosol of guard cells at the end of the dark phase under SD and is not degraded by light exposure

In the chapter 2, we defined that *MIDA9* expression is localized in the hypocotyl and in the apical hook of dark-grown seedlings, and that MIDA9 protein is localized to the nucleus and the cytosol. Previous data predicted that *MIDA9* is expressed in guard cells (Fig 4.8B), but the protein subcellular localization was ill-defined. To test the subcellular localization of MIDA9 in guard cells at the end of the night, we analysed 3-day-old SD-grown 35S::MIDA9:GFP (MIDA9-GFP-OX #2.2) at ZT23 by confocal microscopy. The results showed that MIDA9 is expressed and accumulates in guard cells, and as in hook or hypocotyl cells, MIDA9-GFP fusion was found in the nucleus and in the cytosol of guard cells (Fig 4.12). Notably, GFP fluorescence appeared stable after 1 hour of white

light treatment (4dSD ZT1), suggesting that, in contrast to PIF3, MIDA9 protein is not degraded by light in guard cells (Fig 4.12). Together, these results suggest that MIDA9 protein is localized in the nucleus and in the cytosol of guard cells at the end of the dark period under SD and is not light-degraded at dawn.

MIDA9 is required to maintain stomata closed at the end of the night under SD

Given that *MIDA9* is PIFs- and dark-induced at the end of the night, when PIFs accumulation is required to induce stomata opening during the subsequent light phase, we decided to analyse the possible contribution of *MIDA9* in regulating stomata movements. To this end, we measured stomata pore aperture in 4-day-old SD-grown over 9 hours after dawn in Col-0, *mida9* and MIDA9-GFP-OX #1.4/#2.2 (Fig 4.13). At dawn (ZT0), *mida9* experienced a statistically significant more open stomata than Col-0. In addition, MIDA9-GFP-OX #2.2 was not able to open the stomata compared to Col-0 at ZT0. However,

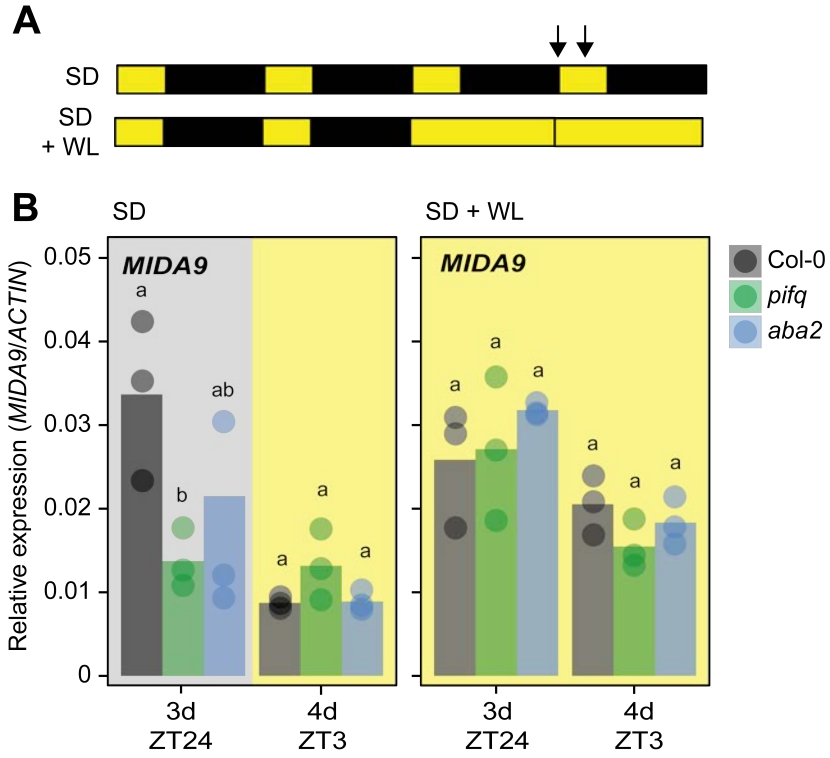

Figure 4.11. *MIDA9* accumulation is not regulated by endogenous ABA at the end of the night under SD.
A. Schematic diagram of growth regime used for B. **B.** Left: *MIDA9* levels in Col-0, *pifq* and *aba2* seedlings at 3d ZT24 and 4d ZT3 under SD conditions. Right: *MIDA9* levels in Col-0, *pifq* and *aba2* seedlings at 3d ZT24 and 4d ZT3 under SD + WL conditions. *MIDA9* expression levels were normalized to *ACTIN2*. Bars represent mean values, dots indicate individual measurements. N=3 biological replicates. Different letters denote statistical differences between means for each time point by ANOVA test ($P<0.05$) followed by post-hoc Tukey-b test.

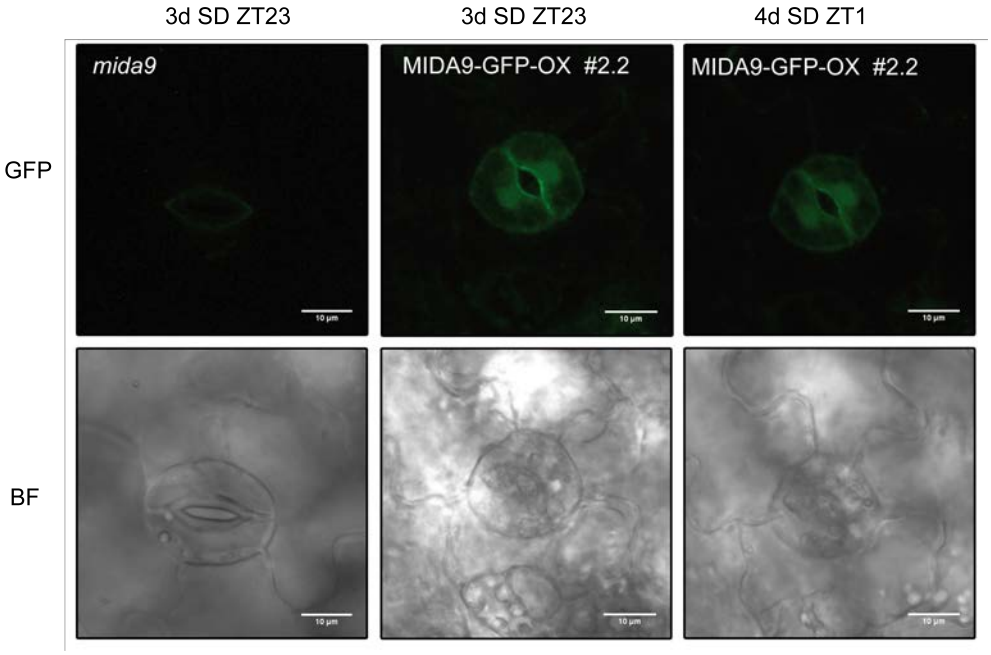

Figure 4.12. MIDA9 localizes in the nucleus of the guard cells and is not degraded by 1 hour white light. MIDA9-GFP localization in guard cells at 3-day-old SD-grown (ZT23) and 4-day-old SD-grown (ZT1) after 1 hour of white light. Same stomata was measured. *mida9* was used as a control. Bar = 10 µm.

no differences in stomata aperture were shown between Col-0 and MIDA9-GFP-OX #1.4. The differences in stomata aperture between MIDA9-GFP-OX #1.4 and #2.2 are in accordance with the fact that #2.2 have greater *MIDA9* levels compared to #1.4 (Fig 2.3B and 2.3C). At 3 hours after dawn (ZT3), Col-0 was able to fully open the stomata in response to light, and no significant difference was observed in *mida9* (Fig 4.13). In contrast, consistent with the role of *mida9* as repressor of stomata opening, the MIDA9-GFP-OX #1.4 and #2.2 were not able to open the stomata as Col-0 at ZT3. At the end of the light period (ZT6), Col-0 was capable to close the stomata. Moreover, no differences in stomata aperture were shown in Col-0 compared to *mida9*, MIDA9-GFP-OX #1.4 and #2.2. Finally, at the beginning of the night (ZT9), same stomata aperture than ZT6 time point were observed for all genotypes (Fig 4.13). These results suggest that *MIDA9* is necessary to keep stomata closure during the dark.

Altogether, we concluded that, similar to KAT*1*, PIFq members induce *MIDA9* expression at the end of the night. Interestingly, in contrast to KAT1, MIDA9 appears to repress stomata opening at night.

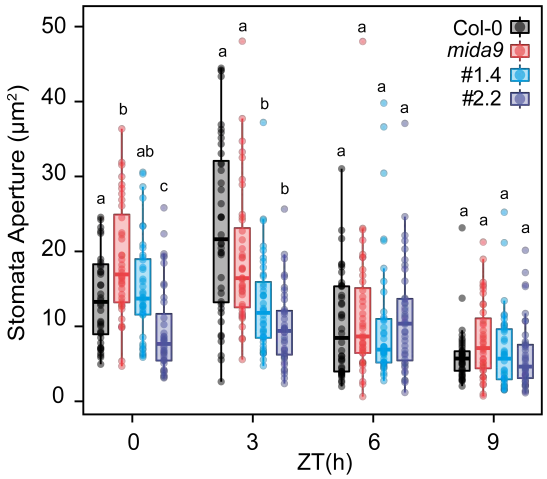

Figure 4.13 *MIDA9* represses stomata aperture at the end of the of the night under SD. Stomata aperture of Col 0, *mida9*, MIDA9-GFP-OX #1.4 and #2.2 at ZT0, 3, 6 and 9 at 4-day-old SD-grown seedlings are represented. Different letters denote statistical differences between means by Kruskal-Wallis test ($P<0.05$) followed by a post-hoc Dunn test. n=40.

DISCUSSION

The ability of plants to perceive and integrate external and endogenous signals allows proper coordination of developmental and physiological responses end ensures adaptation to the ever changing environment. In chapter 3, we defined that PIFs accumulation at the end of the night is necessary to promote stomata aperture at dawn. However, the molecular network downstream of PIFs that modulates these responses was still unclear. In this chapter, we identified PIF-regulated genes that are involved in the regulation of stomata movements under SD conditions.

Through initial microarray comparison analyses, *MIDA9* and *KAT1* appeared as potential candidates in the regulation of stomata aperture mediated by the PIFs. *KAT1* belongs to a family of potassium channels (Hedrich, 2012), and other members in this family have been involved in the regulation of stomata movements (Kollist *et al.*, 2014), and here we describe a novel interplay between light/PIFs, ABA and KAT1 under a diurnal context. On the other hand, although no direct evidence had been previously described for *MIDA9* participation in the control of stomata movements, it is has been proposed that *MIDA9* mediates cell expansion through the proton pump AHA2 (Spartz *et al.*, 2014), and interestingly this gene has been involved in stomata movements (Wang *et al.*, 2014).

KAT1 is necessary to promote stomata aperture during the light phase under SD

Photobiological experiments in chapter 3 let us to postulate that PIFs accumulate and induce the expression of an unknown factor at the end of the dark/night period in SD that is required for the light-induced stomata opening in the morning of the next day. In

this chapter we provide evidence that this unknown factor is KAT1, which belongs to a potassium channel family. KAT1 localizes in the plasma membrane and is activated through the action of H^+-ATPase activity (AHA2) that hyperpolarizes the plasma membrane. This mechanism leads to K^+ uptake trough KAT1 creating an osmotic gradient that triggers water entry inside the guard cells that results in stomata opening.

First, we determined that *KAT1* is a direct target of PIF3, and its expression is induced at the end of the night by the PIFq members (Figs. 4,4 and 4.6). Secondly, genetic analysis of *kat1* T-DNA insertion mutants (Nozue *et al.*, 2015)establishes that KAT1 is required for the transient stomata opening in response to light observed at ZT3 (Fig 4.7). Importantly, our hypothesis has been contrasted by the observation that treatment/genotype conditions with limited *KAT1* expression result in a failure in morning-induced stomata opening, such as *pifq*-SD and Col-WL (Figs. 3.6 and 4.4).

Intriguingly, *KAT1* involvement in stomata movements is apparently in conflict with an old study, in which an *A. thaliana kat1* mutant created with a maize (*Zea mays*) *En-1* transposon insertion in the *KAT1* gene showed no differences in stomata aperture compared to WT control plants (Szyroki *et al.*, 2001). In that study, the data were obtained from guard cell impalement measurements, and showed similar inward ionic current amplitudes in WT compared to mutant plants. Given that other potassium channels were detected by RT-PCR in the mutant, authors proposed a possible redundancy between potassium family channels expressed in guard cells. However, because low expression levels of endogenous *KAT1* mRNA were still detected in the mutant (Szyroki *et al.*, 2001), an alternative explanation is that actually the reported mutant was not a knock-out allele. In fact, *En-1* transposon insertion mutants have been reported to be unstable and get lost, a phenomenon that can interfere with the molecular and cellular analyses of the mutants (Weisshaar *et al.*, 1998). Indeed, parallel studies demonstrated that overexpression of dominant negative *KAT1* mutant inhibits light-induced stomatal opening (Kwak *et al.*, 2001), which is in accordance with our observations.

MIDA9 is required to close the stomata at the end of the night in SD

In chapter 2, we characterized the role of *MIDA9* in the regulation of apical hook formation in etiolated seedlings. Here, we propose a novel *MIDA9* function as a repressor of stomata aperture downstream of the PIFs under diurnal conditions. First, we provide evidence that PIFq members promote *MIDA9* expression at the end of the night in SD (Fig 4.10). The phenotypic analysis of *mida9* mutants shows that *MIDA9* act as repressor stomata opening at the end of the night at ZT24 (Fig 4.13), since stomata are more open in *mida9* than in Col-0 plants. Consistent with this observation, overexpression of the MIDA9 repressors results in unopened stomata in response to light at ZT3 (Fig 4.13). Intriguingly, because no stomata phenotype is observed in *pifq* mutant at the end of the night in SD even when this mutant shows reduced *MIDA9* levels (Figs. 3.5 and 4.10), the

data suggest that repressors other than MIDA9 might be involved in the proper stomata closure in *pifq*. Our results suggest that ABA is a good candidate for mediating this repressor function in *pifq*.

The mechanism by which *MIDA9* regulates stomata aperture is unclear. It has been previously described that MIDA9 interacts and inhibits a proton pump (AHA2) that is required for cell expansion in hypocotyls of diurnally-grown seedlings (Spartz *et al.*, 2014; Ren *et al.*, 2018). Cell expansion is then triggered by SAURs, which interact and inhibit MIDA9 to activate AHA2. We suggest that a similar system could be acting to regulate stomata movements. In fact, it has been published that blue light signal is perceived by phototropins (phot) and transmitted to the plasma membrane H^+-ATPases that drive stomata opening (Kinoshita and Shimazaki, 1999; Christie, 2007; Inoue and Kinoshita, 2017). Moreover, overexpression of *AHA2* using a strong guard cell promoter enhanced light-induced stomata opening (Yang *et al.*, 2008; Wang *et al.*, 2014), suggesting that AHA2 is indeed able to promote stomata movements. Least but no less, SAUR19-overexpressing plants displayed enhanced water loss in detached leaves, wilted faster than WT control plants upon cessation of watering, and importantly, exhibited delayed stomatal closure (Spartz *et al.*, 2014). Taken together and based in our observations, we can conclude that *MIDA9* is involved in stomata movements under SD. Specifically, *MIDA9* is necessary to maintain stomata closure at the end of the night right before dawn in SD. Furthermore, the above described evidences further support the idea that the mechanism by which *MIDA9* regulates cell expansion in hypocotyls might also be involved in the regulation of stomata movements.

A model for PIF-mediated stomata movements

We showed that dark accumulation of PIFs is necessary to induce *KAT1* expression at the end of the night (3d ZT24), and we propose that this night-accumulation of the KAT1 potassium channel is required to promotes stomata aperture in response to light after dawn. This model assumes that a factor inhibits KAT1 activity during the night to keep the stomata closed. Interestingly, it has been described that ABA prevents stomata aperture at the end of the night (3d ZT24) through alternative pathways (Daszkowska-Golec and Szarejko, 2013) including the endocytosis of KAT1 channel (Sutter *et al.*, 2007). Therefore, we suggest that ABA acts during the night to post-translationally repress KAT1 function. In addition to this mechanism, we demonstrate that PIFq also induces the expression of *MIDA9*, which we defined as a repressor of stomata aperture, to prevent stomata aperture at the end of the night (3d ZT24). Both strategies would gate the aperture of stomata at the right moment of the day under SD conditions.

In contrast to dark conditions, when the light turns on at dawn (4d ZT0), PIFs are degraded by light in a phy-dependent manner resulting in a reduction in *MIDA9* repressor

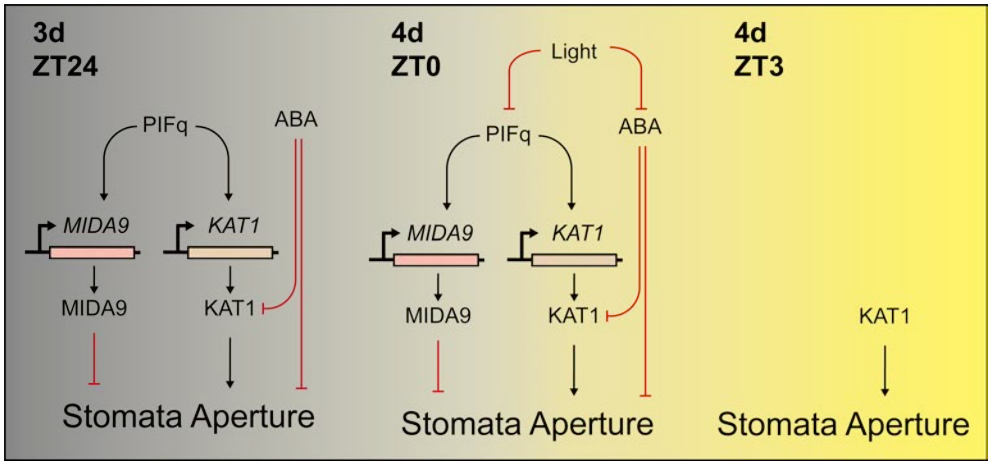

Figure 4.14 Proposed model of the signal transduction pathway mediated by PIFq and endogenous ABA under SD conditions.
Arrows indicate positive regulation and blunt-red arrows indicate negative regulation. Information delivered from literature and data presented in this chapter.

expression. Importantly, it has been suggested that light induces a reduction in bioactive ABA through two different mechanisms: (i) the hydroxylation of ABA by P-450 type monoxygenases that triggers ABA degradation, and (ii) inactivation through esterification of ABA to ABA-glucose ester (ABA-GE) (Nová Ková *et al.*, 2005; Finkelstein, 2013). Moreover, some evidences indicates that light might induce ABA catabolism (Sawada *et al.*, 2008; Nambara *et al.*, 2010) . Considering these antecedents, we propose that light inactivation of ABA reverses the endocytic process of KAT1, and results in availability of the channel at the plasma membrane of guard cells that leads to K^+ uptake, generating osmotic gradient. Following this gradient, water entry and results in stomata opening. The transient nature of this process might be in part mediated by the light repression of the PIFs, as it results in a downregulation of *KAT1* expression. Together, we propose a working model in which stomata opening after dawn is gated by PIFs and endogenous ABA at the end of the night through the regulation of *KAT1* and *MIDA9* expression (Fig 4.14).

It is interesting to note that recently it has been demonstrated that the guard cell circadian oscillator differs from the central oscillator (Hassidim *et al.*, 2017). Authors reported that the guard cell oscillator may be important for the correct regulation of photoperiod pathway genes that have been previously reported to control stomatal aperture such as CONSTANTS (CO) and FLOWERING LOCUS T (FT) (Ando *et al.*, 2013; Hassidim *et al.*, 2017). For this reason, we cannot rule out the possibility that mechanisms other than the one described here, such as one involving the guard cell oscillator, modulate other photoperiod pathways to gate stomata aperture in SD conditions.

SUPPLEMENTAL DATA

Table S4.1. Primers used for gene experssion analyses.

Gene	AGI	Forward	Reverse
KAT1	At5g46240	GCAATAAGGTACCTTTCGAC	AAGCCTTGCAAATAGCGAGC
MIDA9	At5g02760	TCATGTTGCTTGGCAGGAGTG	ACTCCACCTCTCTCAGATC
ACTIN2	At3g18780	CTGGATCGGTGGTTCCATTC	CCTGGACCTGCCTCATCATAC

Table S4.2. Primers used for ChiP-qPCR analyses.

Gene	AGI	Binding region	Forward	Reverse
KAT1	At5g46240	P1	GCATGGGAAGTGAAACTCTAAG	CGAGTGAGAAGAGAGTTTGGG
		P2	GCAAGCAATATGTCTTTGTTG	CCGACGGGAATGAGAAGTATG
		P3 (genomic)	CCAAACTTCTCACTTGCAAGTC	GATCCATATTGCAGCTCAAGC

Table S4.3. Genes identified in guard cells that are PIF- and ABA-regulated under SD conditions.

			Log_2 Fold change		
AGI	**Gene name**	**Gene symbol**	**Guard cells / Leaves**	**+ABA / -ABA (Guard cells)**	***pifq* / WT**
At1g06850	Basic leucine-zipper 52	*bZIP52*	-3,51	-2,00	-1,12
At1g15290	Tetratricopeptide repeat-containing protein	*Atg15290*	-1,63	-1,31	1,61
At1g29660	GDSL esterase/lipase	*At1g29660*	-4,67	-2,37	-0,88
At1g64660	Methionine gamma-lyase	*MgL*	-2,55	-1,17	-1,51
At1g75450	Cytokinin dehydrogenase 5	*CKX5*	-4,37	-1,62	-0,49
At1g78700	BES1/BZR1 homolog 4	*BEH4*	-1,30	-0,94	-0,98
At2g32100	Ovate family protein 16	*OFP16*	-1,12	-1,96	1,04
At3g12610	DNA-damage-repair/toleration protein DRT100	*DRT100*	-2,64	-2,98	-0,67
At5g02020	Hypothetical protein	*At5g02020*	-2,91	1,41	-1,27
At5g02540	NAD(P)-binding Rossmann-fold superfamily protein	*At5g02540*	-3,67	-4,24	-1,01
At5g07000	sulfotransferase 2B	*St2B*	-1,45	-1,61	-0,68
At5g13700	Polyamine oxidase 1	*PAO1*	-3,79	1,66	-0,55
At5g02760	Protein phosphatase 2C clade D	*MIDA9*	-2,25	-5,82	-0,90

			Log$_2$ Fold change		
AGI	**Gene name**	**Gene symbol**	**Guard cells / Leaves**	**+ABA / -ABA (Guard cells)**	***pifq* / WT**
At5g20270	Heptahelical transmembrane protein1	*HHP1*	-3,20	1,46	-1,14
At4g18970	GDSL esterase/lipase	*At4g18970*	-3,18	-2,10	-0,77
At5g46240	Potassium channel	*KAT1*	-3,15	-3,81	-0,84
At3g55090	ABC transporter G family member 16	*At3g55090*	-0,36	4,11	-1,11
At1g22330	RNA recognition motif-containing protein	*At1g22330*	-1,90	-2,91	-1,69
At3g05880	Hydrophobic protein	*RCI2A*	-0,53	1,13	-0,66

chapter 5

General Discussion

At the beginning of this thesis the transcriptional network downstream of PIFs had been widely studied during skotomorphogenesis and photomorphogenesis. Four novel PIF3-regulated genes *MISEXPRESSED IN THE DARK (MIDAs)* had been identified in our laboratory, and they had been involved in different facets of photomorphogenesis such as hypocotyl elongation (*MIDA11*), hook maintenance (*MIDA9* and *MIDA10*) and cotyledon appression (*MIDA1*) (Sentandreu *et al.*, 2011). In chapter 2, we characterized *MIDA9,* one of the nine members of the PP2C clade D family, over the three phases of hook development in etiolated seedlings. We defined that *MIDA9* is necessary to promote hook formation during the first hours of post-germinative growth (Fig 2.2) by inducing cell elongation in the outer edge of the hook. This process is necessary to establish the asymmetric growth that results in apical hook formation (Fig 2.3). Moreover, we defined the temporally-space function of the PP2C clade D family and the genetic interaction between *PD1*, *PD6* and *MIDA9* during hook development during skotomorphogenesis (Fig 2.5).

In chapter 3 we defined novel PIF-mediated rhythmic processes under diurnal growth conditions. Previous studies had described in 5-week-old *V. faba* leaves that stomata close during the night and open during the light period under photoperiodic conditions (Talbott and Zeiger, 1996). Furthermore, it was defined that blue light is implicated in stomata movements, specifically inducing stomata opening (Inoue and Kinoshita, 2017). However, little was known about the regulation of stomata movements mediated by red/far-red light through PIFs-phy interaction (Wang *et al.*, 2010). Here, we defined a new PIFs function under SD conditions, in which PIFs accumulation at the end of the night is necessary to induce stomata aperture during the subsequent light phase under SD conditions.

Finally, in chapter 4, we decided to identify and characterize PIF-regulated genes that might be involved in the regulation of stomata movements under SD conditions. At the beginning of this thesis, several transcriptomic analysis and ChiP data using single and multiple *pif* mutants and PIF-tagged transgenic lines had been reported under diurnal conditions to shed light into the regulatory network downstream of PIFs. Furthermore, genome-wide analysis in guard cells had been published to define ABA-regulated genes in guard cells. By comparison analysis, we proposed that *KAT1* and *MIDA9* act downstream of PIFs to regulate stomata movements (Fig 4.1). Specifically, we defined that PIF3 directly regulates *KAT1* expression at the end of the night under SD (Fig 4.6). It was previously suggested that *KAT1* regulates stomata movements (Kwak *et al.*, 2001), and here we define an interplay between light/PIFs and ABA to regulate stomata aperture through KAT1. However, there was no evidence describing the implication of *MIDA9* in stomata

aperture regulation. In chapter 2 we conclude that *MIDA9* is necessary to promote apical hook formation. Other studies have demonstrated that *MIDA9* physically interacts with the proton pump AHA2 and SAUR19 to regulate cell expansion in the hypocotyl (Spartz *et al.*, 2014). We propose that the mechanism by which *MIDA9* regulates cell expansion in hypocotyls might also be operating to regulate stomata movements.

To conclude, in this thesis we studied the network downstream of PIFs from skotomorphogenesis to photomorphogenesis. It is well-known that PIFs integrate internal and external signals to regulate growth responses. The findings presented in this thesis not only add knowledge on novel PIFs-regulated genes and their mechanism of action, but also open the door to investigate processes other than growth in which PIFs might be involved such as stomata movements.

Conclusions

We conclude that the PP2C clade D phosphatase *MIDA9*, a PIF3-regulated gene, is required to promote hook formation during apical hook development in etiolated seedlings. Furthermore, three members of the PP2C Clade D (*PD1*, *PD6* and *MIDA9*) act collectively to regulate temporal aspects of hook development, such as formation, maintenance and aperture.

- *MIDA9* induce cell expansion in the outer edge of the hook, which is required to establish the asymmetric growth necessary for hook formation.
- MIDA9 localizes to the nucleus and cytosol in the apical hook**.**
- *MIDA9* might regulate ethylene biosynthesis by inducing *ACS* (*1-AMINOCYCLOPROPANE-1-CARBOXULATE SYNTHASE*) expression in dark-grown seedlings. An interplay between *MIDA9* and ethylene might determine apical hook formation.

We define that stomata movements oscillate during early Arabidopsis deetiolation under diurnal short day (SD) conditions, and show a transient aperture during the day/light phase with a peak at ZT3. Moreover, we conclude that PIFs accumulation during the night and light-induced inactivation of endogenous ABA is necessary to promote stomata aperture in the morning.

- A PIF-induced factor during the night period under SD is required to induce stomata opening in response to light at dawn.
- PIF3 localizes in the guard cell nucleus at the end of the dark phase under SD and is degraded by light at dawn.
- Endogenous ABA is required for stomata closure at night under SD conditions.
- Stomata closure at the end of the day/light period is partially independent of the endogenous ABA, and the signal appears to be generated during the dark/night period of the previous day.

We describe that PIFs gate stomata aperture after dawn under diurnal conditions through the regulation of *KAT1* and *MIDA9* expression.

- *KAT1* expression is induced in the dark and peaks at the end of the night in SDs, and is repressed by exogenous ABA in guard cells.
- End-of-night expression of *KAT1* under SD requires the action of PIFq members but not endogenous ABA.

- *KAT1* expression is directly regulated by PIF3 at the end of the dark period under SD.

- *KAT1* is required to induce morning stomata opening at dawn in response to light under SD.

- *MIDA9* expression is induced in the dark and peaks at the end of the night in SD, and is repressed by exogenous ABA in guard cells.

- End-of-night expression of *MIDA9* under SD requires the action of PIFq members but not endogenous ABA.

- *MIDA9* is required to maintain stomata closed at the end of the night under SD.

Summary

Plants perceive and integrate external (such as light and temperature) and internal (such as hormones or the circadian clock) signals to optimize growth and development in a changing environment. Light is used not only as a source of energy for plant photosynthesis, but also as a source of information to perceive the surrounding environment. Plants are armed with light sensitive proteins called photoreceptors that sense and transduce light signals to a core regulatory network that implements different facets of photomorphogenesis throughout plant life cycle. Studies in the model plant *Arabidopsis thaliana* have established that several transcriptional regulators such as the PHYTOCHROME INTERACTING FACTORS (PIFs) play a key role in this transcriptional network by regulating the expression of genes involved in different photomorphogenic processes such as seed germination, seedling deetiolation, diurnal and thermal growth, shade avoidance, or flowering. The downstream functions of this network and the implication of PIFs in other physiological and developmental responses remains poorly understood.

The main objective of this work is to expand current understanding of the regulatory network acting downstream of PIFs during photomorphogenesis, and to define novel regulatory roles of PIFs during plant development.

Previous studies had shown that MIDA9, a PIF3-regulated protein phosphatase 2C, regulates hook development during the post-germinative growth of the seedling. One of the aims of this thesis was to perform detailed genetic and phenotypic characterization of MIDA9 function, and we established that MIDA9 promotes the asymmetric growth required for the apical hook formation, possibly by altering ethylene biosynthesis.

A second aim consisted in the definition of a novel role of PIFs in regulating stomata movements under diurnal conditions. We propose that PIFs accumulate at the end of the night to induce the expression of a factor that is necessary to promote stomata aperture in response to light at dawn. Moreover, light is suggested to reduce bioactive levels of ABA (Abscisic Acid) and release the repression that this hormone exerts during the night.

Finally, we identified and characterized the function of *KAT1* and *MIDA9* as genes that modulate stomata movements downstream of the PIFs.

Because regulation of stomata movements is essential to control water balance in plants, the identified regulatory components are candidate molecular targets for the development of drought resistant plants. Moreover, the described regulation of the apical hook development might contribute to the establishment and survival of the postgerminative seedling.

Resum

El desenvolupament i creixement de les plàntules està influenciat per senyals ambientals com ara la llum o la temperatura, i per senyals internes com ara les hormones o el rellotge circadià. Les plantes utilitzen la llum com a font d'energia per a realitzar la fotosíntesis i també com a font d'informació per percebre els canvis en l'entorn que les envolta. Per aquesta raó, les plantes tenen unes proteïnes sensibles a la llum anomenades fotoreceptors, que capten la llum i envien el senyal a una xarxa de regulació gènica que desencadena respostes fotomorfogèniques durant tot el seu cicle de vida. Els estudis fets en la planta model *Arabidopsis thaliana* han establert que els factors de transcripció anomenats Phytochrome Interacting Factors (PIFs) juguen un paper important durant aquesta resposta, regulant l'expressió de gens involucrats en processos fotomorfogènics com per exemple: la germinació, la desetiolació, el creixement diürn, la regulació del creixement a través de la temperatura, la resposta a la fugida de l'ombra i la floració. Altres processos fisiològics regulats per aquesta xarxa gènica encara estan poc estudiats.

El principal objectiu d'aquest treball és ampliar el coneixement de la xarxa de regulació gènica controlada pels PIFs durant la fotomorfogènesis i definir noves funcions regulades pels PIFs durant el desenvolupament de la planta.

En primer lloc, estudis previs han demostrat que MIDA9, una fosfatasa del tipus 2C, regula la formació del ganxo apical durant la postgerminació de la plàntula en foscor. Durant la tesi hem realitzat estudis genètics per caracteritzar la funció de MIDA9 i hem establert que és necessari per a promoure el creixement asimètric en l'hipocòtil, el qual és imprescindible per la formació del ganxo apical. Per altra banda, la majoria dels treballs publicats s'han focalitzat en entendre la funció dels PIFs durant el creixement de la planta. Per contra, pocs estudis s'han centrat a descobrir altres respostes fisiològiques regulades pels PIFs durant el creixement diürn. En aquest treball hem definit que l'acumulació dels PIFs al final de la nit és necessària per a regular el moviment dels estomes. Finalment, tot i que la funció de la xarxa gènica regulada pels PIFs ha estat caracteritzada durant aquests anys, en aquesta tesi hem identificat KAT1 i MIDA9 com a nous gens regulats pels PIFs, els quals participen en la modulació del moviment dels estomes.

Ja que prèviament s'ha descrit que el control del moviment dels estomes és essencial per a regular el balanç hídric en plantes, aquest treball podria contribuir a la identificació de components que podrien ser dianes moleculars per a la generació de plantes resistents a la sequera. A més a més, hem contribuït a entendre millor el mecanisme involucrat en el desenvolupament del ganxo apical, un procés vital per a la supervivència de les plàntules.

References

Al-Sady, B., Ni, W., Kircher, S., Schä, E., and Quail, P.H. (2006). Photoactivated Phytochrome Induces Rapid PIF3 Phosphorylation Prior to Proteasome-Mediated Degradation. Mol. Cell **23**: 439–446.

Ando, E., Ohnishi, M., Wang, Y., Matsushita, T., Watanabe, A., Hayashi, Y., Fujii, M., Ma, J.F., Inoue, S. -i., and Kinoshita, T. (2013). TWIN SISTER OF FT, GIGANTEA, and CONSTANS Have a Positive But Indirect Effect on Blue Light-Induced Stomatal Opening in Arabidopsis. Plant Physiol. **162**: 1529–1538.

Ang, L.-H., Chattopadhyay, S., Wei, N., Oyama, T., Okada, K., Batschauer, A., and Deng, X.-W. (1998). Molecular Interaction between COP1 and HY5 Defines a Regulatory Switch for Light Control of Arabidopsis Development.

Araújo, W.L., Fernie, A.R., and Nunes-Nesi, A. (2014). Control of stomatal aperture. Plant Signal. Behav. **6**: 1305–1311.

Arve, L.E., Terfa, M.T., Gislerød, H.R., Olsen, J.E., and Torre, S. (2013). High relative air humidity and continuous light reduce stomata functionality by affecting the ABA regulation in rose leaves. Plant, Cell Environ. **36**: 382–392.

Assmann, S.M. and Shimazaki, K.-I. (1999). The Multisensory Guard Cell. Stomatal Responses to Blue Light and Abscisic Acid. PLANT Physiol.

Bae, G. and Choi, G. (2008). Decoding of Light Signals by Plant Phytochromes and Their Interacting Proteins.

Bates, G.W., Rosenthal, D.M., Sun, J., Chattopadhyay, M., Peffer, E., Yang, J., Ort, D.R., and Jones, A.M. (2012). A Comparative Study of the Arabidopsis thaliana Guard-Cell Transcriptome and Its Modulation by Sucrose. PLoS One.

Bauer, D., Vicziá, A., Kircher, S., Nobis, T., Nitschke, R., Kunkel, T., Panigrahi, K.C., bet Fejes, E., Schä fer, E., and Nagy, F. (2004). Constitutive Photomorphogenesis 1 and Multiple Photoreceptors Control Degradation of Phytochrome Interacting Factor 3, a Transcription Factor Required for Light Signaling in Arabidopsis. Plant Cell **16**: 1433–1445.

Bauer, H. et al. (2013). Report The Stomatal Response to Reduced Relative Humidity Requires Guard Cell-Autonomous ABA Synthesis. Curr. Biol. **23**: 53–57.

Bernardo-García, S., de Lucas, M., Martínez, C., Espinosa-Ruiz, A., Davière, J.M., and Prat, S. (2014). BR-dependent phosphorylation modulates PIF4 transcriptional activity and shapes diurnal hypocotyl growth. Genes Dev. **28**: 1681–1694.

Van Buskirk, E.K., Decker, P. V., and Chen, M. (2012). Photobodies in Light Signaling. Plant Physiol. **158**: 52–60.

Casson, S.A., Franklin, K.A., Gray, J.E., Grierson, C.S., Whitelam, G.C., and Hetherington, A.M. (2009). phytochrome B and PIF4 Regulate Stomatal Development in Response to Light Quantity. Curr. Biol. **19**.

Castillon, A., Shen, H., and Huq, E. (2007). Phytochrome Interacting Factors: central players in phytochrome-mediated light signaling networks. Trends Plant Sci. **12**: 514–521.

Charron, J.-B.F., He, H., Elling, A.A., and Deng, X.W. (2009). Dynamic Landscapes of Four Histone Modifications during Deetiolation in Arabidopsis W. Plant Cell.

Chaves, I., Pokorny, R., Byrdin, M., Hoang, N., Ritz, T., Brettel, K., Essen, L.-O., van der Horst, G.T.J., Batschauer, A., and Ahmad, M. (2011). The Cryptochromes: Blue Light Photoreceptors in Plants and Animals. Annu. Rev. Plant Biol. **62**: 335–364.

Cheng, W.-H., Endo, A., Zhou, L., Penney, J., Chen, H.-C., Arroyo, A., Leon, P., Nambara, E., Asami, T., Seo, M., Koshiba, T., and Sheen, J. (2002). A Unique Short-Chain Dehydrogenase/Reductase in Arabidopsis Glucose Signaling and Abscisic Acid Biosynthesis and Functions. Plant Cell **14**: 2723–2743.

Christie, J.M. (2007). Phototropin Blue-Light Receptors. Annu. Rev. Plant Biol.

Christie, J.M., Blackwood, L., Petersen, J., and Sullivan, S. (2015). Plant Flavoprotein Photoreceptors. Plant Cell Physiol.

Cominelli, E., Galbiati, M., Vavasseur, A., Conti, L., Sala, T., Vuylsteke, M., Leonhardt, N., Dellaporta, S.L., and Tonelli, C. (2005). A Guard-Cell-Specific MYB Transcription Factor Regulates Stomatal Movements and Plant Drought Tolerance. Curr. Biol. **15**: 1196–1200.

Daszkowska-Golec, A. and Szarejko, I. (2013). Open or close the gate stomata action under the control of phytohormones in drought stress conditions. Front. Plant Sci. **4**: 1–16.

Deng, X.W., Caspar, T., and Quail, P.H. (1991). Cop1 : a regulatory locus involved m hght-controlled development and gene expression in Arabidopsis. Genes Dev. **5**: 1172–1182.

Ding, Z., Li, S., An, X., Liu, X., Qin, H., and Wang, D. (2009). Transgenic expression of MYB15 confers enhanced sensitivity to abscisic acid and improved drought tolerance in Arabidopsis thaliana.

Fankhauser, C. and Christie, J.M. (2015). Plant Phototropic Growth. Curr. Biol. **25**: R384–R389.

Fehér, B., Kozma-Bognár, L., Kevei, É., Hajdu, A., Binkert, M., Davis, S.J., Schäfer, E., Ulm, R., and Nagy, F. (2011). Functional interaction of the circadian clock and UV RESISTANCE LOCUS 8-controlled UV-B signaling pathways in Arabidopsis thaliana. Plant J. **67**: 37–48.

Feng, S. et al. (2008). Coordinated regulation of Arabidopsis thaliana development by light and gibberellins. Nature **451**: 475–479.

Fierro, A.C., Leroux, O., De Coninck, B., Cammue, B., P.A., Marchal, K., Prinsen, E., Van Der Straeten, D., and Vandenbussche, F. (2015). Ultraviolet-B radiation stimulates downward leaf curling in Arabidopsis thaliana. Plant Physiol. Biochem. **93**: 9–17.

Finkelstein, R. (2013). Abscisic Acid Synthesis and Response. Arab. B. **11**: e0166.

Franklin, K.A. and Quail, P.H. (2009). Phytochrome functions in Arabidopsis development. J. Exp. Bot. **61**: 11–24.

Furuya, M. (1993). Phytochromes: Their molecular species, gene families, and functions. Annu. Rev. Plant Physiol. Plant Mol. Bioi **44**: 617–45.

Gallego-Bartolomé, J., Arana, M. V, Vandenbussche, F., Zádníkova, P., Minguet, E.G., Guardiola, V., Van Der Straeten, D., Benkova, E., Alabadí, D., and Blázquez, M.A. (2011). Hierarchy of hormone action controlling apical hook development in Arabidopsis. Plant J. **67**: 622–634.

Galvão, V.C. and Fankhauser, C. (2015). Sensing the light environment in plants: Photoreceptors and early signaling steps. Curr. Opin. Neurobiol. **34**: 46–53.

Gidda, S.K., Miersch, O., Levitin, A., Schmidt, J., Wasternack, C., and Varin, L. (2003). Biochemical and molecular characterization of a hydroxyjasmonate sulfotransferase from Arabidopsis thaliana. J. Biol. Chem. **278**: 17895–17900.

Gommers, C.M.M. and Monte, E. (2017). Seedling establishment: a dimmer switch-regulated process between dark and light signaling. Plant Physiol. **176**: pp.01460.2017.

Hassidim, M., Dakhiya, Y., Turjeman, A., Hussien, D., Shor, E., Anidjar, A., Goldberg, K., and Green, R.M. (2017). CIRCADIAN CLOCK ASSOCIATED 1 (CCA1) and the circadian control of stomatal aperture. Plant Physiol. **175**: pp.01214.2017.

Hedrich, R. (2012). ION CHANNELS IN PLANTS. In Physiological Reviews, pp. 1777–1811.

Holtkotte, X., Ponnu, J., Ahmad, M., and Hoecker, U. (2017). The blue light-induced interaction of cryptochrome 1 with COP1 requires SPA proteins during Arabidopsis light signaling. PLoS Genet.

Hornitschek, P., Kohnen, M. V., Lorrain, S., Rougemont, J., Ljung, K., López-Vidriero, I., Franco-Zorrilla, J.M., Solano, R., Trevisan, M., Pradervand, S., Xenarios, I., and Fankhauser, C. (2012). Phytochrome interacting factors 4 and 5 control seedling growth in changing light conditions by directly controlling auxin signaling. Plant J. **71**: 699–711.

Inoue, S.-I. and Kinoshita, T. (2017). Blue Light Regulation of Stomatal Opening and the Plasma Membrane H + -ATPase. PLANT Physiol. **174**: 531–538.

Ito, S., Song, Y.H., and Imaizumi, T. (2012). LOV Domain-Containing F-Box Proteins: Light-Dependent Protein Degradation Modules in Arabidopsis. Mol. Plant **5**: 573–582.

Jander, G. and Joshi, V. (2009). Aspartate-derived Amino Acid Biosynthesis in Arabidopsis thaliana. Arab. B. **7**: e0121.

Jang, I.-C., Henriques, R., Seo, H.S., Nagatani, A., and Chua, N.-H. (2010). Arabidopsis PHYTOCHROME INTERACTING FACTOR Proteins Promote Phytochrome B Polyubiquitination by COP1 E3 Ligase in the Nucleus. Plant Cell Online **22**: 2370–2383.

Jenkins, G.I. (2014). Structure and function of the UV-B photoreceptor UVR8. Plant Cell **29**: 52–57.

Ji, H., Peng, Y., Meckes, N., Allen, S., Stewart, C.N., and Traw, M.B. (2014). ATP-Dependent Binding Cassette Transporter G Family Member 16 Increases Plant Tolerance to Abscisic Acid and Assists in Basal Resistance against Pseudomonas syringae DC3000. Plant Physiol. **166**: 879–888.

Josse, E.-M. and Halliday, K.J. (2008). Skotomorphogenesis: The Dark Side of Light Signalling. Curr. Biol. **18**.

Jung, C., Seo, J.S., Han, S.W., Koo, J., Kim, C.H., Song, S.I., Nahm, H., Choi, Y. Do, and Cheong, J.-J. (2008). Overexpression of AtMYB44 Enhances Stomatal Closure to Confer Abiotic Stress Tolerance in Transgenic Arabidopsis. Plant Physiol. **146**: 623–635.

Kami, C., Lorrain, S., Hornitschek, P., and Fankhauser, C. (2010). Light-regulated plant growth and development. In Current Topics in Developmental Biology, pp. 29–66.

Khanna, R., Shen, Y., Marion, C.M., Tsuchisaka, A., Theologis, A., Schafer, E., and Quail, P.H. (2007). The Basic Helix-Loop-Helix Transcription Factor PIF5 Acts on Ethylene Biosynthesis and Phytochrome Signaling by Distinct Mechanisms. Plant Cell **19**: 3915–3929.

Kim, J., Song, K., Park, E., Kim, K., Bae, G., and Choi, G. (2016). Epidermal Phytochrome B Inhibits Hypocotyl Negative Gravitropism Non-Cell-Autonomously. Plant Cell.

Kim, T.-H., Böhmer, M., Hu, H., Nishimura, N., and Schroeder, J.I. (2010). Guard Cell Signal Transduction Network: Advances in Understanding Abscisic Acid, CO 2 , and Ca 2+ Signaling. Annu. Rev. Plant Biol.

Kinoshita, T. and Shimazaki, K.-I. (1999). Blue light activates the plasma membrane H-ATPase by phosphorylation of the C-terminus in stomatal guard cells.

Klose, C., Viczián, A., Kircher, S., Schäfer, E., and Nagy, F. (2015). Molecular mechanisms for mediating light-dependent nucleo/cytoplasmic partitioning of phytochrome photoreceptors. New Phytol. **206**: 965–971.

Kollist, H., Nuhkat, M., and Roelfsema, M.R.G. (2014). Closing gaps: linking elements that control stomatal movement. New Phytol. **203**: 44–62.

Kwak, J.M., Murata, Y., Baizabal-Aguirre, V.M., Merrill, J., Wang, M., Kemper, A., Hawke, S.D., Tallman, G., and Schroeder, J.I. (2001). Dominant Negative Guard Cell K+ Channel Mutants Reduce Inward-Rectifying K+ Currents and Light-Induced Stomatal Opening in Arabidopsis. Plant Physiol. **127**: 473–485.

Lee, J.-H., Jung, J.-H., and Park, C.-M. (2017). Light Inhibits COP1-Mediated Degradation of ICE Transcription Factors to Induce Stomatal Development in Arabidopsis. Plant Cell Adv. Publ.

Leivar, P. and Monte, E. (2014). PIFs: Systems Integrators in Plant Development. Plant Cell.

Leivar, P., Monte, E., Al-Sady, B., Carle, C., Storer, A., Alonso, J.M., Ecker, J.R., and Quail, P.H. (2008a). The Arabidopsis Phytochrome-Interacting Factor PIF7, Together with PIF3 and PIF4, Regulates Responses to Prolonged Red Light by Modulating phyB Levels W. Plant Cell **20**: 337–352.

Leivar, P., Monte, E., Oka, Y., Liu, T., Carle, C., Castillon, A., Huq, E., and Quail, P.H. (2008b). Multiple Phytochrome-Interacting bHLH Transcription Factors Repress Premature Seedling Photomorphogenesis in Darkness. Curr. Biol. **18**: 1815–1823.

Leivar, P. and Quail, P.H. (2011). PIFs: pivotal components in a cellular signaling hub. Trends Plant Sci. **16**: 19–28.

Leivar, P., Tepperman, J.M., Monte, E., Calderon, R.H., Liu, T.L., and Quail, P.H. (2009). Definition of early transcriptional circuitry involved in light-induced reversal of PIF-imposed repression of photomorphogenesis in young Arabidopsis seedlings. Plant Cell **21**: 3535–3553.

Leonhardt, N., Kwak, J.M., Robert, N., Waner, D., Leonhardt, G., and Schroeder, J.I. (2004). Microarray Expression Analyses of Arabidopsis Guard Cells and Isolation of a Recessive Abscisic Acid Hypersensitive Protein Phosphatase 2C Mutant. Plant Cell **16**.

Leung, J., Merlot, S., and Giraudat, J. (1997). The Arabidopsis ABSCISIC ACID-INSENSITIVE2 (AB12) and ABIf Genes Encode Homologous Protein Phosphatases 2C Involved in Abscisic Acid Signal Transduction. Plant Cell **9**: 579–771.

Li, J., Li, G., Wang, H., and Wang Deng, X. (2011). Phytochrome signaling mechanisms. Arab. B. **9**: e0148.

Li, K., Yu, R., Fan, L.-M.M., Wei, N., Chen, H., and Deng, X.W. (2016). DELLA-mediated PIF degradation contributes to coordination of light and gibberellin signalling in Arabidopsis. Nat. Commun. **7**: 1–11.

Li, L. et al. (2012). Linking photoreceptor excitation to changes in plant architecture Linking photoreceptor excitation to changes in plant architecture. Genes Dev. **26**: 785–790.

Li, W.-X., Oono, Y., Zhu, J., He, X.-J., Wu, J.-M., Iida, K., Lu, X.-Y., Cui, X., Jin, H., and Zhu, J.-K. (2008). The Arabidopsis NFYA5 Transcription Factor Is Regulated Transcriptionally and Posttranscriptionally to Promote Drought Resistance. Plant Cell **20**.

Liu, B., Zuo, Z., Liu, H., Liu, X., and Lin, C. (2011a). Arabidopsis cryptochrome 1 interacts with SPA1 to suppress COP1 activity in response to blue light. Res. Commun.

Liu, H., Liu, B., Zhao, C., Pepper, M., and Lin, C. (2011b). The action mechanisms of plant cryptochromes. Trends Plant Sci **16**: 684–691.

Lorrain, S., Trevisan, M., Pradervand, S., and Fankhauser, C. (2009). Phytochrome interacting factors 4 and 5 redundantly limit seedling de-etiolation in continuous far-red light. Plant J. **60**: 449–461.

De Lucas, M., Davière, J.M., Rodríguez-Falcón, M., Pontin, M., Iglesias-Pedraz, J.M., Lorrain, S., Fankhauser, C., Blázquez, M.A., Titarenko, E., and Prat, S. (2008). A molecular framework for light and gibberellin control of cell elongation. Nature **451**: 480–484.

Lymperopoulos, P., Msanne, J., and Rabara, R. (2018). Phytochrome and phytohormones: Working in tandem for plant growth and development. Front. Plant Sci. **9**: 1037.

Ma, D., Li, X., Guo, Y., Chu, J., Fang, S., Yan, C., Noel, J.P., and Liu, H. (2016). Cryptochrome 1 interacts with PIF4 to regulate high temperature-mediated hypocotyl elongation in response to blue light. PNAS **113**: 224–229.

Mao, J., Zhang, Y.-C., Sang, Y., Li, Q.-H., and Yang, H.-Q. (2005). A role for Arabidopsis cryptochromes and COP1 in the regulation of stomatal opening. PNAS **102**.

Martín, G. et al. (2018). Circadian Waves of Transcriptional Repression Shape PIF-Regulated Photoperiod-Responsive Growth in Arabidopsis. Curr. Biol. **28**: 311–318. e5.

Martin, G., Soy, J., and Monte, E. (2016). Genomic Analysis Reveals Contrasting PIFq Contribution to Diurnal Rhythmic Gene Expression in PIF-Induced and -Repressed Genes. Front. Plant Sci. **7**: 962.

Martínez-García, J.F., Huq, E., and Quail, P.H. (2000). Direct Targeting of Light Signals to a Promoter Element–Bound Transcription Factor. Sci. Mag. **288**.

Mazzella, M.A. (2014). Hormonal networks involved in apical hook development in darkness and their response to light. Front. Plant Sci.: 1–13.

Medina, J., Rodríguez-Franco, M., Peñalosa, A., Carrascosa, M.J., Neuhaus, G., and Salinas, J. (2005). Arabidopsis mutants deregulated in RCI2A expression reveal new signaling pathways in abiotic stress responses. Plant J. **42**: 586–597.

Meyer, K., Leube, M.P., and Grill, E. (1994). A Protein Phosphatase 2C Involved in ABA Signal Transduction in Arabidopsis thaliana.

Mockler, T.C., Michael, T.P., and Priest, H.D. (2007). The Diurnal Project : Diurnal and Circadian Expression Profiling , Model-based Pattern Matching , and Promoter Analysis The Diurnal Project : Diurnal and Circadian Expression Profiling , Model-based Pattern Matching , and Promoter Analysis. Cold Spring Harb Symp Quant Biol **LXXII**: 353–363.

Monte, E., Tepperman, J.M., Al-Sady, B., Kaczorowski, K.A., Alonso, J.M., Ecker, J.R., Li, X., Zhang, Y., and Quail, P.H. (2004). The phytochrome-interacting transcription factor, PIF3, acts early, selectively, and positively in light-induced chloroplast development.

Moon, J., Zhu, L., Shen, H., Huq, E., and Lagarias, J.C. (2008). PIF1 directly and indirectly regulates chlorophyll biosynthesis to optimize the greening process in Arabidopsis. PNAS **105**: 9433–9438.

Nakamichi, N., Kiba, T., Kamioka, M., Suzuki, T., Yamashino, T., Higashiyama, T., Sakakibara, H., and Mizuno, T. (2012). Transcriptional repressor PRR5 directly regulates clock-output pathways. Proc. Natl. Acad. Sci. **109**: 17123–17128.

Nambara, E., Okamoto, M., Tatematsu, K., Yano, R., Seo, M., and Kamiya, Y. (2010). Abscisic acid and the control of seed dormancy and germination. Seed Sci. Res. **20**: 55–67.

Neff, M.M., Fankhauser, C., and Chory, J. (2000). Light: an indicator of time and place. Genes Dev. **14**: 257–271.

Ni, W., Xu, S.-L., Chalkley, R.J., Pham, T.N.D., Guan, S., Maltby, D.A., Burlingame, A.L., Wang, Z.-Y., and Quail, P.H. (2013). Multisite Light-Induced Phosphorylation of the Transcription Factor PIF3 Is Necessary for Both Its Rapid Degradation and Concomitant Negative Feedback Modulation of Photoreceptor phyB Levels in Arabidopsis. Plant Cell **25**: 2679–2698.

Ni, W., Xu, S.-L., González-Grandío, E., Chalkley, R.J., Huhmer, A.F.R., Burlingame, A.L., Wang, Z.-Y., and Quail, P.H. (2017). PPKs mediate direct signal transfer from phytochrome photoreceptors to transcription factor PIF3. Nat. Commun. **8**: 15236.

Nieto, C., López-Salmerón, V., Davière, J.M., and Prat, S. (2015). ELF3-PIF4 interaction regulates plant growth independently of the evening complex. Curr. Biol. **25**: 187–193.

Niwa, Y., Yamashino, T., and Mizuno, T. (2009). The Circadian Clock Regulates the Photoperiodic Response of Hypocotyl Elongation through a Coincidence Mechanism in Arabidopsis thaliana. Plant Cell Physiol. **50**: 838–854.

Nomoto, Y., Kubozono, S., Yamashino, T., Nakamichi, N., and Mizuno, T. (2012). Circadian clock-and PIF4-controlled plant growth: A coincidence mechanism directly integrates a hormone signaling network into the photoperiodic control of plant architectures in arabidopsis thaliana. Plant Cell Physiol. **53**: 1950–1964.

Nová Ková, M., Clav Motyka, V., Dobrev, P.I., Malbeck, J., Gaudinová, A., and Vanková, R. (2005). Diurnal variation of cytokinin, auxin and abscisic acid levels in tobacco leaves. J. Exp. Bot. **56**: 2877–2883.

Nozue, K., Covington, M.F., Duek, P.D., Lorrain, S., Fankhauser, C., Harmer, S.L., and Maloof, J.N. (2007). Ehythmic growth explained by coincidence between internal and external cues. Nature **448**.

Nozue, K., Harmer, S.L., and Maloof, J.N. (2011). Genomic Analysis of Circadian Clock-, Light-, and Growth-Correlated Genes Reveals PHYTOCHROME-INTERACTING FACTOR5 as a Modulator of Auxin Signaling in Arabidopsis 1[C][W][OA]. PLANT Physiol. **156**: 357–372.

Nozue, K., Tat, A. V, Devisetty, U.K., Robinson, M., Mumbach, M. r, Ichihashi, Y., Lekkala, S., and Maloof, J.N. (2015). Shade Avoidance Components and Pathways in Adult Plants Revealed by Phenotypic Profiling. PLoS Genet.: 1–26.

Nusinow, D.A., Helfer, A., Hamilton, E.E., King, J.J., Imaizumi, TakatoSchultz, T.F., Farré, E.M., and Kay, S.A. (2012). The ELF4-ELF3-LUX Complex Links the Circadian Clock to Diurnal Control of Hypocotyl Growth. Nature **475**: 398–402.

Oh, E., Zhu, J.-Y., and Wang, Z.-Y.Y. (2012). Interaction between BZR1 and PIF4 integrates brassinosteroid and environmental responses. Nat. Cell Biol. **14**: 802–809.

On Sun Lau, A., Song, Z., Zhou, Z., Hui Zhuang Tay, I., Wigge, P.A., and Bergmann, D.C. (2018). Direct Control of SPEECHLESS by PIF4 in the High-Temperature Response of Stomatal Development. Curr. Biol. **28**: 1273–1280.e3.

Pandey, S., Wang, R.-S., Wilson, L., Li, S., Zhao, Z., Gookin, T.E., Assmann, S.M., and Albert, R. (2010). Boolean modeling of transcriptome data reveals novel modes of heterotrimeric G-protein action. Mol. Syst. Biol. **6**.

Pandey, S., Zhang, W., and Assmann, S.M. (2007). Roles of ion channels and transporters in guard cell signal transduction. FEBS Lett. **581**: 2325–2336.

Park, E., Kim, J., Lee, Y., Shin, J., Oh, E., Chung, W. Il, Jang, R.L., and Choi, G. (2004). Degradation of phytochrome interacting factor 3 in phytochrome-mediated light signaling. Plant Cell Physiol. **45**: 968–975.

Park, E., Park, J., Kim, J., Nagatani, A., Lagarias, J.C., and Choi, G. (2012). Phytochrome B inhibits binding of Phytochrome-Interacting Factors to their target promoters. Plant J. **72**: 537–546.

Pedmale, U. V, Carol Huang, S., Zander, M., Cole, B.J., Hetzel, J., Ljung, K., B Reis, P.A., Sridevi, P., Nito, K., Nery, J.R., Ecker, J.R., and Chory, J. (2016). Cryptochromes interact directly with PIFs to control plant growth in limiting blue light HHS Public Access. Cell **164**: 233–245.

Pfeiffer, A., Nagel, M.-K., Popp, C., Wust, F., Bindics, J., Viczian, A., Hiltbrunner, A., Nagy, F., Kunkel, T., and Schafer, E. (2012). Interaction with plant transcription factors can mediate nuclear import of phytochrome B. Proc. Natl. Acad. Sci. **109**: 5892–5897.

Pfeiffer, A., Shi, H., Tepperman, J.M., Zhang, Y., and Quail, P.H. (2014). Combinatorial Complexity in a Transcriptionally Centered Signaling Hub in Arabidopsis. Mol. Plant **7**: 1598–1618.

Pillitteri, L.J. and Dong, J. (2013). Stomatal Development in Arabidopsis. In The arabidopsis book, pp. 1–26.

Quail, P.H. (2002a). Photosensory perception and signalling in plant cells: new paradigms? Curr. Opin. Cell Biol. **14**: 180–188.

Quail, P.H. (2002b). Phytochrome photosensory signalling networks. Nat. Rev. Mol. Cell Biol. **3**: 85–93.

Quail, P.H., Boylan, M.T., Parks, B.M., Short, T.W., Xu, Y., and Wagner, D. (1995). Phytochromes: photosensory perception and signal transduction. Science. **268**: 675–680.

Raz, V. and Koornneef, M. (2001). Cell division activity during apical hook development. Plant Physiol. **125**: 219–226.

Ren, H., Park, M.Y., Spartz, A.K., Wong, J.H., and Gray, W.M. (2018). A subset of plasma membrane-localized PP2C.D phosphatases negatively regulate SAUR-mediated cell expansion in Arabidopsis. PLoS Biol.

Rizzini, L., Favory, J.J., Cloix, C., Faggionato, D., O'Hara, A., Kaiserli, E., Baumeister, R., Schäfer, E., Nagy, F., Jenkins, G.I., and Ulm, R. (2011). Perception of UV-B by the arabidopsis UVR8 protein. Science (80-.). **332**: 103–106.

Rodriguez, P.L., Benning, G., and Grill, E. (1998). ABI2, a second protein phosphatase 2C involved in abscisic acid signal transduction in Arabidopsis. FEBS Lett. **421**: 185–190.

Sang, Y., Li, Q.-H., Rubio, V., Zhang, Y.-C., Mao, J., Deng, X.-W., and Yang, H.-Q. (2005). N-Terminal Domain-Mediated Homodimerization Is Required for Photoreceptor Activity of Arabidopsis CRYPTOCHROME 1. Plant Cell **17**.

Sawada, Y., Aoki, M., Nakaminami, K., Mitsuhashi, W., Tatematsu, K., Kushiro, T., Koshiba, T., Kamiya, Y., Inoue, Y., Nambara, E., and Toyomasu, T. (2008). Phytochrome- and Gibberellin-Mediated Regulation of Abscisic Acid Metabolism during Germination of Photoblastic Lettuce Seeds. Plant Physiol. **146**: 1386–1396.

Schweighofer, A., Hirt, H., and Meskiene, I. (2004). Plant PP2C phosphatases: emerging functions in stress signaling. Trends Plant Sci. **9**: 236–243.

Sentandreu, M., Martín, G., Gonzalez-Schain, N., Leivar, P., Soy, J., Tepperman, J.M., Quail, P.H., and Monte, E. (2011). Functional Profiling Identifies Genes Involved in Organ-Specific Branches of the PIF3 Regulatory Network in Arabidopsis. Plant Cell **23**: 3974–3991.

Sharkey, T.D. and Raschke, K. (1981). Effect of Light Quality on Stomatal Opening in Leaves of Xanthium strumarium L.

Sharrock, R.A. and Quail, P.H. (1989). Novel phytochrome sequences in Arabidopsis thaliana: structure, evolution, and differential expression of a plant regulatory photoreceptor family. Genes Dev. **3**: 1745–1757.

Shen, H., Moon, J., and Huq, E. (2005). PIF1 is regulated by light-mediated degradation through the ubiquitin-26S proteasome pathway to optimize photomorphogenesis of seedlings in Arabidopsis. Plant J. **44**: 1023–1035.

Shin, J., Kim, K., Kang, H., Zulfugarov, I.S., Bae, G., Lee, C.-H., Lee, D., and Choi, G. (2009). Phytochromes promote seedling light responses by inhibiting four negatively-acting phytochrome-interacting factors. PNAS **106**.

Song, S.-K. and Clark, S.E. (2005). POL and related phosphatases are dosage-sensitive regulators of meristem and organ development in Arabidopsis. Dev. Biol. **285**: 272–284.

Soy, J., Leivar, P., González-Schain, N., Martín, G., Diaz, C., Sentandreu, M., Al-Sady, B., Quail, P.H., and Monte, E. (2016). Molecular convergence of clock and photosensory pathways through PIF3-TOC1 interaction and co-occupancy of target promoters. PNAS.

Soy, J., Leivar, P., Gonzalez-Schain, N., Sentandreu, M., Prat, S., Quail, P.H., and Monte, E. (2012). Phytochrome-imposed oscillations in PIF3 protein abundance regulate hypocotyl growth under diurnal light/dark conditions in Arabidopsis. Plant J. **71**: 390–401.

Soy, J., Leivar, P., and Monte, E. (2014). PIF1 promotes phytochrome-regulated growth under photoperiodic conditions in Arabidopsis together with PIF3, PIF4, and PIF5. J. Exp. Bot.

Spartz, A.K., Lee, S.H., Wenger, J.P., Gonzalez, N., Itoh, H., Inzé, D., Peer, W.A., Murphy, A.S., Overvoorde, P.J., and Gray, W.M. (2012). The SAUR19 subfamily of SMALL AUXIN UP RNA genes promote cell expansion. Plant J. **70**: 978–990.

Spartz, A.K., Ren, H., Park, M.Y., Grandt, K.N., Lee, S.H., Murphy, A.S., Sussman, M.R., Overvoorde, P.J., and Gray, W.M. (2014). SAUR Inhibition of PP2C-D Phosphatases Activates Plasma Membrane H+-ATPases to Promote Cell Expansion in Arabidopsis. Plant Cell.

Strasser, B., Sánchez-Lamas, M., Yanovsky, M.J., Casal, J.J., and Cerdán, P.D. (2010). Arabidopsis thaliana life without phytochromes. PNAS **107**: 4776–4781.

Sutter, J.-U., Sieben, C., Hartel, A., Eisenach, C., Thiel, G., and Blatt, M.R. (2007). Abscisic Acid Triggers the Endocytosis of the Arabidopsis KAT1 K+ Channel and Its Recycling to the Plasma Membrane.

Szyroki, A., Ivashikina, N., Dietrich, P., Roelfsema, M.R.G., Ache, P., Reintanz, B., Deeken, R., Godde, M., Felle, H., Steinmeyer, R., Palme, K., and Hedrich, R. (2001). KAT1 is not essential for stomatal opening. Proc. Natl. Acad. Sci. **98**: 2917–2921.

Takahashi, Y., Cong, R., Sagor, G.H.M., Niitsu, M., Berberich, T., and Kusano, T. (2010). Characterization of five polyamine oxidase isoforms in Arabidopsis thaliana. Plant Cell Rep. **29**: 955–965.

Talbott, L.D. and Zeiger, E. (1996). Central Roles for Potassium and Sucrose in Guard-Cell Osmoregulation'.

Tallman, G. (2004). Are diurnal patterns of stomatal movement the result of alternating metabolism of endogenous guard cell ABA and accumulation of ABA delivered to the apoplast around guard cells by transpiration? J. Exp. Bot.

Toledo-Ortiz, G., Johansson, H., Lee, K.P., Bou-Torrent, J., and Stewart, K. (2014). The HY5-PIF Regulatory Module Coordinates Light and Temperature Control of Photosynthetic Gene Transcription. PLoS Genet **10**: 1004416.

Vandenbussche, F., Petrásek, J., Zádníkova, P., Hoyerová, K., Pesek, B., Raz, V., Swarup, R., Bennett, M., Zazímalova, E., Benkova, E., and Van Der Straeten, D. (2010). The auxin influx carriers AUX1 and LAX3 are involved in auxin-ethylene interactions during apical hook development in Arabidopsis thaliana seedlings. Development **137**: 597–606.

Waese, J. et al. (2017). ePlant: Visualizing and Exploring Multiple Levels of Data for Hypothesis Generation in Plant Biology. Plant Cell **29**.

Wang, F.-F., Hong-Li, L., Chun-Ying, K., and Hong-Quan, Y. (2010). Phytochrome B Is Involved in Mediating Red Light-Induced Stomatal Opening in Arabidopsis thaliana. Mol. Plant **3**: 246–259.

Wang, R.-S., Pandey, S., Li, S., Gookin, T.E., Zhao, Z., Albert, R., and Assmann, S.M. (2011). Common and unique elements of the ABA-regulated transcriptome of Arabidopsis guard cells. BMC Genomics **12**.

Wang, S., Chang, Y., and Ellis, B. (2016). Overview of OVATE FAMILY PROTEINS, A Novel Class of Plant-Specific Growth Regulators. Front. Plant Sci. **7**: 1–8.

Wang, Y., Noguchi, K., Ono, N., Inoue, S.-I., Terashima, I., and Kinoshita, T. (2014). Overexpression of plasma membrane H + -ATPase in guard cells promotes light-induced stomatal opening and enhances plant growth. PNAS **111**: 533–538.

Weatherwax, S.C., Ong, M.S., Degenhardt, J., Bray, E.A., and Tobin, E.M. (1996). The Interaction of Light and Abscisic Acid in the Regulation of Plant Gene Expression. Plant Physiol. **111**: 363–370.

Weisshaar, B., Wisman, E., Hartmann, U., Sagasser, M., Baumann, E., Palme, K., Hahlbrock, K., and Saedler, H. (1998). Knock-out mutants from an En-1 mutagenized Arabidopsis thaliana population generate phenylpropanoid biosynthesis phenotypes. Proc. Natl. Acad. Sci. U. S. A. **95**: 12432–12437.

Widjaja, I., Lassowskat, I., Bethke, G., Eschen-Lippold, L., Long, H.H., Naumann, K., Dangl, J.L., Scheel, D., and Lee, J. (2010). A protein phosphatase 2C, responsive to the bacterial effector AvrRpm1 but not to the AvrB effector, regulates defense responses in Arabidopsis. Plant J. **61**: 249–258.

Yang, X., Montano, S., and Ren, Z. (2015). How Does Photoreceptor UVR8 Perceive a UV-B Signal. Photochem Photobiol **91**: 29–39.

Yang, Y., Costa, A., Leonhardt, N., Siegel, R.S., and Schroeder, J.I. (2008). Isolation of a strong Arabidopsis guard cell promoter and its potential as a research tool. Plant Methods **4**: 1–15.

Yi, C. and Deng, X.W. (2005). COP1-from plant photomorphogen-esis to mammalian tumorigenesis. Trends Cell Biol.

Yin, Y., Vafeados, D., Tao, Y., Yoshida, S., Asami, T., and Chory, J. (2005). A New Class of Transcription Factors Mediates Brassinosteroid-Regulated Gene Expression in Arabidopsis. Cell **120**: 249–259.

Zadnikova, Petra, Petrasek, J., Marhavy, P., Raz, V., Vandenbussche, F., Ding, Z., Schwarzerova, K., Morita, M.T., Tasaka, M., Hejatko, J., Van Der Straeten, D., and Benkova, E. (2010). Role of PIN-mediated auxin efflux in apical hook development of Arabidopsis thaliana. Development **137**.

Zhang, Y., Mayba, O., Pfeiffer, A., Shi, H., and Tepperman, J.M. (2013). A Quartet of PIF bHLH Factors Provides a Transcriptionally Centered Signaling Hub That Regulates Seedling Morphogenesis through Differential Expression-Patterning of Shared Target Genes in Arabidopsis. PLoS Genet **9**: 1003244.

Zhu, J.-Y., Oh, E., Wang, T., and Wang, Z.-Y.Y. (2016). TOC1-PIF4 interaction mediates the circadian gating of thermoresponsive growth in Arabidopsis. Nat. Commun. **7**: 13692.

Annex

Report

Current Biology

Circadian Waves of Transcriptional Repression Shape PIF-Regulated Photoperiod-Responsive Growth in *Arabidopsis*

Highlights

- Circadian waves transcriptionally control the PIF-regulated diurnal gene network
- The clock components PRR9/7/5/1 sequentially gate PIF-promoted growth from morning onward
- *CDF5* is antagonistically targeted by PRRs and PIFs to restrict growth to dawn
- CDF5 promotes cell elongation downstream of the PRR/PIF module

Authors

Guiomar Martín, Arnau Rovira, Nil Veciana, ..., Karen J. Halliday, Pablo Leivar, Elena Monte

Correspondence

elena.monte@cragenomica.es

In Brief

Martín et al. show that the clock components PRRs dynamically antagonize the phytochrome/PIF-regulated transcriptional network across the diurnal cycle. Sequential morning-to-midnight repression of PIF function by waves of PRRs gate growth to dawn, and the authors identify *CDF5* as a co-target necessary to optimize fitness.

Martín et al., 2018, Current Biology *28*, 311–318
January 22, 2018
https://doi.org/10.1016/j.cub.2017.12.021

CellPress

Current Biology
Report

Circadian Waves of Transcriptional Repression Shape PIF-Regulated Photoperiod-Responsive Growth in *Arabidopsis*

Guiomar Martín,[1] Arnau Rovira,[1] Nil Veciana,[1] Judit Soy,[1] Gabriela Toledo-Ortiz,[3,4] Charlotte M.M. Gommers,[1] Marc Boix,[1] Rossana Henriques,[1] Eugenio G. Minguet,[2] David Alabadí,[2] Karen J. Halliday,[4] Pablo Leivar,[1,5] and Elena Monte[1,6,7,*]
[1]Center for Research in Agricultural Genomics (CRAG), CSIC-IRTA-UAB-UB, Campus UAB, Edifici CRAG, Bellaterra, 08193 Barcelona, Spain
[2]Instituto de Biología Molecular y Celular de Plantas (IBMCP), CSIC-UPV, Ingeniero Fausto Elio s/n, 46022 Valencia, Spain
[3]Lancaster Environment Center, Lancaster University, Lancaster LA1 4YQ, UK
[4]The University of Edinburgh, CH Waddington Building, Max Born Crescent, Edinburgh EH9 3BF, UK
[5]Bioengineering Department, IQS School of Engineering, Via Augusta 390, 08017 Barcelona, Spain
[6]Consejo Superior de Investigaciones Científicas (CSIC), 08028 Barcelona, Spain
[7]Lead Contact
*Correspondence: elena.monte@cragenomica.es
https://doi.org/10.1016/j.cub.2017.12.021

SUMMARY

Plants coordinate their growth and development with the environment through integration of circadian clock and photosensory pathways. In *Arabidopsis thaliana*, rhythmic hypocotyl elongation in short days (SD) is enhanced at dawn by the basic-helix-loop-helix (bHLH) transcription factors PHYTOCHROME-INTERACTING FACTORS (PIFs) directly inducing expression of growth-related genes [1–6]. PIFs accumulate progressively during the night and are targeted for degradation by active phytochromes in the light, when growth is reduced. Although PIF proteins are also detected during the day hours [7–10], their growth-promoting activity is inhibited through unknown mechanisms. Recently, the core clock components and transcriptional repressors PSEUDO-RESPONSE REGULATORS PRR9/7/5 [11, 12], negative regulators of hypocotyl elongation [13, 14], were described to associate to G boxes [15], the DNA motifs recognized by the PIFs [16, 17], suggesting that PRR and PIF function might converge antagonistically to regulate growth. Here we report that PRR9/7/5 and PIFs physically interact and bind to the same promoter region of pre-dawn-phased, growth-related genes, and we identify the transcription factor CDF5 [18, 19] as target of this interplay. In SD, *CDF5* expression is sequentially repressed from morning to dusk by PRRs and induced pre-dawn by PIFs. Consequently, *CDF5* accumulates specifically at dawn, when it induces cell elongation. Our findings provide a framework for recent TIMING OF CAB EXPRESSION 1 (TOC1/PRR1) data [5, 20] and reveal that the long described circadian morning-to-midnight waves of the PRR transcriptional repressors (PRR9, PRR7, PRR5, and TOC1) [21] jointly gate PIF activity to dawn to prevent overgrowth through sequential regulation of common PIF-PRR target genes such as *CDF5*.

RESULTS AND DISCUSSION

Genome-wide analysis of chromatin immunoprecipitation sequencing (ChIP-seq) data for the PHYTOCHROME-INTERACTING FACTOR (PIF) quartet (PIFq) (PIF1, PIF3, PIF4, and PIF5)-associated [16] and PSEUDO-RESPONSE REGULATOR 5 (PRR5)-, PRR7-, and/or PRR9-associated [15] loci revealed an overlap of 1,460 genes between PIF-bound genes (57.5% of all PIF-bound genes) and at least one of the three PRRs examined (“PIF-PRR genes”) (Figure 1A, left; Data S1). The overlap between PIF-bound and PRR5-, PRR7-, or PRR9-bound genes, when examined individually or in combination, is shown in the middle panel of Figure 1A (Data S1). The distance between PRR and PIF binding sites indicates that PRRs and PIFs associate to the same genomic regions (Figure 1A, right), in accordance with results showing enrichment of G-box-containing motifs in PRR-bound regions [15, 22]. We detected interaction of PIF3 and PIF4 with PRR5 (PIF4 in accordance with [20]), PRR7, and PRR9 by yeast two-hybrid assays (Figure S1A). We further confirmed PIF3-PRR interaction *in planta* by bimolecular fluorescence complementation (BiFC) assays (Figure 1B). These data suggest that, similarly to recent findings for TIMING OF CAB EXPRESSION 1 (TOC1) and PIF3 and PIF4 [5, 20], PIFs and PRRs may bind together at G boxes to co-regulate the expression of shared PIF-PRR target genes. Based on the described activity of PRRs as transcriptional repressors [11, 12, 20], PIF-PRR interaction also agrees with the possibility that PRR5/7/9 might target PIFs to repress their ability to activate shared PIF-PRR target genes, as shown recently for TOC1 and PIFs [5, 20].

Functional classification indicated that “PIF-PRR” genes are enriched in growth-related categories (Figure S1B) and are over-represented at the elongation phases 18–23 specifically under short days (SD) (Figures 1C and S1C; Data S1), suggesting that PIFs and PRRs jointly target genes involved in the induction

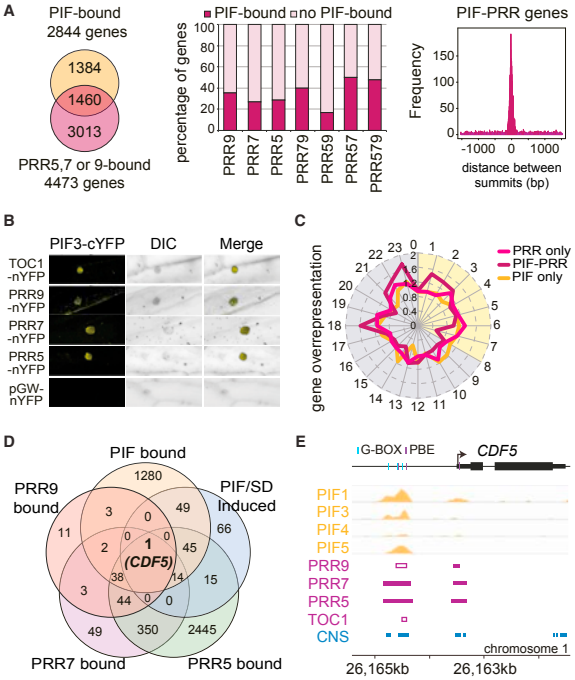

Figure 1. Analysis of Coincident Co-binding of PRRs and PIFs to Dawn-Phased Genes under SD Identifies *CDF5* as a PIF- and PRR5/7/9-Bound Gene

(A) Left: comparison of PIF-bound [16] and PRR5-, 7- and/or PRR9-bound [15] genes (gene lists are provided in Data S1) defines three groups of genes: "PIF only" (1,384 genes), "PRR only" (3,013 genes), and "PIF-PRR" (1,460 genes). Middle: percentage of PIF-bound genes in genes bound by single or a combination of PRRs. Right: frequency of pairwise distance in base pairs (bp) between the PIF- and PRR-binding sites in each of the "PIF-PRR" co-bound genes.

(B) BiFC assay of the PRRs and PIF3 fusions to N- and C-terminal fragments of YFP, respectively, in transfected onion cells. The combinations of PIF3-cYFP and TOC1-nYFP or pGW-nYFP were used as positive and negative control, respectively. Left: YFP fluorescence image. Center: bright-field image. Right: merge of YFP fluorescence and bright-field image.

(C) Expression phases in SD of gene sets defined in (A): "PIF-PRR" (purple), "PRR only" (pink), and "PIF only" (yellow). Phases are indicated on the circumference, and fold-change phase enrichment of genes (count/expected) is indicated on the radius. Day is shown in yellow, and night in gray.

(D) Comparison of PIF- [16], PRR5-, 7-, and PRR9-bound [15], and "PIF/SD-induced" [4] genes (see Data S1 for details).

(E) Visualization of ChIP-seq and ChIP-qPCR data in the genomic region encompassing the *CDF5* locus co-bound by PIFs, PRRs, and TOC1. For PIF (orange), ChIP-seq tracks show the pileup of all the reads obtained from MACS (model-based analysis of ChIP-seq) analyses of the dataset from each experiment [16]. Each corresponding WT-ChIP/input control is overlaid in dark gray. For PRR (purple), filled rectangles indicate the PRR9, PRR7, and PRR5 peaks defined by ChIP-seq in [15]. Empty rectangles indicate peaks only described by ChIP-qPCR, in [22] for PRR9 and in Figure 2A for TOC1. Conserved non-coding sequences (CNS; blue) are defined in [23]. For G and PBE box, vertical lines indicate motif positions. See also Figure S1 and Data S1.

of growth under SD conditions. We compared PRR- and PIF-bound genes with the recently defined PIF- and SD-induced (PIF/SD-induced) gene set of PIFq-regulated genes under SD containing dawn-phased and growth-related genes [4]. Strikingly, one gene (*CDF5*) was PIF/SD induced and bound by all PRRs and PIFs (Figure 1D; Data S1). Previous ChIP experiments showed binding of PRR5/7/9 and possibly TOC1 to this G-box/PBE-containing region [15, 22, 24] (Figure 1E; see legend for details). This region coincides with conserved noncoding sequences (CNSs) among crucifer regulatory regions (Figure 1E) [23], suggesting that the binding sites on the *CDF5* promoter have been subjected to selective constraint, consistent with functionality relevance.

We verified binding of PRR7, TOC1, PIF3, and PIF4 to the *CDF5* promoter (*pCDF5*) region encompassing the G/PBE boxes at different times under SD conditions by time-course analysis using ChIP-qPCR (quantitative PCR). Statistically significant and robust PRR7 binding to *pCDF5* was observed at ZT8 and ZT14 (ZT, zeitgeber time) and was substantially decreased at ZT24, whereas maximum of TOC1 binding was at ZT14 (Figure 2A). For PIF3 and PIF4, tagged lines driven by the endogenous PIF3 promoter and 35S were used, respectively [25, 26] (Figure S2A). Statistically significant binding of PIF3 to *pCDF5* was detected at ZT24, whereas significant PIF4 binding was detected in all three time points and incremented along the night (Figure 2A). These binding dynamics are consistent with the pattern of accumulation of each protein in SD [5, 8, 27]. Together, these data are consistent with binding of the PIFs, PRRs, and TOC1 proteins in SD to the same region of the *CDF5* promoter located approximately 1,000 bp upstream of the transcription start site (TSS) and with binding dictated by their protein abundance.

To examine how PIF and PRR7 interaction (Figures 1B and S1A) and binding to the *CDF5* promoter (Figure 2A) affect *CDF5* expression, we first tested *CDF5* expression in *pif* and *prr7* mutants under SD at ZT9, when PRR7 levels are maximum and PIFs start to accumulate [7, 8, 10, 27, 28]. *CDF5* levels were upregulated in *prr7* (Figure 2B), an effect strongly suppressed by

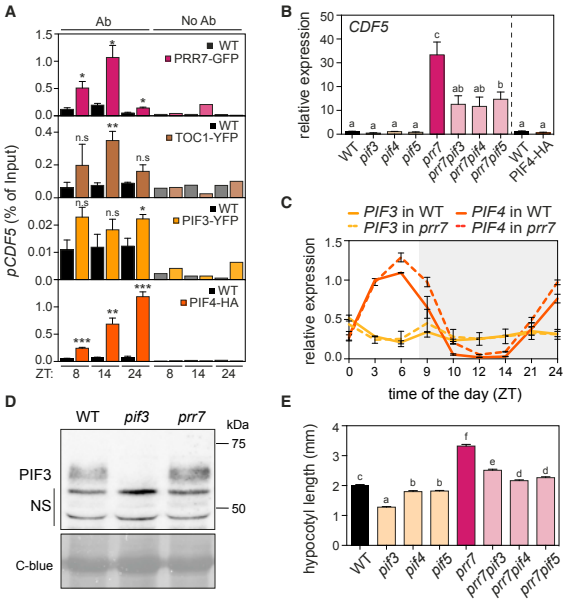

Figure 2. PRR7 Represses PIF3 Ability to Induce *CDF5* Expression in SD

(A) PRR7, TOC1, PIF3, and PIF4 binding to the G-box-containing region of the *CDF5* promoter at ZT8, ZT14, and ZT24 under SD. For ChIP-qPCR analysis, samples of SD-grown *pPRR7::PRR7-GFP* (PRR7-GFP), *pTOC1::TOC1:YFP* (TOC1-YFP), *pPIF3::YFP:PIF3* (YFP-PIF3), and *35S::PIF4-HA* (PIF4-HA) were harvested at the indicated times during the third day and were immunoprecipitated with anti-GFP or anti-HA antibodies. Data are from three independent ChIP experiments, and error bars indicate the SE. Statistically significant differences between mean values by Student's t test relative to the WT are shown (*$p < 0.05$, **$p < 0.01$, ***$p < 0.001$; n.s., not significant). WT controls were Col-0 for YFP-PIF3, PIF4-HA, and PRR7-GFP and C24 for TOC1-YFP seedlings. Ab, samples immunoprecipitated with antibody; No Ab, control samples immunoprecipitated without antibody.

(B) *CDF5* expression levels in WT, *pif3*, *pif4*, *pif5*, *prr7*, *prr7pif3*, *prr7pif4*, *prr7pif5*, and PIF4-HA. Samples were harvested at ZT9 during the third day of growth (ZT8 for PIF4-HA), analyzed by qRT-PCR, and normalized to *PP2A*. Data are from three independent biological replicates relative to the WT set at one. Different letters denote statistically significant differences among means by Tukey b test ($p < 0.05$). Error bars indicate the SE.

(C) WT and *prr7* seedlings grown for 2 days in SD conditions were harvested during the third day at the indicated times. Expression levels of *PIF3* and *PIF4* were analyzed by qRT-PCR, and values were normalized to *PP2A*. Data plotted are the mean ± SE relative to *PIF4* WT at ZT3 set at one, with n = 2 independent biological experiments, each assayed in triplicate.

(D) PIF3 protein levels in 3-day-old SD-grown WT and *prr7* seedlings at ZT24. C-blue, Coomassie blue; NS, non-specific bands.

(E) Hypocotyl length in seedlings as in (B) (except for PIF4-HA) grown for 3 days in SD. Different letters denote statistically significant differences among means by Tukey b test ($p < 0.05$). Data are the means ± SE of at least 50 seedlings.

See also Figure S2.

the *pif* mutations in the *prr7pif* double mutants (Figure 2B), suggesting that PIFs and PRR7 regulate *CDF5* expression antagonistically as transcriptional activator and repressor, respectively. Interestingly, because PIF3 transcript and protein levels are not affected in *prr7* (Figures 2C and 2D); together, these data suggest that, as described for TOC1 [5], PRR7 acts directly as transcriptional repressor of PIF3 activity in the regulation of *CDF5*. In agreement, the *prr7* long hypocotyl phenotype was also partially suppressed with genetic removal of PIF3 (Figure 2E). However, because the detected binding of PIF3 to the *CDF5* promoter at ZT8 or ZT14 was not statistically significant (Figure 2A), we cannot discard that the effect of PRRs on PIF3 might involve inhibition of PIF3 binding to the *CDF5* promoter. Suppression of hypocotyl phenotype was also observed for *prr7pif4* and *prr7pif5* compared to *prr7* (Figure 2E), which suggests that PRR7 directly represses PIF4 transcriptional activity, as previously shown for TOC1 and PIF4 [20] and might also repress PIF5. This scenario might be potentially more complex given that *PIF4/5* transcription is regulated by the clock under SD [2] and that at least *PIF4* transcript levels are slightly higher in *prr7* (Figure 2C), in accordance with recent data showing *PIF4* de-repression in *prr* multiple mutants [29]. However, the observation that *CDF5* expression in overexpressing PIF4-HA lines at ZT8 was similar to *pif4* (Figure 2B), a time point at which both PRR7 and PIF4 are co-bound to the *pCDF5* (Figure 2A), provides strong support that PRR7 directly suppresses PIF4 transcriptional activation activity toward *CDF5*.

We next examined the antagonistic PIF-PRR interaction in the direct regulation of *CDF5* across the diurnal cycle. Under SD, phytochrome imposes oscillation of PIF3 and probably PIF1 proteins to progressively accumulate during the night and to degrade rapidly in the morning maintaining residual levels during the day [8, 9]. For PIF4 and possibly PIF5, clock and light regulation result in PIF accumulation also during daytime (Figure 2C) [7, 10]. In contrast, PRR accumulation is sequential (PRR9/7/5/TOC1) from morning to midnight (Figure 3A) [21, 27]. We therefore expected *CDF5* to oscillate with a peak in the early morning and at the end of the night (when the presence of the PIFs is at a maximum) and a trough from morning to midnight (when PRRs accumulate). Indeed, *CDF5* in the wild-type (WT) was detected during the first part of the day (ZT0–ZT3), declined to almost undetectable levels through ZT15, and accumulated after ZT15 to peak at dawn (Figure 3B). Expression at dawn in *pifq* SD and in WT LL (continuous light; a free-running condition in which

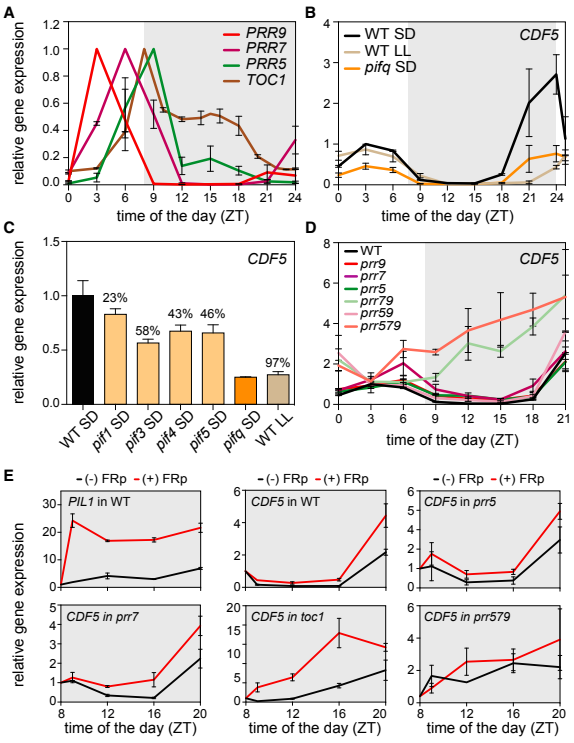

Figure 3. PRRs and PIFs Antagonistically Regulate *CDF5* to Dawn-Phase Its Expression under Diurnal SD Conditions

(A) Transcriptional waves of *PRR9/7/5* and *TOC1* expression during the third day in SD at the indicated times. Each gene is expressed relative to its maximum expression value set at one.

(B–D) *CDF5* expression in WT, *pif*, and *prr* analyzed by qRT-PCR.

(B) Expression in 2-day-old SD-grown seedlings harvested during the third day at the indicated times in seedlings kept under SD or moved to continuous light (LL). Data are relative to WT SD at ZT3.

(C) Expression in 3-day-old seedlings at ZT24 grown as in (B). Data are from two independent biological replicates and are relative to WT samples set at one. The percentage is the contribution of each PIF to *CDF5* expression in SD considering *pifq* and WT values as 0% and 100%, respectively. Error bars indicate the SE.

(D) Expression in WT, *prr5*, *prr7*, *prr9*, *prr59*, *prr79*, and *prr579* seedlings grown for 2 days in SD conditions during the third day at the indicated times. Expression is relative to *CDF5* WT at ZT3.

(E) *PIL1* and *CDF5* expression in WT, *prr* and *toc1* analyzed by qRT-PCR. Two-day-old SD-grown seedlings were treated with a 15-min far-red pulse (FRp) at ZT8 on the third day ((+) FRp samples, in red), and harvested during the night at ZT9, ZT12, ZT16, and ZT20. (−) FRp control samples (in black) did not receive a FRp. Data are relative to ZT8 set at one for each genotype.

(A–E) All samples were normalized to *PP2A*.

(A, B, D, and E) Data plotted are the mean ± SE, with n = 2 independent biological experiments, each assayed in triplicate.

See also Figures S2 and S3.

PIFs do not accumulate) [28] was lower than WT SD (Figure 3B), supporting the notion that transcript induction leading to the oscillatory pattern of *CDF5* expression in SD depends on the presence of the PIFs (Figure 3B). Analysis of *CDF5* levels in single *pif* and multiple *pifq* (defective in PIF1/3/4/5) mutants at ZT24 showed that the PIFq collectively induces *CDF5* expression at dawn, with PIF1 having a lesser contribution (Figure 3C). *CDF5* transcript levels dropped in the WT after 1 hr of morning light (Figure 3B), concurrent with phy-induced PIF degradation. In contrast, at ZT9, when *CDF5* expression in the WT is almost non-detectable, *CDF5* expression was significantly higher in *prr5*, *prr7*, *prr79*, *prr59*, and *prr579*, with a major contribution for PRR7 (Figure S2B). Compared to the WT, *CDF5* expression was higher in *prr7* from ZT3 through midnight (Figure 3D), whereas in *prr59* and *prr79* mutants, *CDF5* expression was only slightly higher at dawn in *prr59* and higher from dusk to dawn in *prr79* (Figure 3D). In *toc1*, de-repression of *CDF5* was early compared to the WT (Figure S2C), similar to other PIF-TOC1 co-targets [5]. Because cross-regulation was described in the PRRs [30], with nuclear accumulation of TOC1 depending partly on PRR5, it is likely that TOC1 contributes to the phenotype of PRR5-deficient mutant backgrounds. We also characterized *PRR5* and *PRR7* expression in *prr79* and *prr59* double mutants, respectively. Levels of *PRR5* and *PRR7* were ~1.5-fold higher in *prr59* and *prr79* compared to the WT, and *PRR5* phase was delayed in *prr79*, indicative of intricate cross-regulatory pathways (Figure S2D). Significantly, *CDF5* expression in the *prr579* mutant from ZT3–ZT21 was almost linear (Figure 3D), in accordance with the PRRs (with TOC1 possibly also contributing) being responsible for the repression of *CDF5* expression from morning to midnight.

To further examine the PIF-PRR antagonistic interplay, we artificially induced PIF accumulation at the beginning of the night period when PRR levels are high (Figure 3A) [27] by giving a far-red light pulse (FRp) at ZT8 [5, 28]. As control, we used *PIL1*, a direct PIF target and marker gene for PIF abundance and activity [8]. *PIL1* levels accumulated in the WT immediately after the FRp (Figure 3E), in agreement with the rapid accumulation of PIF proteins after a FRp [9, 25, 31], as well as with PRRs not interfering significantly with PIF activity in the regulation of *PIL1* given that *PIL1* is not a direct target of all PRRs [15]. In striking contrast,

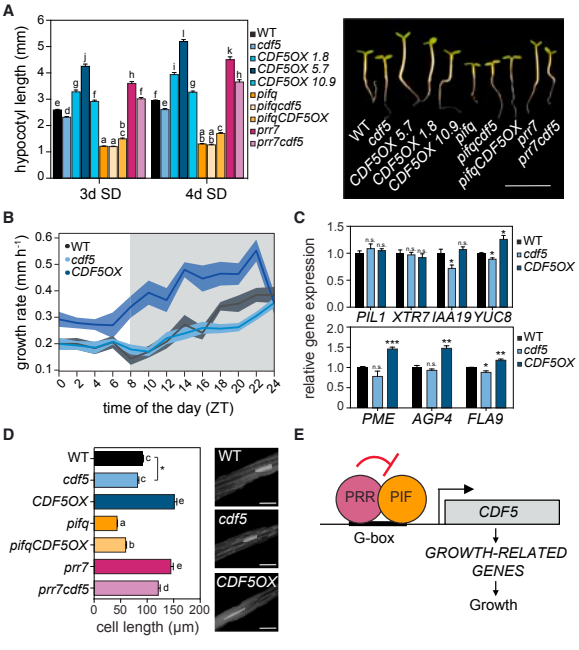

Figure 4. PRR- and PIF-Mediated Regulation of Cell Elongation Requires CDF5

(A) Hypocotyl length of WT, *cdf5*, *CDF5OX*, *pifq*, *pifqCDF5OX*, *prr7*, and *prr7cdf5* grown for 3 and 4 days in SD (left). Data are the means ± SE of at least 35 seedlings. Different letters denote statistically significant differences among means by Tukey b test ($p < 0.05$). Visible phenotypes of 3-day-old seedlings are shown on the right. Scale bar, 5 mm.

(B) Hypocotyl elongation rate for WT, *cdf5*, and *CDF5OX 5.7* under SD conditions. Seedling growth was monitored every 2 hr during the third day. The average of 12 seedlings is shown, and the SE is indicated by the shaded area.

(C) Expression of PIF-regulated growth marker genes (top) and cell wall genes (bottom) in 3-day-old SD-grown WT, *cdf5*, and *CDF5OX 5.7* seedlings at ZT24, analyzed by qRT-PCR and normalized to *PP2A*. Data are from three independent biological replicates normalized to the WT set at one. Error bars indicate the SE. Statistically significant differences between mean values by Student's t test relative to WT are shown (*$p < 0.05$, **$p < 0.01$, ***$p < 0.001$; n.s., not significant).

(D) Left: quantification of cell length in WT, *cdf5*, *CDF5OX 5.7*, *pifq*, *pifqCDF5OX*, *prr7*, and *prr7cdf5*. Seedlings were grown for 3 days in SD. Data are means ± SE of at least 100 cells from three to four independent seedlings. Different letters or an asterisk denote statistically significant differences among means by Tukey b test ($p < 0.05$) or by Student's t test ($p < 0.05$), respectively. Right: visual phenotypes of cell area in 3-day-old SD-grown WT, *cdf5* and *CDF5OX 5.7* seedling hypocotyls. Scale bar, 200 μm.

(E) Model of the proposed role of PRRs as repressors of PIF activity to regulate cell elongation through CDF5. PIFs bind to the *CDF5* promoter and induce *CDF5* transcription in the absence of PRRs. If PRRs are present, PRRs repress PIF transcriptional activity though direct PIF-PRR interaction. Based on current data, PRRs and PIFs could bind to the same or different nearby G boxes, or alternatively, PRRs could bind indirectly to G boxes through DNA-bound PIFs or other G box and PRR-binding factors. Sequential PRR9/7/5 and PRR1/TOC1 accumulation from morning to midnight gate PIF induction of *CDF5* to dawn, when it induces hypocotyl cell elongation by upregulating growth-related genes like *YUC8* or *FLA9*.

See also Figures S3 and S4.

expression induction of the PIF-PRR target *CDF5* was repressed in the WT during the first part of the night (ZT8–ZT16) after a FRp, similarly to the control (−FRp) samples (Figure 3E). Interestingly, this repression was much lower in *prr5* and *prr7* and was not observed in *prr579*. In *toc1*, early *CDF5* expression compared to the WT (Figures 3E and S2C) was more evident in +FRp samples.

Although part of the effect seen in *prr* mutants might come from elevated PIF4/5 levels due to their transcriptional derepression (Figure 2C) [2, 29], together these data support the conclusion that the PRR9/7/5 and TOC1 prevent the transcriptional activation of *CDF5* by PIFs. Given the sequential pattern of expression of *PRR9*, *PRR7*, *PRR5*, and *TOC1* (Figure 3A) [21] and the progressive accumulation of the PIFs along the night in SD conditions [8], our results suggest that *CDF5* is sequentially targeted by *PRR9*, *PRR7*, *PRR5*, and *TOC1* to repress its expression from morning to midnight (when PRR and TOC1 levels are high), to gate PIF direct induction of *CDF5* to dawn when the levels of PRRs and TOC1 are low and PIFs reach a peak in abundance. We propose that *CDF5* might be a novel target of this PRR and PIF interplay in the promotion of hypocotyl elongation.

Our findings suggest a model in which the antagonistic regulation of *CDF5* gene expression by PRRs and PIFs described above might underlie rhythmic growth under SD. In agreement, we observed correlation between the magnitude of hypocotyl length under our SD conditions and *CDF5* levels in *prr* and *pifq* mutants (Figures S3A and S3B). To test this model genetically, we generated seedlings ectopically expressing *CDF5* in a *cdf5* mutant background (*CDF5OX*) (Figure S3C) and quantified the hypocotyl phenotype of WT, *CDF5OX,* and *cdf5* lines under SD. *cdf5* mutants were slightly shorter than WT SD-grown seedlings, whereas *CDF5OX* lines suppressed the *cdf5* phenotype and showed a range from subtle to robustly elongated hypocotyls compared to the WT (Figures 4A). We analyzed the elongation rate of *cdf5* and *CDF5OX* lines under SD compared to the WT (Figure 4B). As described, the growth rate of WT seedlings is highest during the second half of the night [2]. Elongation rate of *cdf5* seedlings was similar to the WT during the day and first part of the night, but it was reduced during the last part of

the night, when *CDF5* expression in the WT is maximum, consistent with their short phenotype. Interestingly, elongation rate of *CDF5OX* seedlings was constantly high during the day and most part of the night (Figure 4B). Together, our data suggest that transcriptional control of *CDF5* expression by the PIFs and PRRs is a key regulatory mechanism in growth control.

Next, to genetically test the interplay between CDF5, PIFs and PRRs, we generated *prr7cdf5*, *pifqcdf5*, and *pifqCDF5OX* mutants (Figure S3C) to study their hypocotyl phenotypes. We observed that in SD, the quintuple *pifqcdf5* mutant displayed a phenotype similar to *pifq*, indicating that the *cdf5* mutation did not have an additive effect on *pifq* mutation (Figure 4A). This result agrees with PIFq and CDF5 acting in the same signaling pathway. Overexpression of *CDF5* in the *pifq* background partially restored the *pifq* phenotype (Figures 4A), providing additional evidence that CDF5 contributes to growth downstream of the PIFs. Finally, comparison of *prr7* with *prr7cdf5* mutants showed that the long phenotype of *prr7* under SD is reduced when CDF5 is removed in *prr7cdf5* (Figures 4A), suggesting that exaggerated growth in *prr7* is partially a consequence of having elevated levels of CDF5. Together, our results confirm our model in which PRRs and PIFs directly and antagonistically regulate *CDF5* expression to precisely gate CDF5 growth-promoting activity to the end of the night.

We hypothesized that CDF5 might control the expression of growth-related genes at dawn downstream of PIFq. We selected a few PIF-regulated [4], growth-related cell-wall [32] and SD growth-marker genes [6, 8] to test for their expression in *cdf5* and *CDF5OX* lines. As shown in Figure 4C, *PIL1* and *XTR7* were not significantly affected in *cdf5* or *CDF5OX*, and *IAA19*, *YUCCA8*, and three selected cell-wall-related genes (*AGP4*, *PME*, and *FLA9*) show significant downregulation in *cdf5* (*IAA19*), upregulation in *CDF5OX* (*PME* and *AGP4*), or both (*YUC8* and *FLA9*) compared to the WT. Interestingly, *AGP4* and *PME* are not PIF-bound genes. These results suggest branching downstream of PIFq, with CDF5 regulating a subset of the PIFq-regulated growth-related genes, in accordance to the partial suppression of the *pifq* phenotype by *CDF5OX* shown above (Figure 4A). Examination of the hypocotyl cell size in SD-grown WT, *cdf5*, and *CDF5OX* seedlings by confocal microscopy imaging clearly showed elongated cells in *CDF5OX* hypocotyls compared to the WT, whereas cells in *cdf5* appeared shorter (Figure 4D, right), which was confirmed by quantification of the hypocotyl cell length (Figure 4D, left). Next, we tested *prr7*, which exhibited a longer cell phenotype partially suppressed by genetic removal of *CDF5* in *prr7cdf5* (Figure 4D). In contrast, cell length in *pifq* was shorter than WT, a phenotype that was partially recovered by *CDF5OX* (Figure 4D, left). Together, these results support a role for CDF5 in the promotion of cell elongation under the inductive growth condition of SDs downstream of PRRs and PIFs.

Conclusions

Here we found that members of the PRR family of transcriptional repressors (PRR5, PRR7, and PRR9), with a key role in the regulation of the central circadian oscillator and clock output processes in plants [12], target growth-related genes that are directly induced by the growth-promoting PIF transcription factors. Given the coincident DNA-binding specificity of PRRs and PIFs (Figure 1A) [15, 33], the PIF-PRR physical interaction in the nucleus (Figures 1B and S1A), and their accumulation dynamics during SD photoperiods (Figure 3A) [2, 7, 8, 11, 21], we propose a model in which successive binding of the PRR9, PRR7, and PRR5 to the G box elements of shared PIF and PRR target genes (like the growth-promoting *CDF5*) acts to sequentially repress transcription of the PIF-induced transcriptional network starting in the morning (Figures 4E and S4). Given that PRR9/7/5 have not been shown to bind DNA directly, our results agree with the possibility that PIFs might bridge the binding of PRRs to DNA, although competition by direct binding of PRR to G boxes, or through a PRR- and G-box-binding factor different than PIFq, cannot be completely discarded based on our results. These findings define an expanded framework for previous results showing PRR1/TOC1 repression of PIF transcriptional activity at midnight [5]. At dawn, PRRs and TOC1 are not present, PIF protein accumulation reaches a maximum, and elongation is promoted by PIF-induced expression of growth-promoting genes like *CDF5* (Figure 4E). Collectively, our data reveal that gating of growth occurs not only at the post-dusk hours of the night as previously described for TOC1 [5], but instead starts in the morning and covers all the day period until midnight through the sequential action of the PRR family of transcriptional repressors. The molecular mechanism described here could explain why growth rate under SD photoperiods is low [2] from morning to midnight in the presence of low PIF3 and PIF1 [9, 34] and considerable high amounts of PIF4 (and most likely PIF5) [7, 10], a regulation critical for fitness by preventing overgrowth (Figure 4A). Our results reveal that gating of growth has evolved in plants to encompass the orchestrated sequential action of members of the PRR family (PRR9/7/5/1) of transcriptional repressors that peak in waves from morning to midnight. This function highlights the dual role of the PRR family of clock oscillator components, as regulators of central clock components and cycling outputs [11, 21, 35], and as repressors of the physiological output of growth in combined regulation with light pathways that control accumulation of PIFs.

STAR★METHODS

Detailed methods are provided in the online version of this paper and include the following:

- KEY RESOURCES TABLE
- CONTACT FOR REAGENT AND RESOURCE SHARING
- EXPERIMENTAL MODEL AND SUBJECT DETAILS
- METHOD DETAILS
  - Seedling Growth and Hypocotyl and Cell Measurements
  - ChIP-seq Data Analysis and Visualization
  - Chromatin Immunoprecipitation (ChIP) Assays
  - Yeast Two-Hybrid Assays
  - Bimolecular Fluorescence Complementation (BiFC) Assays
  - Protein Extraction and Immunoblot
  - Gene Expression Analysis
- QUANTIFICATION AND STATISTICAL ANALYSIS

SUPPLEMENTAL INFORMATION

Supplemental Information includes four figures, one table, and one data file and can be found with this article online at https://doi.org/10.1016/j.cub.2017.12.021.

ACKNOWLEDGMENTS

We thank D. Somers, S. Prat, G. Coupland, and R. McClung for sharing seed and plasmid resources. We thank G. Steele for generating double and triple *prr* mutants and the *prrpif* mutant combinations. The work in this manuscript was supported by grants from the Spanish "Ministerio de Economía y Competitividad" (MINECO) (BIO2012-31672 and BIO2015-68460-P) and the Generalitat de Catalunya (2014-SGR-1406) to E.M.; by Marie Curie IRG grant PIRG06-GA-2009-256420 to P.L.; by the European Commission (PCIG2012-GA-2012-334052) and MINECO (BIO2015-70812-ERC and RYC-2011-09220) to R.H.; by Royal Society grant RG2016R1 to G.T.-O.; by MINECO BIO2013-43184-P to D.A.; and by MINECO AGL2014-57200-JIN to E.G.M. We acknowledge financial support by the CERCA programme/Generalitat de Catalunya and from MINECO through the "Severo Ochoa Programme for Centers of Excellence in R&D" 2016-2019 (SEV-2015-0533).

AUTHOR CONTRIBUTIONS

G.M., P.L., and E.M. conceived and designed the study. G.M., A.R., N.V., J.S., G.T.-O., C.M.M.G., M.B., R.H., E.G.M., D.A., K.J.H., P.L., and E.M. acquired, analyzed, and interpreted data. G.M., P.L., and E.M. wrote the manuscript.

DECLARATION OF INTERESTS

The authors declare no competing interests.

Received: January 15, 2017
Revised: July 27, 2017
Accepted: December 8, 2017
Published: January 11, 2018

REFERENCES

1. Niwa, Y., Yamashino, T., and Mizuno, T. (2009). The circadian clock regulates the photoperiodic response of hypocotyl elongation through a coincidence mechanism in Arabidopsis thaliana. Plant Cell Physiol. *50*, 838–854.
2. Nozue, K., Covington, M.F., Duek, P.D., Lorrain, S., Fankhauser, C., Harmer, S.L., and Maloof, J.N. (2007). Rhythmic growth explained by coincidence between internal and external cues. Nature *448*, 358–361.
3. Nomoto, Y., Kubozono, S., Yamashino, T., Nakamichi, N., and Mizuno, T. (2012). Circadian clock- and PIF4-controlled plant growth: a coincidence mechanism directly integrates a hormone signaling network into the photoperiodic control of plant architectures in Arabidopsis thaliana. Plant Cell Physiol. *53*, 1950–1964.
4. Martín, G., Soy, J., and Monte, E. (2016). Genomic Analysis Reveals Contrasting PIFq Contribution to Diurnal Rhythmic Gene Expression in PIF-Induced and -Repressed Genes. Front. Plant Sci. *7*, 962.
5. Soy, J., Leivar, P., González-Schain, N., Martín, G., Diaz, C., Sentandreu, M., Al-Sady, B., Quail, P.H., and Monte, E. (2016). Molecular convergence of clock and photosensory pathways through PIF3-TOC1 interaction and co-occupancy of target promoters. Proc. Natl. Acad. Sci. USA *113*, 4870–4875.
6. Nozue, K., Harmer, S.L., and Maloof, J.N. (2011). Genomic analysis of circadian clock-, light-, and growth-correlated genes reveals PHYTOCHROME-INTERACTING FACTOR5 as a modulator of auxin signaling in Arabidopsis. Plant Physiol. *156*, 357–372.
7. Bernardo-García, S., de Lucas, M., Martínez, C., Espinosa-Ruiz, A., Davière, J.-M., and Prat, S. (2014). BR-dependent phosphorylation modulates PIF4 transcriptional activity and shapes diurnal hypocotyl growth. Genes Dev. *28*, 1681–1694.
8. Soy, J., Leivar, P., González-Schain, N., Sentandreu, M., Prat, S., Quail, P.H., and Monte, E. (2012). Phytochrome-imposed oscillations in PIF3 protein abundance regulate hypocotyl growth under diurnal light/dark conditions in Arabidopsis. Plant J. *71*, 390–401.
9. Monte, E., Tepperman, J.M., Al-Sady, B., Kaczorowski, K.A., Alonso, J.M., Ecker, J.R., Li, X., Zhang, Y., and Quail, P.H. (2004). The phytochrome-interacting transcription factor, PIF3, acts early, selectively, and positively in light-induced chloroplast development. Proc. Natl. Acad. Sci. USA *101*, 16091–16098.
10. Yamashino, T., Nomoto, Y., Lorrain, S., Miyachi, M., Ito, S., Nakamichi, N., Fankhauser, C., and Mizuno, T. (2013). Verification at the protein level of the PIF4-mediated external coincidence model for the temperature-adaptive photoperiodic control of plant growth in Arabidopsis thaliana. Plant Signal. Behav. *8*, e23390.
11. Nakamichi, N., Kiba, T., Henriques, R., Mizuno, T., Chua, N.-H., and Sakakibara, H. (2010). PSEUDO-RESPONSE REGULATORS 9, 7, and 5 are transcriptional repressors in the Arabidopsis circadian clock. Plant Cell *22*, 594–605.
12. Farré, E.M., and Liu, T. (2013). The PRR family of transcriptional regulators reflects the complexity and evolution of plant circadian clocks. Curr. Opin. Plant Biol. *16*, 621–629.
13. Nakamichi, N., Kita, M., Ito, S., Yamashino, T., and Mizuno, T. (2005). PSEUDO-RESPONSE REGULATORS, PRR9, PRR7 and PRR5, together play essential roles close to the circadian clock of Arabidopsis thaliana. Plant Cell Physiol. *46*, 686–698.
14. Kaczorowski, K.A., and Quail, P.H. (2003). Arabidopsis PSEUDO-RESPONSE REGULATOR7 is a signaling intermediate in phytochrome-regulated seedling deetiolation and phasing of the circadian clock. Plant Cell *15*, 2654–2665.
15. Liu, T.L., Newton, L., Liu, M.-J., Shiu, S.-H., and Farré, E.M. (2016). A G-box-like motif is necessary for transcriptional regulation by circadian pseudo-response regulators in Arabidopsis. Plant Physiol. *170*, 528–539.
16. Pfeiffer, A., Shi, H., Tepperman, J.M., Zhang, Y., and Quail, P.H. (2014). Combinatorial complexity in a transcriptionally centered signaling hub in Arabidopsis. Mol. Plant *7*, 1598–1618.
17. Martínez-García, J.F., Huq, E., and Quail, P.H. (2000). Direct targeting of light signals to a promoter element-bound transcription factor. Science *288*, 859–863.
18. Fornara, F., de Montaigu, A., Sánchez-Villarreal, A., Takahashi, Y., Ver Loren van Themaat, E., Huettel, B., Davis, S.J., and Coupland, G. (2015). The GI-CDF module of Arabidopsis affects freezing tolerance and growth as well as flowering. Plant J. *81*, 695–706.
19. Fornara, F., Panigrahi, K.C.S., Gissot, L., Sauerbrunn, N., Rühl, M., Jarillo, J.A., and Coupland, G. (2009). Arabidopsis DOF transcription factors act redundantly to reduce CONSTANS expression and are essential for a photoperiodic flowering response. Dev. Cell *17*, 75–86.
20. Zhu, J.-Y., Oh, E., Wang, T., and Wang, Z.-Y. (2016). TOC1-PIF4 interaction mediates the circadian gating of thermoresponsive growth in Arabidopsis. Nat. Commun. *7*, 13692.
21. Matsushika, A., Makino, S., Kojima, M., and Mizuno, T. (2000). Circadian waves of expression of the APRR1/TOC1 family of pseudo-response regulators in Arabidopsis thaliana: insight into the plant circadian clock. Plant Cell Physiol. *41*, 1002–1012.
22. Nakamichi, N., Kiba, T., Kamioka, M., Suzuki, T., Yamashino, T., Higashiyama, T., Sakakibara, H., and Mizuno, T. (2012). Transcriptional repressor PRR5 directly regulates clock-output pathways. Proc. Natl. Acad. Sci. USA *109*, 17123–17128.
23. Haudry, A., Platts, A.E., Vello, E., Hoen, D.R., Leclercq, M., Williamson, R.J., Forczek, E., Joly-Lopez, Z., Steffen, J.G., Hazzouri, K.M., et al. (2013). An atlas of over 90,000 conserved noncoding sequences provides insight into crucifer regulatory regions. Nat. Genet. *45*, 891–898.
24. Huang, W., Pérez-García, P., Pokhilko, A., Millar, A.J., Antoshechkin, I., Riechmann, J.L., and Mas, P. (2012). Mapping the core of the

Arabidopsis circadian clock defines the network structure of the oscillator. Science *336*, 75–79.

25. Lorrain, S., Allen, T., Duek, P.D., Whitelam, G.C., and Fankhauser, C. (2008). Phytochrome-mediated inhibition of shade avoidance involves degradation of growth-promoting bHLH transcription factors. Plant J. *53*, 312–323.
26. Al-Sady, B., Ni, W., Kircher, S., Schäfer, E., and Quail, P.H. (2006). Photoactivated phytochrome induces rapid PIF3 phosphorylation prior to proteasome-mediated degradation. Mol. Cell *23*, 439–446.
27. Fujiwara, S., Wang, L., Han, L., Suh, S.-S., Salomé, P.A., McClung, C.R., and Somers, D.E. (2008). Post-translational regulation of the Arabidopsis circadian clock through selective proteolysis and phosphorylation of pseudo-response regulator proteins. J. Biol. Chem. *283*, 23073–23083.
28. Soy, J., Leivar, P., and Monte, E. (2014). PIF1 promotes phytochrome-regulated growth under photoperiodic conditions in Arabidopsis together with PIF3, PIF4, and PIF5. J. Exp. Bot. *65*, 2925–2936.
29. Hayama, R., Sarid-Krebs, L., Richter, R., Fernández, V., Jang, S., and Coupland, G. (2017). PSEUDO RESPONSE REGULATORs stabilize CONSTANS protein to promote flowering in response to day length. EMBO J. *36*, 904–918.
30. Wang, L., Fujiwara, S., and Somers, D.E. (2010). PRR5 regulates phosphorylation, nuclear import and subnuclear localization of TOC1 in the Arabidopsis circadian clock. EMBO J. *29*, 1903–1915.
31. Shen, H., Moon, J., and Huq, E. (2005). PIF1 is regulated by light-mediated degradation through the ubiquitin-26S proteasome pathway to optimize photomorphogenesis of seedlings in Arabidopsis. Plant J. *44*, 1023–1035.
32. Pelletier, S., Van Orden, J., Wolf, S., Vissenberg, K., Delacourt, J., Ndong, Y.A., Pelloux, J., Bischoff, V., Urbain, A., Mouille, G., et al. (2010). A role for pectin de-methylesterification in a developmentally regulated growth acceleration in dark-grown Arabidopsis hypocotyls. New Phytol. *188*, 726–739.
33. Heyndrickx, K.S., Van de Velde, J., Wang, C., Weigel, D., and Vandepoele, K. (2014). A functional and evolutionary perspective on transcription factor binding in Arabidopsis thaliana. Plant Cell *26*, 3894–3910.
34. Huq, E., Al-Sady, B., Hudson, M., Kim, C., Apel, K., and Quail, P.H. (2004). Phytochrome-interacting factor 1 is a critical bHLH regulator of chlorophyll biosynthesis. Science *305*, 1937–1941.
35. Kamioka, M., Takao, S., Suzuki, T., Taki, K., Higashiyama, T., Kinoshita, T., and Nakamichi, N. (2016). Direct Repression of Evening Genes by CIRCADIAN CLOCK-ASSOCIATED1 in the Arabidopsis Circadian Clock. Plant Cell *28*, 696–711.
36. Kikis, E.A., Khanna, R., and Quail, P.H. (2005). ELF4 is a phytochrome-regulated component of a negative-feedback loop involving the central oscillator components CCA1 and LHY. Plant J. *44*, 300–313.
37. Más, P., Alabadí, D., Yanovsky, M.J., Oyama, T., and Kay, S.A. (2003). Dual role of TOC1 in the control of circadian and photomorphogenic responses in Arabidopsis. Plant Cell *15*, 223–236.
38. Leivar, P., Monte, E., Oka, Y., Liu, T., Carle, C., Castillon, A., Huq, E., and Quail, P.H. (2008). Multiple phytochrome-interacting bHLH transcription factors repress premature seedling photomorphogenesis in darkness. Curr. Biol. *18*, 1815–1823.
39. Khanna, R., Shen, Y., Marion, C.M., Tsuchisaka, A., Theologis, A., Schäfer, E., and Quail, P.H. (2007). The basic helix-loop-helix transcription factor PIF5 acts on ethylene biosynthesis and phytochrome signaling by distinct mechanisms. Plant Cell *19*, 3915–3929.
40. Michael, T.P., Salomé, P.A., Yu, H.J., Spencer, T.R., Sharp, E.L., McPeek, M.A., Alonso, J.M., Ecker, J.R., and McClung, C.R. (2003). Enhanced fitness conferred by naturally occurring variation in the circadian clock. Science *302*, 1049–1053.
41. Fujimori, T., Yamashino, T., Kato, T., and Mizuno, T. (2004). Circadian-controlled basic/helix-loop-helix factor, PIL6, implicated in light-signal transduction in Arabidopsis thaliana. Plant Cell Physiol. *45*, 1078–1086.
42. Ni, M., Tepperman, J.M., and Quail, P.H. (1998). PIF3, a phytochrome-interacting factor necessary for normal photoinduced signal transduction, is a novel basic helix-loop-helix protein. Cell *95*, 657–667.
43. Tanaka, Y., Kimura, T., Hikino, K., Goto, S., Nishimura, M., Mano, S., and Nakagawa, T. (2012). Gateway Vectors for Plant Genetic Engineering: Overview of Plant Vectors, Application for Bimolecular Fluorescence Complementation (BiFC) and Multigene Construction (InTech).
44. Nicol, J.W., Helt, G.A., Blanchard, S.G., Jr., Raja, A., and Loraine, A.E. (2009). The Integrated Genome Browser: free software for distribution and exploration of genome-scale datasets. Bioinformatics *25*, 2730–2731.
45. Huang, D.W., Sherman, B.T., Tan, Q., Collins, J.R., Alvord, W.G., Roayaei, J., Stephens, R., Baseler, M.W., Lane, H.C., and Lempicki, R.A. (2007). The DAVID Gene Functional Classification Tool: a novel biological module-centric algorithm to functionally analyze large gene lists. Genome Biol. *8*, R183.
46. Liu, T., Carlsson, J., Takeuchi, T., Newton, L., and Farré, E.M. (2013). Direct regulation of abiotic responses by the Arabidopsis circadian clock component PRR7. Plant J. *76*, 101–114.
47. Toledo-Ortiz, G., Johansson, H., Lee, K.P., Bou-Torrent, J., Stewart, K., Steel, G., Rodríguez-Concepción, M., and Halliday, K.J. (2014). The HY5-PIF regulatory module coordinates light and temperature control of photosynthetic gene transcription. PLoS Genet. *10*, e1004416.
48. Wang, L., Kim, J., and Somers, D.E. (2013). Transcriptional corepressor TOPLESS complexes with pseudoresponse regulator proteins and histone deacetylases to regulate circadian transcription. Proc. Natl. Acad. Sci. USA *110*, 761–766.
49. Martín, G., Leivar, P., Ludevid, D., Tepperman, J.M., Quail, P.H., and Monte, E. (2016). Phytochrome and retrograde signalling pathways converge to antagonistically regulate a light-induced transcriptional network. Nat. Commun. *7*, 11431.

STAR★METHODS

KEY RESOURCES TABLE

REAGENT or RESOURCE	SOURCE	IDENTIFIER
Antibodies		
Anti-GFP	Invitrogen	Cat# A11122
Peroxidase-linked anti rabbit secondary antibody	Sigma	Cat# NA934
Anti-PIF3	[26]	N/A
Anti-HA	Abcam	Cat# 9110
Bacterial and Virus Strains		
AH109	Clontech	N/A
E. coli DH5α	N/A	N/A
A. tumefaciens GV3031	N/A	N/A
Chemicals, Peptides, and Recombinant Proteins		
Formaldehyde	ThermoFisher Scientific	Cat# 28908
Glycine	GE Healthcare Life Sciences	Cat# 17-1323-01
EDTA	Thermo Scientific	Cat# 17892
Tris-HCL	Sigma	Cat# C4706-2G
Proteinase K	ThermoFisher Scientific	Cat# EO0491
Sucrose	Applichem	Cat# A1125.1000
MgCl2	Calbiochem	Cat# 442611
PMSF	Applichem	Cat# A0999,0025
MG132	Merck	Cat# 474790
Proteinase Inhibitor Cocktail	Roche	Cat# 4693116001
Triton X-100	Applichem	Cat# A1388.10000
NaCl	Scharlau	Cat# SO02271000
LiCl	Merck	Cat# 1,056,790,250
NP40	Sigma	Cat# 74385
Deoxycholic acid sodium	Sigma	Cat# D6750
$NaHCO_3$	Merck	Cat# 6329
Dropout medium (-AHLT)	Clontech	Cat# 630428
Yeast Nitrogen Base w/o aa & ammonium sulfate	Conda	Cat# 1553.00
Ammonium Sulfate	Sigma	Cat# A4418
D-Glucose	Applichem	Cat# 3O000431
European bacteriological Agar	Conda	Cat# 1800.00
His	Sigma	Cat# H8125
Trp	Sigma	Cat# T0254
Leu	Sigma	Cat# L8912
Ade	Sigma	Cat# A9126
Propidium iodine	Calbiochem	Cat# 537059-
Ortho-nitrophenyl- β-D-galacpyranoside	ThermoFisher Scientific	Cat# 34055
DNase I	Ambion	Cat# AM2224
RNase Out	Invitrogen	Cat# 10777019
SYBR Premix Ex Taq	Roche	Cat# 04707516001
MOPS (pH 7.6)	Sigma	Cat# M1254
SDS	Amresco	Cat# 0227
Glycerol	Applichem	Cat# A2926
EDTA	Thermo Scientific	Cat# 17892
Aprotinin	Applichem	Cat# A2132

(*Continued on next page*)

Continued

REAGENT or RESOURCE	SOURCE	IDENTIFIER
Leupeptin	Applichem	Cat# A2183
Pepsatin	Applichem	Cat# A2205
PMSF	Applichem	Cat# A0999
β-mercaptoethanol	Fluka	Cat# 03700
GFP Agarose Beads	MBL	Cat# D153-8
rProtein A-Sepharose	Bionova	Cat# 1-888-752-2568
Hikari solution	Nacalai Tesque	Cat# 02270-81
Sodium metabisulfite	Sigma	Cat# 255556
XmaI	Roche	Cat# ER0171
BamHI	Roche	Cat# 10 220 612 001
EcoRI	Roche	Cat# 10 703 737 001
T4 DNA Ligase	NZYtech	Cat# MB00703
BP Clonase II	Gateway	Cat# 11789-020
LR Clonase II	Gateway	Cat# 11791-020
Critical Commercial Assays		
RNeasy Plant Mini	QIAGEN	Cat# 74904
SuperScript III reverse transcriptase	Invitrogen	Cat# 18080044
Protein DC	Bio-Rad	Cat# 5000121
SuperSignal West Femto chemiluminescence	Thermo Scientific	Cat# 34095
QIAquick gel extraction kit	QIAGEN	Cat# QIA28704
Dynabeads	Invitrogen	Cat# 10004D
Immobilon-P membrane	Millipore	Cat# IPVH00010
Experimental Models: Organisms/Strains		
Col-0	N/A	N/A
C24	N/A	N/A
cdf5-1	[19]	N/A
toc1-101	[36]	N/A
pPRR7::PRR7-GFP (PRR7-GFP)	[27]	N/A
pPIF3::YFP:PIF3 (YFP-PIF3)	[26]	N/A
p35S::PIF4-HA (PIF4-HA)	[25]	N/A
pTOC1::TOC1:YFP (TMG or TOC1-YFP)	[37]	N/A
pif1-1	[34]	N/A
pif3-3	[9]	N/A
pif4-2	[38]	N/A
pif5-3	[39]	N/A
pifq	[38]	N/A
prr5-1	[40]	N/A
prr7-3	[40]	N/A
prr9-1	[40]	N/A
pif3-1	[9]	N/A
pif4-101	[25]	N/A
pil6-1 (pif5)	[41]	N/A
prr7-3pif3-1 (*prr7pif3*)	This paper	N/A
prr7-3pif4-101 (*prr7pif4*)	This paper	N/A
prr7-3pil6-1 (*prr7pif5*)	This paper	N/A
prr7-3prr9-1 (*prr79*)	This paper	N/A
prr5-1prr9-1 (*prr59*)	This paper	N/A
prr5-1prr7-3prr9-1 (*prr579*)	This paper	N/A
prr7-3cdf5-1 (*prr7cdf5*)	This paper	N/A

(*Continued on next page*)

Continued		
REAGENT or RESOURCE	SOURCE	IDENTIFIER
35S::CDF5-GFP (*CDF5OX*)	This paper	N/A
pifqCDF5OX	This paper	N/A
pifqcdf5	This paper	N/A
Oligonucleotides		
See Table S1	N/A	N/A
Recombinant DNA		
pH7FWG2	Gateway	N/A
PIF3 in pGAD424	[42]	N/A
PIF4 in pGADT7	[7]	N/A
NZY-A PCR cloning kit	NZYTech	Cat# MB05302
pGBKT7	Clontech	Cat# PT3248-5
pGWcY	[43]	N/A
pGWnY	[43]	N/A
Software and Algorithms		
ActiveWebCam software (http://www.pysoft.com)	N/A	N/A
Integrated Genome Browser (IGB)	[44]	N/A
PHASER (http://phaser.mocklerlab.org)	N/A	N/A
DAVID system	[45]	N/A
IBM SPSS Statistics Software	N/A	N/A
Excel	N/A	N/A

CONTACT FOR REAGENT AND RESOURCE SHARING

Further information and requests for resources and reagents should be directed to and will be fulfilled by the Lead Contact, Elena Monte (elena.monte@cragenomica.es).

EXPERIMENTAL MODEL AND SUBJECT DETAILS

The *Arabidopsis thaliana* (L.) accession Columbia (Col-0), C24, and mutants used here were obtained from the mentioned references or generated in this work (see Key Resources Table).

METHOD DETAILS

Seedling Growth and Hypocotyl and Cell Measurements

Arabidopsis thaliana seeds used in this manuscript include the previously described *cdf5-1* [19], *toc1-101* [36], *pPRR7::PRR7-GFP* (PRR7-GFP) [27], *pPIF3::YFP:PIF3* (YFP-PIF3) [26], *p35S::PIF4-HA* [25], *pif1-1* [34], *pif3-3* [9], *pif4-2* [38], *pif5-3* [39], *pifq* [38], *prr5-1*, *prr7-3*, and *prr9-1* [40], *pif3-1* [9], *pif4-101* [25], *pil6-1* (*pif5* mutant) [41], and the newly generated *prr7-3pif3-1* (*prr7pif3*), *prr7-3pif4-101* (*prr7pif4*), *prr7-3pil6-1* (*prr7pif5*), *prr7-3prr9-1* (*prr79*), *prr5-1prr9-1* (*prr59*), *prr5-1prr7-3prr9-1* (*prr579*), and *prr7-3cdf5-1* (*prr7cdf5*) in Col-0 ecotype, and *pTOC1::TOC1:YFP* (TMG) [37] in C24 ecotype. *CDF5OX* lines were generated by cloning the *CDF5* ORF under the regulation of the 35S promoter in the pH7FWG2 vector. The resulting 35S::CDF5-GFP construct was transformed into *cdf5* to generate *CDF5OX* lines, and into *pifq* to generate *pifqCDF5OX* lines.

Seeds were sterilized and plated on Murashige and Skoog medium without sucrose. Seedlings were stratified for 4d at 4C in darkness, and seedling growth was done in short days (8 hr light + 16 hr dark) or continuous white light (85 μmol·m-2·s-1) for the time indicated in each experiment. Hypocotyl measurements in Figures 2E and 4A and S3B were done using ImageJ (National Institutes of Health). Saturating FR pulses were 30 μmol·m-2·s-1 for 15min. Samples at ZT0 and ZT24 were collected in the dark, whereas at ZT8 were in the light. For hypocotyl growth rate measurements (Figure 4B), image acquisition was done using the ActiveWebCam software (http://www.pysoft.com) under infrared light background using modified webcams (Microsoft Life Cam Studio). Twelve seedlings were measured individually every 2 hr throughout the diurnal cycle, the difference in hypocotyl length between the two time points was calculated, and the elongation rate was expressed as mm/h. The mean and SE for the 12 seedlings are represented. Cell size was visualized in seedlings stained with propidium iodine (10 μg/mL) (Calbiochem) using a confocal laser microscope Leica SP5 (570 nm-666 nm). Cell length was measured in pictures taken with an optic microscope (AixoPhot DP70) (Figure 4D).

ChIP-seq Data Analysis and Visualization

Comparison of ChIP-seq data shown in Figure 1A was performed using PIF- [16] and PRR9/7/5-associated peaks from [15], which contained novel PRR9 and re-analyzed ChIP-seq data for PRR5 [22] and PRR7 [46], considering only the PRR binding sites located upstream of the transcriptional start site TSS as in [16]. The same comparison was performed in Figure 1D adding the PIF/SD-induced gene set from [4]. Distance between PIF and PRR peaks was calculated separately for all the different pairwise combinations associated to a given gene. To jointly visualize the Chip-Seq data for PRR [15] and PIFs [16], and the conserved noncoding sequences (CNS) regions [23] (Figure 1E), the Integrated Genome Browser (IGB) [44] was used. Data was obtained from http://mustang.biol.mcgill.ca (CNS), GEO: GSE71397 (PRRs) and GEO: GSE43286 (PIFs). Expression phases shown in Figures 1C and S1C were analyzed using the PHASER tool (http://phaser.mocklerlab.org) for SD (Col-0_SD), LD (longday), and LL (LL23_LDHH). The PHASER tool generated over-representation p values for each phase (Data S1). DAVID system [45] was used to identify enriched GO biological terms (Figure S1B).

Chromatin Immunoprecipitation (ChIP) Assays

Chromatin immunoprecipitation (ChIP) and ChIP-qPCR assays (Figure 2A) were performed as in [5, 47]. For PIF3-YFP, all process was performed in the dark under green safelight. Seedlings (3g) were vacuum-infiltrated with 1% formaldehyde and cross-linking was quenched by vacuum infiltration with 0.125 M glycine for 5 min. Tissue was ground, and nuclei-containing cross-linked protein and DNA were purified by sequential extraction on Extraction Buffer 1 (0.4M Sucrose, 10 mM Tris-HCL pH8, 10mM $MgCl_2$, 5mM β-mercaptoethanol, 0.1mM PMSF, 50 μM MG132, proteinase inhibitor cocktail), Buffer 2 (0.25M Sucrose, 10mM Tris-HCL pH8, 10mM $MgCl_2$, 1% Triton X-100, 5mM β-mercaptoethanol, 0.1mM PMSF, 50 μM MG132, proteinase inhibitor cocktail), and Buffer 3 (1.7M Sucrose, 10 mM Tris-HCL pH8, 0.15% Triton X-100, 2mM $MgCl_2$, 5mM β-mercaptoethanol, 0.1mM PMSF, 50 μM MG132, proteinase inhibitor cocktail). Nuclei were resuspended in nuclei lysis buffer (50 mM Tris-HCL pH8, 10 mM EDTA, 1% SDS, 50 μM MG132, proteinase inhibitor cocktail), sonicated for 10X 30sec, and diluted 10X in Dilution Buffer (0.01% SDS, 1% Triton X-100, 1.2 mM EDTA, 16.7 mM Tris-HCL pH8, 167 mM NaCl). Overnight incubation was performed with the corresponding antibody (or with no antibody as control) at 4C overnight, and immunoprecipitation was performed using dynabeads. Washes were done sequentially in Low Salt Buffer (0.1% SDS, 1% Triton X-100, 2 mM EDTA, 20 mM Tris-HCL pH8, 150 mM NaCl), High Salt Buffer (0.1% SDS, 1% Triton X-100, 2 mM EDTA, 20 mM Tris-HCL pH8, 500 mM NaCl), LiCl Buffer (0.25M LiCl, 1% NP40, 1% deoxycholic acid sodium, 1 mM EDTA, 10 mM Tris-HCL pH8), and TE X1. Immunocomplexes were eluated in Elution Buffer (1%SDS, 0.1M $NaHCO_3$), de-cross-linked overnight at 65C in 10 mM NaCl, and then treated with proteinase K. DNA was purified using QIAGEN columns, eluted in 100 uL of QIAGEN elution buffer, and 2 μL were used for qPCR (ChIP-qPCR) using *CDF5* promoter-specific primers (Table S1) spanning the region containing the predicted binding sites for the PIFs [16]. Three biological replicates were performed for all the "Antibody" samples (two for WT C24 at ZT8), and one for the "No Antibody." Calculations of percent input were done following the protocol available at http://www.thermofisher.com.

Yeast Two-Hybrid Assays

For yeast two-hybrid assays shown in Figure S1A, we used PIF3 (pGAD424) and PIF4 (pGADT7) described previously [7, 42]. PRR fragments were PCR-amplified from PRR templates [48] with primers containing restriction sites (XmaI/BamHI for PRR5 and PRR9, EcoRI/XmaI for PRR7) (Table S1), cloned into pTOPO vector (NZYTech), sequenced and cloned into pGBKT7 (Clontech). To assess interactions, constructs were co-transformed into yeast AH109 cells (Clontech). Yeast transformants were selected on synthetic dropout medium (SD) deficient in leucine and tryptophan (-LT), and interaction was assayed quantitatively by a β-Galactosidase assay performed using ortho-nitrophenyl- β-D-galacpyranoside as a substrate following manufacturer's instructions.

Bimolecular Fluorescence Complementation (BiFC) Assays

For bimolecular fluorescence complementation (BiFC) shown in Figure 1B, the coding regions of PIF3 and TOC1 [5] were cloned into pGWcY and pGWnY vectors [43], respectively. PRR5-, PRR7- and PRR9-nYFP are from [48]. Preparation of samples and bombardment of onion cells were done as in [5]. Briefly, the inner layers of spring onions were cut in 2 × 2 cm squares and used for particle bombardment. Each sample was transfected with 1 μg of each plasmid coupled to tungsten particles using a Biolistic Particle Delivery System PDS-1000 (Bio-Rad). After bombardment, onions were exposed to a saturating 15 min FR pulse and incubated overnight in dark conditions. The upper epidermal layer was removed, placed in a microscope slide and visualized using a confocal laser scanning microscope Olympus FV1000 (Objective Lens UPLSAPO 20X, Laser Wavelength: 514 nm, Emission window: 525-600 nm).

Protein Extraction and Immunoblot

Total protein extracts to detect endogenous PIF3 were prepared from 3 day-old SD-grown seedlings harvested at ZT24 in the dark (Figure 2D). Extraction buffer and protein quantification were done essentially as described [49]: Samples were collected and frozen in liquid nitrogen, and manually ground under frozen conditions before resuspension in boiling extraction buffer (100 mM MOPS (pH 7.6), 2% SDS, 10% glycerol, 4mM EDTA, 50mM Sodium metabisulfite ($Na_2S_2O_5$), $2gl^{-L}$ aprotinin, $3gl^{-L}$ leupeptin, $1gl^{-L}$ pepstatin and 2 mM PMSF). Total protein was quantified using a Protein DC kit (Bio-Rad), and β-mercaptoethanol was added just before loading. Aliquots of 100 ug for each sample were treated for 5min at 95C and subjected to 12.5% SDS- PAGE gels. Proteins were then transferred to Immobilon-P membrane (Millipore), and immunodetection of endogenous PIF3 was performed using a anti-PIF3 antibody [26] (1:10,000 dilution) incubated with Hikari solution (Nacalai Tesque). Peroxidase-linked anti rabbit secondary

antibody (1:5,000 dilution) and a SuperSignal West Femto chemiluminescence kit (Pierce) were used for detection of luminescence using LAS-4000 Image imaging system (Fujifilm). The membrane was stained with Coomassie blue as a loading control.

Gene Expression Analysis

Quantitative RT-PCR, RNA extraction, cDNA synthesis and qRT-PCR were done as described [49]. Briefly, 1 mg of total RNA extracted using the RNeasy Plant Mini Kit (QIAGEN) were treated with DNase I (Ambion) according to the manufacturer's instructions. First-strand cDNA synthesis was performed using the SuperScript III reverse transcriptase (Invitrogen) and oligo dT as a primer (dT30). cDNA was then treated with RNase Out (Invitrogen) before 1:20 dilution with water, and 2 μL was used for real-time PCR (Light Cycler 480; Roche) using SYBR Premix Ex Taq (Takara) and primers at a 300 nM concentration. Gene expression in time-course analyses (Figures 2C, 3A, 3B, 3D, 3E, S2C, and S2D) was measured in two independent biological replicates, with three technical replicates for each biological sample, and the mean of the biological replicates ± SE is shown. For specific time points in Figures 2B, 4C, S2A, S2B, and S3C, gene expression was measured in three independent biological replicates, and in two biological replicates in Figure 3C, and each biological sample corresponds to the mean of three technical replicates. *PP2A* (*AT1G13320*) was used for normalization.

QUANTIFICATION AND STATISTICAL ANALYSIS

Differences between means were statistically analyzed by one-way analysis of variance using Tukey-b post hoc multiple comparison test (IBM SPSS Statistics Software) or homoscedastic Student's t test (Excel Microsoft), as indicated in the figure legends. Statistically significant differences were defined as those with a p value < 0.05. Significance level is indicated as * $p < 0.05$, ** $p < 0.01$ and *** $p < 0.001$.